

MOLECULAR ECOLOGY

Comparing RADseq and microsatellites to infer complex phylogeographic patterns, an empirical perspective in the Crucian carp, *Carassius carassius*, L.

Journal:	<i>Molecular Ecology</i>
Manuscript ID	MEC-15-1040.R2
Manuscript Type:	Original Article
Date Submitted by the Author:	n/a
Complete List of Authors:	Jeffries, Daniel; University of Hull, School of Biological, Biomedical and Environmental Science Copp, Gordon; Centre for Environment, Fisheries and Aquaculture Science, ; Bournemouth University, Department of Life and Environmental Sciences Lawson Handley, Lori; University of Hull, School of Biological, Biomedical and Environmental Science Olsen, Hakan; Södertörn University, School of Natural Science, Technology and Environmental Studies Sayer, Carl; University College London, Department of Geography Haenfling, Bernd; University of Hull, School of Biological, Biomedical and Environmental Science
Keywords:	Approximate Bayesian Computation, Postglacial recolonisation, Landscape Genetics, Conservation Biology, Study design, Population structure

SCHOLARONE™
Manuscripts

"This is the peer reviewed version of the following article: Jeffries, D. L., Copp, G. H., Lawson Handley, L., Olsén, K. H., Sayer, C. D. and Hänfling, B. (2016), Comparing RADseq and microsatellites to infer complex phylogeographic patterns, an empirical perspective in the Crucian carp, *Carassius carassius*, L.. Mol Ecol. doi:10.1111/mec.13613, which has been published in final form at <http://onlinelibrary.wiley.com/doi/10.1111/mec.13613/abstract>. This article may be used for non-commercial purposes in accordance with Wiley Terms and Conditions for Self-Archiving."

1 Comparing RADseq and microsatellites to infer
2 complex phylogeographic patterns, an empirical
3 perspective in the Crucian carp, *Carassius carassius*,
4 L.

5

6 **Authors:** ¹Daniel L Jeffries, ²Gordon H Copp, ¹Lori Lawson Handley, ³K. Håkan Olsén, ⁴Carl D
7 Sayer, ¹Bernd Hänfling

8

9 ¹ *Evolutionary Biology Group, School of Biological, Biomedical and Environmental Sciences,*
10 *Hardy Building, University of Hull, Hull, HU6 7RX, UK*

11 ² *Salmon & Freshwater Team, Cefas, Pakefield Road, Lowestoft, Suffolk NR33 0HT, UK, and*
12 *Department of Life and Environmental Sciences, Faculty of Science and Technology, Bournemouth*
13 *University, Poole, UK*

14 ³ *School of Natural Science, Technology and Environmental Studies, Södertörn University, Alfred*
15 *Nobels allé 7, Flemingsberg, 141 89 Huddinge, Sweden*

16 ⁴ *Environmental Change Research Centre, Department of Geography, University College London,*
17 *Pearson Building, Gower Street, London, WC1E 6BT, UK*

18

19 **Keywords**

20 Approximate Bayesian Computation, Postglacial recolonisation, Landscape Genetics, Conservation Biology,
21 Study design, Population structure

22

23 **Corresponding author:** Daniel Jeffries (dljeffries86@gmail.com) *Evolutionary Biology Group,*
24 *School of Biological, Biomedical and Environmental Sciences, Hardy Building, University of Hull,*
25 *Hull, HU6 7RX, UK*

26

27 **Running title:** The complex phylogeography of the crucian carp

28

29 Abstract

30 The conservation of threatened species must be underpinned by phylogeographic knowledge. This
31 need is epitomised by the freshwater fish *Carassius carassius*, which is in decline across much of
32 its European range. Restriction site associated DNA sequencing (RADseq) is increasingly used for
33 such applications, however RADseq is expensive, and limitations on sample number must be
34 weighed against the benefit of large numbers of markers. This trade-off has previously been
35 examined using simulation studies, however, empirical comparisons between these markers,
36 especially in a phylogeographic context, are lacking. Here, we compare the results from
37 microsatellites and RADseq for the phylogeography of *C. carassius* to test whether it is more
38 advantageous to genotype fewer markers (microsatellites) in many samples, or many markers
39 (SNPs) in fewer samples. These datasets, along with data from the mitochondrial cytochrome b
40 gene, agree on broad phylogeographic patterns; showing the existence of two previously
41 unidentified *C. carassius* lineages in Europe; one found throughout northern and central-eastern
42 European drainages, and a second almost exclusively confined to the Danubian catchment. These
43 lineages have been isolated for approximately 2.15 M years, and should be considered separate
44 conservation units. RADseq recovered finer population structure and stronger patterns of IBD than
45 microsatellites, despite including only 17.6% of samples (38% of populations and 52% of samples
46 per population). RADseq was also used along with Approximate Bayesian Computation to show
47 that the postglacial colonisation routes of *C. carassius* differ from the general patterns of freshwater
48 fish in Europe, likely as a result of their distinctive ecology.

49 Introduction

50 Phylogeographic studies have revealed that the contemporary distributions of European taxa and
51 their genetic diversity have been largely shaped by the glacial cycles of the Pleistocene epoch, and
52 in particular by range shifts during recolonisation from glacial refugia (Hewitt 1999). In freshwater
53 fishes, the dynamics of recolonisation are tightly linked to the history of river drainage systems
54 (Bianco 1990; Bănărescu 1990, 1992; Bernatchez & Wilson 1998; Reyjol *et al.* 2006). For example,
55 watersheds pose a significant barrier to fish dispersal, often resulting in strong genetic structuring
56 across separate drainage systems (Durand *et al.* 1999; Hänfling *et al.* 2002). However, during
57 glacial melt periods, ephemeral rivers and periglacial lakes can arise, providing opportunities for
58 colonisation (Gibbard *et al.* 1988) of otherwise isolated drain basins (Grosswald 1980; Arkhipov *et al.*
59 *al.* 1995). These processes have resulted in complicated recolonisation scenarios in Europe, which,
60 in contrast to North America (Bernatchez & Wilson 1998), appear to possess few general patterns
61 of population structure. Furthermore, previous phylogeographic studies have predominantly focused
62 on highly mobile, obligatory or facultatively lotic species, with more sedentary, lentic species being
63 largely overlooked.

64

65 The crucian carp, *Carassius carassius* (Linnaeus 1758), is native to parts of central, eastern and
66 northern Europe and almost exclusively restricted to lentic ecosystems, including lakes, ponds and
67 river floodplains (Copp 1991; Copp *et al.* 2008). *C. carassius*, has recently experienced sharp
68 declines in the number and sizes of populations throughout its native range, leading to some local
69 population extinctions. The reasons for these declines include habitat loss through drought and
70 terrestrialisation in England (Copp 1991; Wheeler 2000; Sayer *et al.* 2011), acidification
71 (Holopainen & Oikari 1992), poor water quality in the Danube river catchment (Navodaru *et al.*
72 2002), and hybridisation with several non-native species (Copp *et al.* 2010; Savini *et al.* 2010;
73 Mezhzherin *et al.* 2012; Wouters *et al.* 2012; Rylková *et al.* 2013). The susceptibility of *C.*

74 *carrassius* to genetic isolation and bottlenecks is compounded by small population sizes (Hänfling
75 *et al.* 2005) and low dispersal (Holopainen *et al.* 1997). Strong geographic structure is therefore
76 likely in this species. Although the threats to *C. carassius* populations are recognised on a regional
77 level (Lusk *et al.* 2004; Mrakovčić *et al.* 2007; Wolfram & Mikschi 2007; Simic, V *et al.* 2009;
78 Copp & Sayer 2010), a global conservation strategy is missing. Broad scale phylogeographic data
79 and definition of evolutionary significant units are essential for informing unified conservation
80 efforts for this species (Frankham *et al.* 2002).

81

82 Phylogeographic data have traditionally been collected using mitochondrial gene regions and/or
83 nuclear markers such as AFLPs and microsatellites. However, cost and time often limits the number
84 of these nuclear markers used, which can result in low power for addressing phylogeographic
85 questions (Cornuet & Luikart 1996; Luikart & Cornuet 2008; Landguth *et al.* 2012; Peery *et al.*
86 2012; Hoban *et al.* 2013). Single nucleotide polymorphisms (SNPs) are increasingly used in
87 phylogeography for assessments of population structure (for example see Morin *et al.* 2010;
88 Emerson *et al.* 2010; Hess *et al.* 2011; Hauser *et al.* 2011). However, being bi-allelic, SNP loci
89 contain less information than highly polymorphic microsatellites (Coates *et al.* 2009) and therefore
90 large numbers of SNPs are needed to provide adequate statistical power. SNP discovery and assay
91 development, which has been costly and slow in the past, has recently been greatly facilitated by the
92 invention of restriction site associated DNA sequencing (RADseq, (Miller *et al.* 2006)), which
93 enables the fast identification of thousands of orthologous SNP markers in non-model organisms.
94 Nevertheless, although next generation sequencing costs are falling, RADseq remains a relatively
95 expensive approach, which often constrains the number of biological samples that can be included
96 in a given study. Researchers are, therefore, faced with a trade-off between the number of samples
97 and loci during study design. The optimal balance between the two is likely to be based on several
98 important but often unknown properties of the study system in question, for example the strength of
99 population structure (i.e. F_{ST}). Identifying these properties and comparing the relative strengths and

100 weaknesses of different molecular markers have recently been highlighted as priority topics in
101 landscape genetics and phylogeography (Epperson *et al.* 2010; Balkenhol & Landguth 2011).
102 Recent simulation studies have provided some important insights into this trade-off, for example,
103 Schwartz & McKelvey (2009) find that patchy geographic sampling along an IBD gradient could
104 result in falsely identified distinct lineages, whereas Landguth *et al.* (2012) find that increasing the
105 number of loci can strengthen the correlation between genetic and geographic distance for a given
106 sample set. To date, comprehensive empirical comparisons between microsatellite and SNP markers
107 in a phylogeographic context are lacking (but see Bradbury *et al.* 2015).

108

109 In the present study, we use a combination of mitochondrial DNA (mtDNA), microsatellites and
110 genome-wide SNPs obtained from RADseq in order to: 1) produce a comprehensive
111 phylogeography for *C. carassius* as a basis for Europe-wide conservation strategies, 2) test
112 competing scenarios of postglacial recolonisation that have potentially contributed to the
113 contemporary distribution of the species, and 3) compare the power of microsatellites and RADseq
114 based population structure analyses, in the context of the first two objectives. In this third aim, we
115 specifically ask, whether the benefits gained by the high numbers of markers obtained from
116 RADseq outweigh the potential loss of power associated by the reduction in the number of samples
117 in our system.

118 Materials and Methods

119 *Sample collection and DNA extraction*

120 *C. carassius* is a Cyprinid native to much of continental Europe; latitudinally from the North Sea
121 and Baltic Sea basins, through central Europe north of the Alps down to the Ponto-Caspian region
122 and longitudinally from Belgium and perhaps northern France into Siberia (Lelek 1980). However,
123 the true extent of this native range is unknown, largely due to difficulties in morphologically
124 distinguishing it from three closely related, introduced and widespread species: *Carassius auratus*,

125 *Carassius gibelio*, and *Cyprinus carpio* (Wheeler 2000; Hickley & Chare 2004). We initially
126 collected 1354 samples from 72 populations across 13 European countries, but due to frequent
127 hybridisation between the *C. carassius* and the three species mentioned above, it was necessary to
128 identify and remove hybrids from this sample set. To this end, all samples were first genotyped at 6
129 species diagnostic microsatellite loci. We removed all samples identified as hybrids from the dataset
130 and, to safeguard against cryptic hybridisation, we also removed all *C. carassius* that were
131 sympatric with hybrids (see SI text for full details of species identification and hybrid detection).
132 This left 867 *C. carassius* samples from 57 populations across the species' distribution in central
133 and northern Europe (Table 1, Fig. 1). Sample sizes ranged from n=4 to n=37, with a mean of n=17
134 (Table 1). Fish were anaesthetised by a UK Home Office (UKHO) personal license holder (GHC) in
135 a 1 mL L⁻¹ bath of 2-phenoxyethanol prior to collection of a 1 cm² tissue sample from the lower-
136 caudal fin, and wounds were treated with a mixture of adhesive powder (Orahesive) and antibiotic
137 (Cicatrín) (Moore *et al.* 1990). Tissue samples were immediately placed in ≥95% ethanol, and
138 stored at -20°C. DNA was extracted from 2–4 mm² of each tissue sample using either the Genra
139 Puregene DNA isolation kit or the DNeasy DNA purification kit (both Qiagen, Hilden, Germany).
140 For the RADseq library, DNA was quantified using the Quant-iT™ PicoGreen® dsDNA Assay kit
141 (Invitrogen) and normalised to concentrations ≥50 ng ml⁻¹. Gel electrophoresis was then used to
142 check that DNA extractions contained high molecular weight DNA.

143

144 *Molecular markers and methods*

145 Three types of molecular markers were used in this study. Mitochondrial DNA sequencing was
146 used to identify highly distinct lineages and to date the divergence between them through
147 phylogenetic analysis. Two sets of nuclear markers; microsatellites and RADseq-derived SNPs,
148 were used to investigate more recent and complex structure in a population genetics framework and
149 to compare the relative power of each marker to do so.

150

151 *Mitochondrial DNA amplification*

152 A total of 83 *C. carassius* individuals, randomly chosen from a subset of 30 populations, which
153 were chosen to represent all major catchment areas and the widest possible geographic range (min.
154 $n = 1$, max. $n = 4$, mean $n = 2.7$), were sequenced at the cytochrome b (*cytb*) gene (Table 1). PCR
155 reactions were carried out following the protocol in Takada *et al.* (2010) using the forward and
156 reverse primers L14736-Glu and H15923-Thru on an Applied Biosciences® Veriti Thermal Cycler.
157 PCR products were sequenced in both directions on an ABI3700 by Macrogen Europe. The forward
158 and reverse *cytb* sequence reads were aligned using a GenBank sequence from the UK (accession
159 no. JN412539, Table 1) as a reference and ambiguous nucleotides were manually edited using
160 CodonCode aligner v.2.0.6 (CodonCode Corporation).

161

162 *Microsatellite amplification*

163 Of the 867 samples identified as pure *C. carassius*, 19 samples were in populations with sample
164 numbers which were too low to be useful for population genetics analyses (< 4). The remaining
165 848 samples, from 49 populations, were genotyped at 13 microsatellite loci, including the six
166 species diagnostic loci used for hybrid identification (Supporting Information (SI) Table 1).
167 Microsatellites were amplified in three multiplex PCR reactions, using the Qiagen multiplex PCR
168 mix with manufacturer's recommended reagent concentrations, including Q solution and 1 μ l of
169 template DNA. Primer concentrations for each locus are provided in SI Table 1 and PCRs were
170 performed on an Applied Biosciences® Veriti Thermal Cycler. The annealing temperature used was
171 54°C for all reactions, and all other PCR cycling parameters were set to Qiagen multiplex kit
172 recommended values. PCR products were run on a Beckman Coulter CEQ 8000 genome analyser

173 using a 400 bp size standard and microsatellite alleles scored using the Beckman Coulter CEQ8000
174 software.

175

176 *RADseq*

177 A total of 160 individuals (18 populations, min. $n = 8$, max. $n = 10$, mean $n = 8.9$), identified as
178 pure *C. carassius* with the diagnostic microsatellites, were used in the RADseq (Table 1). These
179 samples were chosen to represent a wide geographic range and all major phylogeographic clusters
180 identified using the microsatellite data. These samples were split across 13 libraries prepared at
181 Edinburgh Genomics (University of Edinburgh, UK) according to the protocol in Davey *et al.*
182 (2012) using the enzyme *Sbf*1. Libraries were then sequenced using paired-end sequencing across
183 five lanes of two Illumina HiSeq 2000 flowcells (Edinburgh Genomics).

184

185 *Data analyses*

186 *Phylogenetic analysis of mtDNA*

187 In addition to the 83 sequenced samples (SI Table 2), we retrieved 19 published *C. carassius* and
188 three *C. carpio cytb* sequences from GenBank to be used as an outgroup. The *C. carpio* samples
189 were chosen to include samples from multiple, distant lineages of *C. carpio* located in Japan,
190 Greece and India. All sequences used were validated through cross checking with their original
191 publications (Table 1). Sequence alignment was performed in MEGA6 (Tamura *et al.* 2013) using
192 default settings, and DNAsp v.5.0 (Librado & Rozas 2009) was used to calculate sequence
193 divergence and to identify haplotypes.

194

195 Haplotypes of all *C. carassius* samples and the three *C. carpio* outgroup individuals were exported
196 to BEAST v.1.7.5 (Drummond *et al.* 2012) for phylogenetic analyses in order to identify the major

197 phylogenetic lineages within European *C. carassius*. Phylogenetic model testing with jModeltest2
198 v.2.1.7 (Guindon *et al.* 2003; Darriba *et al.* 2012) using Akaike information criterion (AIC),
199 Bayesian Information Criteria (BIC) and the decision-theoretic performance-based (DT) approach
200 showed that HKY (Hasegawa *et al.* 1985) was the most appropriate substitution model for our
201 dataset. Using this model, the splits between the major phylogenetic clades were then dated using a
202 relaxed molecular clock method in BEAST. The widely-used Dowling *et al.* (2002) cyprinid *cytb*
203 divergence rate of 1.05% pairwise sequence divergence / MY was used after converting to a per
204 lineage value of 0.0053 mutations/site/MY for use in BEAST. We used a ‘coalescent: constant size’
205 tree prior, which assumes an unknown but constant population size backwards in time, as
206 recommended for intraspecific phylogenies (Drummond *et al.* 2012) . MCMC chain lengths were 1
207 $\times 10^7$ with samples taken every 1000 iterations. A gamma site heterogeneity model was used, with
208 the default of four categories. Substitution rates, rate heterogeneity and base frequencies were
209 unlinked between each codon position to allow substitution rate to vary between them. Default
210 values were used for all other parameters and priors.

211

212 *Population structure and diversity analyses using microsatellites*

213 Allele dropout and null alleles in the microsatellite data were tested using Microchecker (Van
214 Oosterhout *et al.* 2004). FSTAT v. 2.9.3.2 (Goudet 1995) was then used to check for linkage
215 disequilibrium (LD) between loci (using 10,000 permutations), deviations from Hardy-Weinberg
216 equilibrium (HWE) within populations (126500 permutations) and for all population genetic
217 summary statistics. Genetic diversity within populations was estimated using Nei’s estimator of
218 gene diversity (H_o) (Nei 1987) and Allelic richness (A_r), which was standardised to the smallest
219 sample size ($n = 4$) using rarefaction (Petit *et al.* 1998). Pairwise F_{ST} values were calculated
220 according to (Weir & Cockerham 1984) and 23520 permutations and sequential Bonferroni
221 correction were used to test for significance of F_{ST} .

222

223 IBD was investigated using a Mantel test in the adegenet v1.6 (Jombart & Ahmed 2011) package in
224 R v3.0.1 (R Core Team 2013). We then tested for an association between A_r and longitude and
225 latitude, which is predicted under a stepping-stone colonisation model (Ramachandran *et al.* 2005;
226 Simon *et al.* 2014), using linear regression analysis in R.

227

228 Population structure was then further examined using Discriminant Analyses of Principal
229 Components (DAPC) also in adegenet (DAPC, see SI text and Jombart *et al.* 2010 for more details).
230 DAPC has been shown to perform as well or better than the commonly used program,
231 STRUCTURE (Pritchard *et al.* 2000) for both simple and complex models of population structure
232 (Jombart *et al.* 2010). Furthermore, unlike STRUCTURE, DAPC is free of underlying assumptions
233 of Hardy-Weinberg equilibrium, which are likely to be violated when effective population sizes are
234 small, as is often the case in *C. carassius* (Hänfling *et al.* 2005).

235

236 In preliminary DAPC analysis using all 49 *C. carassius* populations, Sweden (SWE9) was found to
237 be so genetically distinct from the rest of the data set that it masked the variation between the other
238 populations. This population was therefore omitted from further DAPC analyses. To infer the
239 appropriate number of genetic clusters in the data, we used BIC scores (SI Fig. 5a), in all cases
240 choosing lowest number of genetic clusters from the range suggested. Spline interpolation
241 (Hazewinkel 1994) was then used to identify the appropriate number of principal components to use
242 in the subsequent discriminant analysis (SI Fig. 5a).

243

244 *RADseq data filtering and population structure analysis*

245 The quality of the RADseq raw read data was examined using FastQC (Andrews 2010), the dataset
246 was then cleaned, processed and SNPs were called using the Stacks pipeline v 1.19 (Catchen *et al.*
247 2011). Preliminary tests were carried out in order to identify optimal Stacks parameters (See SI
248 text). Final parameter values for the respective Stacks module were as follows; ustacks: M=2, m=8,

249 removal (-r) and deleveraging (-d) algorithms were also used; cstacks: N=2 (n populations = 18, n
250 individuals = 160); populations module: one SNP per RAD locus was used (--write_single_snp) and
251 SNPs were only retained if they were present in 70% of individuals ($r=0.7$) in at least 17 out of the
252 18 populations in the study ($p=17$), which allows for mutations in restriction sites that may cause
253 loci to dropout in certain lineages. All other parameters were kept at default values. Finally, we
254 filtered out loci which had a heterozygosity of > 0.5 and $F_{IS} < 0.0$ in one or more populations in
255 order to control for the possibility of erroneously merging ohnologs resulting from the multiple
256 genome duplications that have occurred the in *Cyprinus* and *Carassius* genera (Henkel *et al.* 2012;
257 Xu *et al.* 2014). The resulting refined SNP set was then used in subsequent phylogeographic
258 analyses. The R package Adegenet v. 1.42 was used to calculate H_o and pairwise F_{ST} , test for IBD
259 and genetic clusters were inferred using DAPC.

260

261 *Reconstructing postglacial colonisation routes in Europe*

262 DIYABC v. 2.0 (Windows, Cornuet *et al.* 2014) was used to reconstruct the most likely *C.*
263 *carassius* recolonisation routes through Europe after the last glacial maximum. We used the
264 RADseq data set for this analysis as it showed a much clearer pattern of population structure than
265 the microsatellite data in DAPC analyses (see Results). Furthermore, preliminary DIYABC
266 analyses using microsatellites failed to identify a scenario which was significantly more likely than
267 its counterparts, suggesting low power in this dataset for reconstructing complex phylogeographic
268 patterns over long timescales.

269

270 As DIYABC is a computationally intensive method, it was necessary to perform analyses on a
271 subset of 1000 randomly-selected SNP loci from the full RADseq dataset to reduce computation
272 time. This SNP subset was first analysed with DAPC to confirm that it produced the same
273 population structure as the full dataset and was then used to compare the likelihood of a number of
274 user defined colonisation scenarios (i.e. a specific population tree topology, together with the

275 parameter prior distributions that are associated with it). First, 1 million datasets were simulated for
276 each scenario. These simulated summary statistic datasets represented the theoretical expectation
277 under each scenario, and were compared to the same summary statistics calculated from the
278 observed data, in order to identify the most likely of the tested scenarios. In DIYABC, two methods
279 of comparison between simulated and observed datasets are used; logistic regression and “direct
280 approach”, the latter method identifies the scenario that produces the largest proportion of the n
281 number of closest scenarios to the observed, where n is specified by the user. The goodness-of-fit of
282 scenarios was also assessed using the model checking function implemented in DIYABC (Cornuet
283 *et al.* 2014). In all analyses, the single-sample summary statistics used were the mean and variance
284 of gene diversity across all polymorphic loci and the mean gene diversity across all loci. The two-
285 sample summary statistics used were the mean and variance of F_{ST} and Nei’s distance for loci with
286 F_{ST} greater than zero between two samples and the mean F_{ST} and Nei’s distance for all loci. Finally,
287 for scenarios including admixture events, the maximum likelihood estimates of admixture
288 proportions were also used. See Cornuet *et al.* (2014) for the exact equations used and their
289 implementation in DIYABC.

290

291 To reduce the number and complexity of possible scenarios, we split DIYABC analysis into three
292 stages (Table 2). In stage 1, we tested 11 broad scale scenarios (Scenarios 1 -11, SI Fig. 1).
293 Populations were grouped into three pools in order to reduce the number and complexity of possible
294 scenarios (Table 2); Pool 1 – all northern European populations (npops = 17, n = 155), Pool 2 – Don
295 population (npops = 1, n = 9), Pool 3 – Danubian population (npops = 1, n = 6). In six scenarios (1,
296 2, 8-11), northern European and the Don population diverged from each other more recently than
297 from Danubian populations. These scenarios differ in the patterns of effective population size
298 change and the presence or absence of a bottleneck. In scenarios 3 and 4, northern European and
299 Danubian populations are more closely related to each other than to the Don population. And in the
300 remaining three scenarios, one pool of populations is the product of an admixture event between the

301 other two. Population poolings and scenarios were both chosen on the basis of the broad
302 phylogeographic structure identified in the mtDNA and RADseq population structure analysis (see
303 Results).

304

305 In the second and third stages, we performed a finer scale analysis, focussing on the 17 northern
306 European populations alone. Populations were again pooled, this time into six groups, on the basis
307 of both population structure and geography (Table 2). In stage 2 we tested five scenarios (Scenarios
308 12-16, see SI Fig. 2a for graphical description of each scenario), with no bottlenecks included,
309 which represented the major topological variants that were most likely, given population structure
310 results from DAPC. We then identified the most likely of these scenarios in DIYABC and took this
311 forward into the final stage of the analysis where we tested 6 multiple bottleneck combinations (SI
312 Fig. 2b) around this scenario. This three stage approach allowed us to systematically build a
313 complex scenario for the European colonisation of *C. carassius*. Finally, we used the posterior
314 distributions of the time parameters, simulated using the scenario identified as most likely in stages
315 one and three, to estimate the times of the major lineage splits in European *C. carassius*. These
316 parameters, calculated by DIYABC in generations, were converted to years using an average
317 generation time of 2 years (Tarkan *et al.* 2010).

318

319 *Comparison of microsatellite and RADseq data*

320 Finally, we compared the results derived from population structure analyses on microsatellite and
321 RADseq data to assess their suitability for addressing our phylogeographic question. It is important
322 to note that differences between the full microsatellite and RADseq datasets could be attributable to
323 one or a combination of the following; the number of populations, the geographic distribution of
324 populations, the number of samples per population, the number of markers, or the information
325 content of the marker type. To disentangle these sources of variation, we created two microsatellite

326 data subsets; M2, which included only individuals used in RADseq, (excluding three individuals for
327 which microsatellite data was incomplete, $n = 146$, npops = 19), and M3, which contained all
328 individuals for which microsatellite data was available in populations that were used in RADseq (n
329 = 313, npops = 19);

For Review Only

330 Table 3). This gave us three pairs of datasets for comparison: 1) RADseq Vs. M2: same individuals
331 but different marker types, 2) M1 vs M2: full microsatellite dataset versus a subset of the
332 populations, and 3) M2 vs M3: same populations but different number of individuals per
333 population. This strategy enabled us to test for the influence of marker, sampling of populations and
334 individuals per population respectively. Comparisons were performed between datasets on
335 heterozygosities and pairwise F_{ST} s using both Pearson's product-moment correlation coefficient and
336 paired Student's t-tests in R. IBD results were compared using Mantel tests (Jombart & Ahmed
337 2011), and DAPC results were compared on the basis of similarity of number of inferred clusters
338 and cluster sharing between populations.

339

340 Results

341 *Phylogenetic analyses of mitochondrial data*

342 The combined 1090 bp alignment of 100 *cytb* *C. carassius* mtDNA sequences yielded 22
343 haplotypes, which were split across two well supported and highly differentiated phylogenetic
344 lineages (Fig. 2, SI Table 3). Lineage 1 was found in all northern European river catchments
345 sampled, as well as eastern European (Dnieper) and southeastern European (Don and Volga)
346 catchments, whereas Lineage 2 was almost exclusively confined to the River Danube catchment.
347 There were, however, a few exceptions to this clear geographical split; two individuals, one from
348 the Elbe and one from the Rhine in northern Germany, belonged to mtDNA Lineage 2, as did one
349 individual from the River Lahn river catchment in western Germany. Also one population in the
350 Czech Republic, located on the border between the Danube and Rhine river catchments, was found
351 to contain individuals belonging to lineages 1 and 2.

352

353 The mean number of nucleotide differences within lineages 1 and 2 was 2.25 and 2.00, respectively,
354 which equated to a sequence divergence 0.2% and 0.18%, respectively. Between the two lineages

355 there was an average of 22.5 nucleotide differences (2.06% mean sequence divergence), with 19 of
356 these being fixed. BEAST molecular clock analysis dated the split between lineages 1 and 2 to be
357 1.30–3.22 million years ago (MYA), with a median estimate of 2.15 MYA (Fig. 2).

358

359 *Nuclear marker datasets and quality checking*

360 Microchecker showed no consistent signs of null alleles or allele dropout in microsatellite loci and
361 no significant LD was found between any pairs of loci. No populations showed significant deviation
362 from Hardy-Weinberg proportions (adjusted nominal level 0.0009).

363

364 After filtering raw RADseq data, *de novo* construction of loci across the 19 populations produced
365 35 709 RADseq loci that were present in at least 70% of individuals in at least 17 populations.

366 These loci contained a total of 29 927 polymorphic SNPs (approx. 0.84 SNPs per locus). Only the
367 first SNP in each RADseq locus was retained, to avoid confounding signals of LD. This yielded a
368 total of 18 908 loci with a mean coverage of 29.07 reads (SI Fig. 3b). Finally 5719 of these SNP
369 loci were filtered out due to high (> 0.5) heterozygosity and/or F_{IS} of < 0.0 in at least one
370 population. In doing so, we removed many high coverage tags (SI Fig. 3a), which was consistent
371 with over-merged ohnologs having higher coverage (*i.e.* reads from more than two alleles) than
372 correctly assembled loci. The final dataset therefore contained 13189 SNP loci, with a mean
373 coverage of 27.72 reads.

374

375 *Within population diversity at nuclear loci*

376 Observed heterozygosity (H_o), averaged across all microsatellite loci within a population, ranged
377 from 0.06 (SWE9) to 0.44 (BLS), with a mean of 0.25 across all populations (SD = 0.105), and was
378 highly correlated with A_r ($t = 19.67$, $P < 0.001$, $df = 40$), which ranged from 1.26 (FIN1) to 2.96

379 (POL3) with a mean of 1.92 (SD = 0.51). Mean H_o averaged across all RADseq loci for all
380 populations was 0.013 (SD = 0.013), ranged from 0.001 to 0.057 and was significantly correlated
381 with H_o from microsatellite loci at populations shared between both datasets ($r = 0.69$, $t = 3.74$, $P =$
382 0.002 , $df = 15$). Microsatellite A_r significantly decreased along an east to west longitudinal gradient
383 (adj. $R^2 = 0.289$, $P < 0.001$, SI Fig. 4b) consistent with decreasing diversity along colonisation
384 routes. However, A_r did not decrease with increasing latitude (adj $R^2 = -0.007$, $P = 0.414$, SI Fig. 4a).
385 We also repeated this analysis after removing samples from mtDNA Lineage 2 in the Danube
386 catchment. Again there was no relationship between A_r and latitude ($R^2 = -0.023$, $P = 0.254$, SI Fig.
387 4c), but the relationship between A_r and longitude was strengthened (adj. $R^2 = 0.316$, $P < 0.001$, SI
388 Fig. 4d).

389

390 *Population Structure in Europe based on nuclear markers*

391 Population structure was strong, as predicted. Using the full (M1) microsatellite dataset, mean
392 pairwise F_{ST} was 0.413 (min = 0.0; BEL2 and BEL3), max = 0.864 (NOR2 vs GBR2), with 861 of
393 the 1128 pairwise population comparisons being significant F_{ST} ($P < 0.05$, SI Table 4). Pairwise F_{ST}
394 calculated from the RADseq dataset also showed strong structure (SI Table 5), ranging from 0.067
395 (DEN1, DEN2) to 0.699 (NOR2, GBR4), and these values were highly correlated with the same
396 population comparisons in the M3 microsatellite dataset ($r = 0.66$, $t = 9.01$, $P < 0.01$, $df = 104$).

397

398 BIC scores obtained from initial DAPC analyses of the microsatellite dataset, using all 49
399 populations, indicated that between 11 and 19 genetic clusters (SI Fig. 5a) would be an appropriate
400 model of the variation in the data. As a conservative estimate of population structure, we chose 11
401 clusters for use in the discriminant analysis, retaining eight principal components as recommended
402 by the spline interpolation a-scores (SI Fig. 5a). This initial analysis showed that populations
403 belonging to Cluster 10 (RUS1, Don river catchment) and Cluster 11 (GER3, GER4, CZE1,

404 Danubian catchment) were highly distinct from clusters found in northern Europe (Fig. 1b). Since
405 the marked genetic differentiation between these three main clusters masked the more subtle
406 population structure among northern European populations (see Fig. 1b), we repeated the DAPC
407 analysis without the populations from the Danube and Don (RUS1, GER3, GER4, CZE1, Fig. 1b).
408 The results of this second DAPC analysis revealed an IBD pattern of population structure, across
409 Europe (Fig. 1). Mantel tests excluding the Danubian and Don populations corroborated these
410 results; showing significant correlation with geographic distance in northern Europe (adjusted $R^2 =$
411 0.287 , $P < 0.001$, SI Fig. 6a), with Danubian populations shown to be more diverged than their
412 geography would predict (data not shown).

413

414 In the RADseq DAPC analysis, BIC scores suggested between four and ten genetic clusters, a lower
415 number than that inferred from the microsatellite data set. Again we chose the lowest number of
416 suggested clusters (four) clusters to take forward in the analysis (SI Fig. 5b). Following spline
417 interpolation, we retained six principal components and kept two of the linear discriminants from
418 the subsequent discriminant analysis (SI Fig. 5b). The inferred population structure showed that the
419 Danubian population (HUN2) and the Don population (RUS1) were highly diverged from the
420 northern European clusters. Unfortunately, HUN2 is not present in the microsatellite dataset for
421 direct comparison, however both datasets, and the mtDNA data show the same pattern of high
422 divergence between northern Europe and Danubian populations. DAPC analyses of RADseq data
423 again showed an IBD pattern in northern European populations, which was confirmed with Mantel
424 tests when the Danubian population HUN2 was excluded (adjusted $R^2 = 0.722$, $P < 0.001$; SI Fig.
425 6b).

426

427 *Postglacial recolonisation of C. carassius in Europe*

428 DAPC results of the 1000 SNP RADseq dataset used in DIYABC showed that it produced the same
429 population structure as the full RADseq dataset (SI Fig. 7). For the broad-scale scenario tests in
430 stage one of the DIYABC analysis, both logistic regression and direct approach identified Scenario
431 9 as being most likely to describe the true broad-scale demographic history (SI Fig. 8). Model
432 checking showed that the observed summary statistics for our data fell well within those of the
433 posterior parameter distributions for scenario 9 (SI Fig. 8c). Scenario 9 agrees with the mtDNA
434 results, suggesting that the Danubian populations have made no major contribution to the
435 colonisation of northern Europe. The median posterior distribution estimate of the divergence time
436 between Danubian and northern European populations is 2.18 MYA (95% CI = 1.03 – 5.12 MYA),
437 assuming a two-year generation time (Tarkan *et al.* 2010)), which is strikingly similar to that of
438 mtDNA dating analysis. Scenario 9 also suggests that the northern European populations
439 experienced a population size decline after the split of Pool 1 from the population in the Don river
440 catchment, which lasted approximately 8920 years (95% CI = 616 – 13700 years) and reduced N_e
441 by 32%.

442

443 In stage two of the DIYABC analysis, we tested the major variant scenarios for the colonisation of
444 northern Europe. In assessing the relative probabilities of scenarios, there was some discrepancy
445 between the direct approach, which revealed Scenario 14 to be most likely, and the logistic
446 regression, which favoured Scenario 13 (with Scenario 14 being the second most likely). However,
447 the goodness-of-fit model checking showed that the observed dataset fell well within the posterior
448 parameter distributions for Scenario 14 (SI Fig. 9a), but not for Scenario 13 (not shown). Therefore,
449 Scenario 14 was carried forward into stage three in which we tested six more scenarios (SI Fig. 2b)
450 to compare combinations of bottlenecks using the same population tree topology as in Scenario 14.
451 Direct approach, logistic regression and model checking all found scenario 14d to be the most likely
452 (SI Fig. 9b), we therefore accepted this as the scenario for the colonisation of *C. carassius* in

453 northern Europe (SI Fig. 9b). This scenario infers an initial split between two sub-lineages in
454 northern Europe approximately 33 600 YBP (Fig. 4), one of which re-colonised northwest Europe
455 and one that re-colonised Finland through the Ukraine and Belarus. Scenario 14d also inferred a
456 secondary contact between these sub-lineages approximately 15 940 YBP, resulting in the
457 populations currently present in Poland; these admixed populations provided the source of one
458 colonisation across the Baltic into Sweden, and a second route was inferred into southern Sweden
459 from Denmark (Table 3, SI Fig. 9b).

460

461 *Comparing microsatellite datasets and RAD sequencing data*

462 The results from the RADseq ($n = 149$, npops = 16) dataset and the full microsatellite dataset (M1,
463 $n = 848$, npops = 49) largely agreed on the inferred structure and cluster identity of populations.
464 However, there were some important differences between them. Firstly, the IBD pattern of
465 population structure in northern Europe was much stronger in the RADseq data ($R^2 = 0.722$, $P <$
466 0.001 , SI Fig. 6) compared to the M1 dataset ($R^2 = 0.287$, $P < 0.001$, excluding Danubian
467 populations and SWE9 from both datasets, SI Fig. 6). Secondly, clusters inferred by the RADseq
468 DAPC analysis are much more distinct, *i.e.* there is much lower within-cluster, and higher between-
469 cluster variation in the RADseq results than in the M1 dataset results (Fig. 3).

470

471 As the properties of the RADseq and M1 datasets differ in four respects, namely marker type,
472 number of populations, number of samples per population (Table 3) and uniformity of sampling
473 locations, (SI Fig. 10) it was not possible to identify the cause of discrepancies in their results.
474 Therefore, below we report the results from the pair-wise dataset comparisons, which isolate the
475 effects of these parameter differences.

476

477 1) *M1 Vs. M3*: the effect that the number of populations and the uniformity of sampling locations
478 might have on inferred population structure. The geographic distribution of sampling locations was
479 more clustered in M1 (full microsatellite dataset) than in M3 (containing microsatellite for samples
480 in populations used in RADseq (SI Fig. 10), and IBD patterns were considerably stronger in the M3
481 subset (adj. $R^2 = 0.447$, $P < 0.001$) than in the full M1 dataset (adj. $R^2 = 0.287$, $P < 0.001$). In
482 contrast DAPC results were very similar between datasets, with inferred cluster number, structure
483 and population identity of clusters generally agreeing well (Fig. 1, Fig. 3c).

484

485 2) *M2 Vs. M3*: the effect of reducing the number of samples per population on the inferred
486 population structure. The number of samples per population in the M2 subset (microsatellite data
487 only for the samples used in RADseq, mean = 9.125 ± 0.8) was significantly lower than that of the
488 M3 subset (mean, 19.6 ± 9.0 , $t = -4.66$, $df = 15$, $P < 0.001$), as was the number of alleles per
489 population (M2 mean = 24.4 ± 7.3 , M3 mean = 27.4 ± 8.1 , $t = -5.72$, $df = 15$, $P < 0.001$). Population
490 heterozygosities were significantly different between M2 and M3 (M2 mean = 0.21, M3 mean =
491 0.23, $t = -2.4$, $df = 15$, $P = 0.012$), but highly correlated ($r = 0.94$, $t = -11.13$, $P < 0.001$, $df = 15$).
492 Pairwise F_{ST} s were very strongly correlated ($r = 0.97$, $t = 46.26$, $P < 0.001$, $df = 105$), but again, still
493 significantly different between the two datasets (M2 mean = 0.46, M3 mean = 0.49, $t = -6.21$, $P <$
494 0.001 , $df = 15$, Table 4). The patterns of IBD were almost identical for M2 ($R^2 = 0.455$, $P < 0.001$)
495 and M3 ($R^2 = 0.447$, $P < 0.001$, SI Fig. 6) and population structure inferred by DAPC was again
496 similar. BIC scores suggested a similar range of cluster number for M2 and M3, the smallest of
497 which was nine in both cases.

498

499 3) *RADseq Vs. M3*: The effect of the number and the type of markers used on the phylogeographic
500 results. We compared the results from the RADseq and M2 datasets, which contain exactly the
501 same samples (with the exception of three individuals missing in M2). Significant correlations were
502 again found between heterozygosities estimated for the two datasets ($r = 0.69$, $t = 3.73$, $P = 0.002$,

503 $df = 15$) and pair-wise F_{ST} s ($r = 0.70$, $t = 10.09$, $P < 0.001$, $df = 105$), but RADseq data yielded
504 much lower pairwise F_{ST} s (mean RAD = 0.29, mean M2 = 0.46, $t = 13.74$, $P < 0.001$, $df = 15$).
505 DAPC analysis of RADseq data resolved populations into much more distinct clusters (Figs. 3a,
506 3b), and the IBD pattern found was considerably stronger in the RADseq ($R^2 = 0.722$, $P < 0.001$)
507 dataset compared to M2 ($R^2 = 0.455$, $P < 0.001$, SI Fig. 6).

508

509 Discussion

510 In this study, we aimed to simultaneously produce a phylogeographic framework on which to base
511 conservation strategies for *C. carassius* in Europe, and compare the relative suitability of genome-
512 wide SNP markers and microsatellite markers for such an undertaking. Through comparison of the
513 inferred population structure from microsatellite and genome-wide SNP data, we show that there
514 are important differences in the results from each data type, attributable predominantly to marker
515 type, rather than within population sampling or spatial distribution of samples. However, despite
516 these differences, all three data types used (mitochondrial, microsatellite and SNP data) agree that,
517 unlike many other European freshwater fish for which phylogeographic data is available, *C.*
518 *carassius* has not been able to cross the Danubian catchment boundary into northern Europe. This
519 has resulted in two, previously unknown, major lineages of *C. carassius* in Europe, which we argue
520 should be considered as separate conservation units.

521

522 *Phylogeography and postglacial recolonisation of C. carassius in Europe*

523 The most consistent result across all three marker types (mtDNA sequences, microsatellites and
524 RADseq) was the identification of two highly-divergent lineages of *C. carassius* in Europe. The
525 distinct geographic distribution of these lineages; Lineage 1 being widely distributed across north
526 and eastern Europe and Lineage 2 generally only in the River Danube catchment, indicates a long-

527 standing barrier to gene flow between these geographic regions. Bayesian inference based on
528 mtDNA phylogeny and ABC analysis of RADseq data showed remarkable agreement, estimating
529 that these lineages have been isolated for 2.15 MYA (95% CI = 1.30–3.22) and 2.18 (95% CI = 2 –
530 6.12) MYA respectively, which firmly places the event at the beginning of the Pleistocene (2.6
531 MYA; (Gibbard & Head 2009). This pattern differs substantially from the general phylogeographic
532 patterns observed in other European freshwater fish. Indeed, previous studies have shown that the
533 Danube catchment has been an important source for the postglacial recolonisation of freshwater fish
534 into northern Europe or during earlier interglacials in the last 0.5 MYA. For example, bullhead
535 *Cottus gobio* (Hänfling & Brandl 1998; Hänfling *et al.* 2002), chub *Leuciscus cephalus* (Durand *et*
536 *al.* 1999), Eurasian perch *Perca fluviatilis* (Nesbø *et al.* 1999), riffle minnow *Leuciscus souffia*
537 (Salzburger *et al.* 2003), grayling *Thymallus thymallus* (Gum *et al.* 2009), European barbel *Barbus*
538 *barbus* (Kotlík & Berrebi 2001), and roach *Rutilus rutilus* (Larmuseau *et al.* 2009) all crossed the
539 Danube catchment boundary into northern drainages such as those of the rivers Rhine, Rhône and
540 Elbe during the mid-to-late Pleistocene. The above species occur in lotic habitats, and most are
541 capable of relatively high dispersal. In contrast *C. carassius* has a very low propensity for dispersal,
542 and a strict preference for the lentic backwaters, isolated ponds and small lakes (Holopainen *et al.*
543 1997; Culling *et al.* 2006; Copp 1991). We therefore hypothesise that these ecological
544 characteristics of *C. carassius* have reduced its ability to traverse the upper Danubian watershed,
545 which lies in a region characterised by the Carpathian Mountains and the Central European
546 Highlands. This region may have acted as a barrier to the colonisation of *C. carassius* into northern
547 European drainages during the Pleistocene. It should be noted, however, that the phylogeography of
548 two species, the spined loach *Cobitis taenia* and European weatherfish *Misgurnus fossilis*, does not
549 support this hypothesis as a general pattern for floodplain species (Janko *et al.* 2005; Culling *et al.*
550 2006). The former is the only species that we know of other than *C. carassius* showing long-term
551 isolation between the Danube and northern European catchments, but has lotic habitat preferences
552 and good dispersal abilities (Janko *et al.* 2005; Culling *et al.* 2006), whereas the latter inhabits

553 similar ecosystems as *C. carassius*, with low dispersal potential, but has colonised northern Europe
554 from the Danube catchment (Bohlen *et al.* 2006, 2007).

555

556 There is one notable exception to the strict separation between Danubian and northern European *C.*
557 *carassius* populations. The population CZE1, located in the River Lužnice catchment (Czech
558 Republic), which drains into the River Elbe, clusters with Danubian populations in both the
559 microsatellite and mtDNA data. This sample site, from the River Lužnice, is very close to the
560 Danubian catchment boundary and is situated in a relatively low lying area. Therefore, some recent
561 natural movements across the watershed between these river catchments, either through river
562 capture events or ephemeral connections, could have been possible. A similar pattern has been
563 shown in some European bullhead *Cottus gobio* populations along the catchment Danube/Rhine
564 catchment border (Riffel & Schreiber 1995). We also observed the presence of two mtDNA
565 haplotypes from Lineage 2 in some individuals from northern German populations (GER1, GER2,
566 GER8), however, one of these haplotypes was shared with Danubian individuals and the results
567 were not confirmed by nuclear markers. Overall this is most likely to be the result of occasional
568 human mediated long-distance dispersal for the purposes of intentional stocking.

569

570 Population structure within Lineage 1 is characterised by a pattern of IBD and a loss of allelic
571 richness from eastern to western Europe. This is consistent with the most likely colonisation
572 scenario identified by the DIYABC analysis, indicating a general southeast to northwest expansion
573 from the Ponto-Caspian region towards central and northern Europe (Fig. 4). The Ponto-Caspian
574 region, and in particular the Black Sea basin, was an important refugium for freshwater fishes
575 during the Pleistocene glacial cycles, and a similar colonisation route has been inferred for many
576 other freshwater species in northern Europe (Nesbø *et al.* 1999; Durand *et al.* 1999; Culling *et al.*
577 2006; Costedoat & Gilles 2009). The DIYABC analysis also suggests that there was an interval of >
578 200 000 years between the split of the Don population (\approx 270 000 years ago) and the next split in

579 the scenario (approx. 33 600 years ago), which marks the main expansion across central and
580 northern Europe. It appears that no further population divergence can be dated back to the time
581 interval between the Riss/Saalian and the Würm/Weichelian glacial periods. This may be because
582 the range of *C. carassius* has not undergone a major change during that time interval, but it is more
583 likely that the signal of expansion during the Riss-Würm interglacial has been eradicated through a
584 subsequent range contraction during the Würm/Weichelian glacial period. The model also suggests
585 that the Würm/Weichelian period was accompanied by a sustained but moderate reduction in
586 population size over almost 9000 years (Bottleneck A, Fig. 4), which may reflect general population
587 size reductions during the Riss glaciations or a series of shorter bottlenecks during subsequent range
588 expansion (Ramachandran et al. 2005, Simon et al 2015, Hewitt 2000).

589

590 DIYABC analyses inferred the colonisation of northern Europe by two sub-lineages within the
591 mtDNA Lineage 1, which were isolated from each other approximately 33 600 years ago. These
592 sub-lineages may reflect two glacial refugia resulting from the expansion of the Weichselian ice cap
593 to its maximum extent roughly 22 000 years ago (see hypothetical refugia II and III in Fig. 4). The
594 western sub-lineage underwent a second long period of population decline (Bottleneck B, Fig. 4),
595 which may again represent successive founder effects during range expansion. There is then
596 evidence of secondary contact between these sub-lineages (node b, approximately \approx 15 940 years
597 ago), contributing to the genetic variation now found in Poland. This inferred admixture event may
598 represent one of the numerous inundation and drainage capture events, which resulted from the
599 melting of the Weichselian ice cap, that are known to have occurred around this time (Grosswald
600 1980; Gibbard *et al.* 1988; Arkhipov *et al.* 1995). However, as the colonisation of Europe was
601 likely to have occurred via the expansion of colonisation fronts (*i.e.* dashed contour lines in Fig. 4),
602 rather than along linear paths, it could also be indicative of the known IBD gradient between the
603 inferred western and eastern sub-lineages. Such a gradient (eg. between northwestern and

604 northeastern Europe) may give false signals of admixture between intermediate populations, such as
605 those in Poland.

606

607 The colonisation of the Baltic sea basin also seems to have been complex, with three independent
608 routes inferred by DIYABC scenario 14d; one recent route through Denmark into southern Sweden,
609 one to the east of the Baltic Sea, through Finland, and one across the Baltic Sea, from populations
610 related to those in Poland (Pool 4). The first of these agrees well with the findings of Janson *et al.*
611 (2014), whereby populations, including SWE8 from our study (SK3P in Janson *et al.* 2014), in this
612 region were found to be distinct from those in central Sweden. The eastern route shows similarities
613 to the colonisation patterns of *P. fluviatilis*, which is hypothesised to have had a refugium east of
614 Finland (Nesbø *et al.* 1999) during the most recent glacial period. This is certainly also plausible in
615 *C. carassius* and may account for the distinctiveness of Finnish populations seen in microsatellites
616 and RADseq DAPC analysis. The last colonisation route, across the Baltic Sea from mainland
617 Europe, may have coincided with the freshwater Lake Ancyclus stage of the Baltic Sea's evolution,
618 which existed from $\approx 10\,600$ to $7\,500$ years ago (Björck 1995; Kostecki 2014). The Lake Ancyclus
619 stage likely provided a window for the colonisation of many of the species now resident in the
620 Baltic, and has been proposed as a possible window for the colonisation of *T. thymallus* (Koskinen
621 *et al.* 2000), *C. taenia*, (Culling *et al.* 2006), *C. gobio* (Kontula & Väinölä 2001) and four
622 *Coregonus* species (Svärdson 1998). Consistent with this, we found strong similarity between
623 populations from Fasta Åland, southern Finland and central Sweden, suggesting that shallow
624 regions in the central part of Lake Ancyclus (what is now the Åland Archipelago), may have
625 provided one route across Lake Ancyclus.

626 It is also likely that the contemporary distribution of *C. carassius* in the Baltic has been influenced
627 by human translocations. *C. carassius* were often used as a food source in monasteries in many
628 parts of Sweden (Janson *et al.* 2014), and the Baltic island of Gotland (Rasmussen 1959; Svanberg
629 *et al.* 2013) was an important trading port of the Hanseatic League – a commercial confederation

630 that dominated trade in northern Europe from the 13th to 17th centuries. Previous data suggest that
631 *C. carassius* was transported from the Scania Province, southern Sweden, where *C. carassius*
632 aquaculture was common at least during the 17th century, to parts further north (Svanberg *et al.*
633 2013; Janson *et al.* 2014).

634

635 *Implications for the conservation of C. carassius in Europe*

636 The two *C. carassius* lineages exhibit highly-restricted gene flow between them and are the highest
637 known organisational level within the species. They therefore meet the genetic criteria for
638 Evolutionarily Significant Units (ESUs) as described in (Fraser & Bernatchez 2001). This is
639 especially important in light of the current *C. carassius* decline in the Danubian catchment
640 (Bănărescu 1990; Navodaru *et al.* 2002; Lusk *et al.* 2010; Savini *et al.* 2010). The conservation of
641 *C. carassius* in central Europe must therefore take these catchment boundaries into consideration, as
642 opposed to political boundaries. A first step would be to include *C. carassius* in Red Lists, not only
643 for individual countries, but at the regional (e.g. European Red List of Freshwater Fishes; (Freyhof
644 & Brooks 2011) and global (IUCN 2015) scales, and we hope that the evidence presented here will
645 facilitate this process. Within the northern European lineage, the Baltic Sea basin shows high levels
646 of population diversity, likely owing to its complex colonisation history. As such, the Baltic
647 represents an important part of the *C. carassius* native range. Although *C. carassius* is not currently
648 thought to be threatened in the Baltic region, *C. gibelio* is invading this region and is considered a
649 threat (Urho & Lehtonen; Deinhardt 2013).

650

651 *Microsatellites vs RADseq for phylogeography*

652 Broad conclusions drawn from each of our RADseq-derived SNPs, full or partial microsatellite
653 datasets are consistent, demonstrating deep divergence between northern and southern European
654 populations and an IBD pattern of population structure in northern Europe. This similarity in spatial
655 signal between marker types was also observed by (Bradbury *et al.* 2015). However, two striking
656 differences exist in the phylogeographic results produced by RADseq compared to those of the
657 microsatellite datasets. Firstly, the IBD pattern inferred from RADseq data was considerably
658 stronger than for any of the microsatellite datasets. This effect was also found by Coates *et al.*
659 (2009) when comparing SNPs and microsatellites, who postulated that it was driven by the
660 differences in mutational processes of the markers. The second major difference between RADseq
661 and microsatellite results was that clusters inferred by DAPC from the RADseq data were
662 considerably more distinct compared to the full microsatellite dataset, emphasising the fine scale
663 structure in the data (which is particularly apparent in the northern Finnish populations). We ruled
664 out the possibility of these differences being caused by the reduction in number of populations, their
665 spatial uniformity or number of individuals per population used in RADseq by creating two partial
666 microsatellite datasets and comparing these to results from the RADseq-SNPs. Differences between
667 marker types were consistently reproducible whether full or partial microsatellite datasets were used
668 in the analyses.

669

670 It is also worth noting that the number of populations or the number of samples per population had
671 no apparent impact on IBD and DAPC results between the microsatellite datasets. This is in contrast
672 to predictions of patchy sampling of IBD made by Schwartz and McKelvey (2009), perhaps
673 because of the strong population structure in *C. carassius*, and likelihood that a sufficiently
674 informative number of populations was included even in the reduced datasets.

675

676 SNP loci provide several advantages over microsatellites additional to those highlighted here. SNPs
677 are more densely and evenly distributed across the genome (Xing *et al.* 2005) and have been shown
678 to display lower error rates during genotyping (Montgomery *et al.* 2005). For example, Morin *et al.*
679 (2009a) showed that HW proportions are very sensitive to microsatellite genotyping errors. SNPs
680 also lend themselves to a plethora of evolutionary applications, including the identification of
681 outlier loci (Hohenlohe *et al.* 2012) or small regions of introgression in the genome (Hohenlohe *et al.*
682 *et al.* 2013). Lastly, SNPs are also much less susceptible to homoplasy than microsatellites (Morin *et al.*
683 *et al.* 2004). Van Oppen *et al.* (2000) found evidence of homoplasy in 10 out of 13 microsatellite loci,
684 which had accumulated in approximately 700,000 years and Cornuet *et al.* (2010) show that such
685 homoplasy makes microsatellites unreliable and error prone when used in DIYABC for inference
686 over long time scales. For these reasons, SNPs have a clear advantage over microsatellites for the
687 purposes of characterising population divergence over long time scales. This may explain why
688 preliminary microsatellite analyses in DIYABC showed insufficient power to identify a most likely
689 colonisation scenario.

690

691 *Conclusions*

692 We have identified the most likely routes of post-glacial colonisation in *C. carassius*, which deviate
693 from the general patterns observed in other European freshwater fishes. This has resulted in two,
694 previously-unidentified major lineages in Europe, which future broad-scale monitoring and
695 conservation strategies should take into account.

696

697 Although our RADseq sampling design included only 17.6% of samples included in the full
698 microsatellite dataset this was sufficient to produce a robust phylogeography in agreement with the
699 microsatellite dataset, and emphasised the fine scale structure among populations. We therefore

700 conclude that, if made to choose between the comprehensively sampled microsatellite approach or
701 the RADseq approach with fewer samples but many more loci, the RADseq approach presents the
702 better option for the phylogeography of *C. carassius*, with the huge number of SNP loci
703 overcoming the limitations imposed by reduced sample number. We also predict that this will hold
704 true for systems with similar genetic characteristics to ours, *i.e.* strong population structure
705 characterised by IBD.

706

707 **Acknowledgements**

708 The authors thank the FSBI (www.fsbi.org.uk) and Cefas (Lowestoft, UK) for funding the PhD of
709 DLJ in which this research was performed. Additionally KHO received financial support from The
710 Foundation for Baltic and Eastern European Studies (Östersjöstiftelsen). We thank the following
711 landowners, and contributors of fish tissue; Keith Wesley, Ian Patmore and Dave Emson (England),
712 L. Urho (Helsinki, Finland), M. Himberg (Salo, Finland), J. Krekula (Steninge Castle, Uppland,
713 Sweden), B.-M. Josephson and G. Josephson (Styrstad Vicarage, Sweden), G. Hellström (Umeå
714 University, Sweden), K.Ø. Gjelland (NINA, Tromsø, Norway), N. Hellenberg (Gotland Island,
715 Sweden), A. Tuvikene (Center for Limnology, Tartu, Estonia), S.V. Mezhzherin (Kiev, Ukraine),
716 K. Lindström (Kvicksund, Sweden), K.-J. Dahlbom and G. Sundberg (Åland Island, Finland), O.
717 Sandström and M. Andersson (Skutab, Öregrund, Sweden), B. Tengelin (Structor Miljöteknik AB),
718 A. Olsén-Wannefjord (Uppsala, Sweden), Müller Tamás (Godollo, Hungary), András Weiperth
719 (Hungary), Peter D Rask Møller and Henrik Carl (Copenhagen, Denmark), Oksana Stoliar,
720 (Ternopil, Ukraine), Manuel Deinhardt (Jyväskylä, Finland), Filip Volckaert and Greg Maes
721 (Leuven, Belgium).

722

723 **References**

- 724 Andrews S (2010) *FastQC: a quality control tool for high throughput sequence data*. Babraham
725 Bioinformatics. Available at www.bioinformatics.babraham.ac.uk/projects/fastqc.
- 726 Arkhipov SA, Ehlers J, Johnson RG, Wright HE Jr (1995) Glacial drainage towards the
727 Mediterranean during the Middle and Late Pleistocene. *Boreas*, **24**, 196–206.
- 728 Balkenhol N, Landguth EL (2011) Simulation modelling in landscape genetics: on the need to go
729 further. *Molecular ecology*, **20**, 667–670.
- 730 Bernatchez L, Wilson CC (1998) Comparative phylogeography of Nearctic and Palearctic fishes.
731 *Molecular ecology*, **7**, 431–452.
- 732 Bianco P (1990) Potential role of the palaeohistory of the Mediterranean and Paratethys basins on
733 the early dispersal of Euro-Mediterranean freshwater fishes. *Ichthyological exploration of*
734 *freshwaters*, **1**, 167 - 184
- 735 Björck S (1995) A review of the history of the Baltic Sea, 13.0-8.0 ka BP. *Quaternary*
736 *international: the journal of the International Union for Quaternary Research*, **27**, 19–40.
- 737 Bohlen J, Šlechtová V, Bogutskaya N, Freyhof J (2006) Across Siberia and over Europe:
738 Phylogenetic relationships of the freshwater fish genus *Rhodeus* in Europe and the phylogenetic
739 position of *R. sericeus* from the River Amur. *Molecular phylogenetics and evolution*, **40**, 856–865.
- 740 Bohlen J, Šlechtová V, Doadrio I, Ráb P (2007) Low mitochondrial divergence indicates a rapid
741 expansion across Europe in the weather loach, *Misgurnus fossilis* (L.). *Journal of fish biology*, **71**,
742 186–194.
- 743 Bănărescu P (1990) *Zoogeography of Fresh Waters. Vol. 1. General Distribution and Dispersal of*
744 *Freshwater Animals*. Aula-Verlag, Wiesbaden.

- 745 Bănărescu P (1992) *Zoogeography of fresh waters. Vol. 2. Distribution and dispersal of freshwater*
746 *animals in North America and Eurasia*. Aula-Verlag, Wiesbaden.
- 747 Bradbury IR, Hamilton LC, Dempson B *et al.* (2015) Transatlantic secondary contact in Atlantic
748 Salmon, comparing microsatellites, a single nucleotide polymorphism array and restriction-site
749 associated DNA sequencing for the resolution of complex spatial structure. *Molecular Ecology* **24**,
750 5130–5144.
- 751 Catchen J, Hohenlohe PA, Bassham S, Amores A, Cresko WA (2013) Stacks: an analysis tool set
752 for population genomics. *Molecular ecology*, **22**, 3124–3140.
- 753 Coates BS, Sumerford DV, Miller NJ *et al.* (2009) Comparative performance of single nucleotide
754 polymorphism and microsatellite markers for population genetic analysis. *The Journal of heredity*,
755 **100**, 556–564.
- 756 Copp GH (1991) Typology of aquatic habitats in the great ouse, a small regulated lowland river.
757 *Regulated Rivers: Research & Management*, **6**, 125–134.
- 758 Copp G, Sayer C (2010) *Norfolk Biodiversity Action Plan–Local Species Action Plan for Crucian*
759 *Carp (Carassius carassius)*. *Norfolk Biodiversity Partnership Reference: LS/3*. Fisheries &
760 Aquaculture Science, Lowestoft.
- 761 Copp G, Tarkan S, Godard M, Edmonds N, Wesley K (2010) Preliminary assessment of feral
762 goldfish impacts on ponds, with particular reference to native crucian carp. *Aquatic invasions*, **5**,
763 413–422.
- 764 Copp GH, Černý J, Kováč V (2008) Growth and morphology of an endangered native freshwater
765 fish, crucian carp *Carassius carassius*, in an English ornamental pond. *Aquatic conservation:*
766 *marine and freshwater ecosystems*, **18**, 32–43.

- 767 Cornuet JM, Luikart G (1996) Description and power analysis of two tests for detecting recent
768 population bottlenecks from allele frequency data. *Genetics*, **144**, 2001–2014.
- 769 Cornuet JM, Ravigne V, Estoup A (2010) Inference on population history and model checking
770 using DNA sequence and microsatellite data with the software DIYABC (v1.0). *BMC*
771 *Bioinformatics* **11**, 401.
- 772 Cornuet J-M, Pudlo P, Veyssier J *et al.* (2014) DIYABC v2.0: a software to make approximate
773 Bayesian computation inferences about population history using single nucleotide polymorphism,
774 DNA sequence and microsatellite data. *Bioinformatics*, **30**, 1187-1189.
- 775 Costedoat C, Gilles A (2009) Quaternary pattern of freshwater fishes in Europe: comparative
776 phylogeography and conservation perspective. *The Open Conservation Biology Journal*, **3**, 36-48.
- 777 Culling MA, Janko K, Boron A *et al.* (2006) European colonization by the spined loach (*Cobitis*
778 *taenia*) from Ponto-Caspian refugia based on mitochondrial DNA variation. *Molecular ecology*, **15**,
779 173–190.
- 780 Darriba D, Taboada GL, Doallo R, Posada D (2012) jModelTest 2: more models, new heuristics
781 and parallel computing. *Nature Methods* **9**, 772.
- 782 Davey JW, Cezard T, Fuentes-Utrilla P *et al.* (2012) Special features of RAD Sequencing data:
783 implications for genotyping. *Molecular ecology*, **22**, 3151–3164.
- 784 Deinhardt M (2013) The invasive potential of Prussian carp in Finland under the light of a novel
785 semi-clonal reproductive mechanism, Masters thesis, University of Jyväskylä.
- 786 Dowling TE, Tibbets CA, Minckley WL, Smith GR, McEachran JD (2002) Evolutionary
787 Relationships of the Plagopterins (Teleostei: Cyprinidae) from Cytochrome b Sequences. *Copeia*,
788 **2002**, 665–678.

- 789 Drummond AJ, Suchard MA, Xie D, Rambaut A (2012) Bayesian phylogenetics with BEAUti and
790 the BEAST 1.7. *Molecular biology and evolution*, **29**, 1969–1973.
- 791 Durand JD, Persat H, Bouvet Y (1999) Phylogeography and postglacial dispersion of the chub
792 (*Leuciscus cephalus*) in Europe. *Molecular ecology*, **8**, 989–997.
- 793 Eaton DAR (2014) PyRAD: assembly of de novo RADseq loci for phylogenetic analyses.
794 *Bioinformatics*, **30**, 1844–1849.
- 795 Emerson KJ, Merz CR, Catchen JM *et al.* (2010) Resolving postglacial phylogeography using high-
796 throughput sequencing. *Proceedings of the National Academy of Sciences*, **107**, 16196–16200.
- 797 Epperson BK, Mcrae BH, Scribner K *et al.* (2010) Utility of computer simulations in landscape
798 genetics. *Molecular ecology*, **19**, 3549–3564.
- 799 Frankham R, Briscoe D, Ballou J (2002) *Introduction to Conservation Genetics*. Cambridge
800 University Press, Cambridge, UK.
- 801 Fraser DJ, Bernatchez L (2001) Adaptive evolutionary conservation: towards a unified concept for
802 defining conservation units. *Molecular ecology*, **10**, 2741–2752.
- 803 Freyhof J, Brooks E (2011) European red list of freshwater fishes. Luxembourg: Publications Office
804 of the European Union.
- 805 Gibbard P, Head MJ (2009) The Definition of the Quaternary System/Era and the Pleistocene
806 Series/Epoch. *Quaternaire*, **20**, 125–133.
- 807 Gibbard PL, Rose J, Bridgland DR (1988) The history of the great northwest European rivers
808 during the past three million years [and discussion]. *Philosophical transactions of the Royal Society*
809 *of London. Series B, Biological sciences*, **318**, 559–602.
- 810 Goudet J (1995) FSTAT, a computer program to calculate F-Statistics. *Heredity*, **86**, 485–486

- 811 Grosswald MG (1980) Late Weichselian ice sheet of Northern Eurasia. *Quaternary Research*, **13**,
812 1–32.
- 813 Gum B, Gross R, Geist J (2009) Conservation genetics and management implications for European
814 grayling, *Thymallus thymallus*: synthesis of phylogeography and population genetics. *Fisheries*
815 *management and ecology*, **16**, 37–51.
- 816 Guindon S, Gascuel O (2003) A simple, fast, and accurate algorithm to estimate large phylogenies
817 by maximum likelihood. *Systematic Biology*, **52**, 696–704.
- 818 Hasegawa M, Kishino H, Yano T (1985) Dating of the human-ape splitting by a molecular clock of
819 mitochondrial DNA. *Journal of molecular evolution*, **22**, 160–174.
- 820 Hauser L, Baird M, Hilborn R, Seeb LW, Seeb JE (2011) An empirical comparison of SNPs and
821 microsatellites for parentage and kinship assignment in a wild sockeye salmon (*Oncorhynchus*
822 *nerka*) population. *Molecular ecology resources*, **11 Suppl 1**, 150–161.
- 823 Hazewinkel M (Ed.) (1994) *Encyclopaedia of Mathematics (set)*. Kluwer, Dordrecht, Netherlands.
- 824 Henkel CV, Dirks RP, Jansen HJ *et al.* (2012) Comparison of the exomes of common carp
825 (*Cyprinus carpio*) and zebrafish (*Danio rerio*). *Zebrafish*, **9**, 59–67.
- 826 Hess JE, Matala AP, Narum SR (2011) Comparison of SNPs and microsatellites for fine-scale
827 application of genetic stock identification of Chinook salmon in the Columbia River Basin.
828 *Molecular ecology resources*, **11**, 137–149.
- 829 Hewitt GM (1999) Post-glacial re-colonization of European biota. *Biological journal of the Linnean*
830 *Society. Linnean Society of London*, **68**, 87–112.
- 831 Hoban SM, Gaggiotti OE, Bertorelle G (2013) The number of markers and samples needed for
832 detecting bottlenecks under realistic scenarios, with and without recovery: a simulation-based study.
833 *Molecular ecology*, **22**, 3444–3450.

- 834 Holopainen IJ, Aho J, Vornanen M, Huuskonen H (1997) Phenotypic plasticity and predator effects
835 on morphology and physiology of crucian carp in nature and in the. *Journal of fish biology*, **50**,
836 781–798.
- 837 Holopainen IJ, Oikari A (1992) Ecophysiological effects of temporary acidification. *Annales*
838 *Zoologici Fennici*, **29**, 29–38.
- 839 Holopainen IJ, Tonn WM, Paszkowski CA (1997) Tales of two fish: the dichotomous biology of
840 crucian carp (*Carassius carassius* (L.)) in northern Europe.
- 841 Hänfling B, Hellemans B, Volckaert F, Carvalho GR (2002) Late glacial history of the cold-adapted
842 freshwater fish *Cottus gobio*, revealed by microsatellites. *Molecular ecology*, **11**, 1717–1729.
- 843 Hänfling B, Bolton P, Harley M, Carvalho GR (2005) A molecular approach to detect hybridisation
844 between crucian carp (*Carassius carassius*) and non-indigenous carp species (*Carassius* spp. and
845 *Cyprinus carpio*). *Freshwater biology*, **50**, 403–417.
- 846 Hickley P, Chare S (2004) Fisheries for non-native species in England and Wales: angling or the
847 environment? *Fisheries management and ecology*, **11**, 203-212.
- 848 IUCN 2015. The IUCN Red List of Threatened Species. Version 2015-4, <http://www.iucnredlist.org>
849 . Downloaded on 19 August 2015.
- 850 Janko K, Culling MA, Ráb P, Kotlík P (2005) Ice age cloning--comparison of the Quaternary
851 evolutionary histories of sexual and clonal forms of spiny loaches (*Cobitis*; Teleostei) using the
852 analysis of mitochondrial DNA variation. *Molecular ecology*, **14**, 2991–3004.
- 853 Janson S, Wouters J, Bonow M, Svanberg I, Olsén KH (2014) Population genetic structure of
854 crucian carp (*Carassius carassius*) in man-made ponds and wild populations in Sweden.
855 *Aquaculture international: journal of the European Aquaculture Society*, **23**, 359-368.

- 856 Jombart T, Ahmed I (2011) adegenet 1.3-1: new tools for the analysis of genome-wide SNP data.
857 *Bioinformatics* , **27**, 3070–3071.
- 858 Jombart T, Devillard S, Balloux F (2010) Discriminant analysis of principal components: a new
859 method for the analysis of genetically structured populations. *BMC genetics*, **11**, 94.
- 860 Kontula T, Väinölä R (2001) Postglacial colonization of Northern Europe by distinct
861 phylogeographic lineages of the bullhead, *Cottus gobio*. *Molecular ecology*, **10**, 1983–2002.
- 862 Koskinen MT, Ranta E, Piironen J *et al.* (2000) Genetic lineages and postglacial colonization of
863 grayling (*Thymallus thymallus*, Salmonidae) in Europe, as revealed by mitochondrial DNA
864 analyses. *Molecular ecology*, **9**, 1609–1624.
- 865 Kostecki R (2014) Stages of the Baltic Sea evolution in the geochemical record and radiocarbon
866 dating of sediment cores from the Arkona Basin. *Oceanological and Hydrobiological Studies*, **43**,
867 237–246.
- 868 Kotlík P, Berrebi P (2001) Phylogeography of the barbel (*Barbus barbus*) assessed by
869 mitochondrial DNA variation. *Molecular ecology*, **10**, 2177–2185.
- 870 Landguth EL, Fedy BC, Oyler-McCance SJ *et al.* (2012) Effects of sample size, number of markers,
871 and allelic richness on the detection of spatial genetic pattern. *Molecular ecology resources*, **12**,
872 276–284.
- 873 Larmuseau MHD, Freyhof J, Volckaert FAM, Van Houdt JKJ (2009) Matrilinear phylogeography
874 and demographical patterns of *Rutilus rutilus*: implications for taxonomy and conservation. *Journal*
875 *of fish biology*, **75**, 332–353.
- 876 Lelek A (1980) Threatened freshwater fishes of Europe. Council of Europe, Strasbourg, France.
- 877 Librado P, Rozas J (2009) DnaSP v5: a software for comprehensive analysis of DNA
878 polymorphism data. *Bioinformatics* , **25**, 1451–1452.

- 879 Luikart G, Cornuet J-M (2008) Empirical Evaluation of a Test for Identifying Recently
880 Bottlenecked Populations from Allele Frequency Data. *Conservation biology*, **12**, 228-237.
- 881 Lusk S, Hanel L, Luskova V (2004) Red List of the ichthyofauna of the Czech Republic:
882 Development and present status. *Folia Zoologica*, **53**, 215–226.
- 883 Lusk S, Lusková, V, Hanel L (2010) Alien fish species in the Czech Republic and their impact on
884 the native fish fauna. *Folia Zoology*, **59**, 57–72.
- 885 Mabuchi K, Senou H, Suzuki T, Nishida M (2005) Discovery of an ancient lineage of *Cyprinus*
886 *carpio* from Lake Biwa, central Japan, based on mtDNA sequence data, with reference to possible
887 multiple origins of koi. *Journal of Fish Biology*, **66**, 1516–1528.
- 888 Mezhzherin SV, Kokodii SV, Kulish AV, Verlatii DB, Fedorenko LV (2012) Hybridization of
889 crucian carp *Carassius carassius* (Linnaeus, 1758) in Ukrainian reservoirs and the genetic structure
890 of hybrids. *Cytology and genetics*, **46**, 28–35.
- 891 Miller MR, Dunham JP, Amores A, Cresko WA, Johnson EA (2006) Rapid and cost-effective
892 polymorphism identification and genotyping using restriction site associated DNA (RAD) markers.
893 *Genome research*, **17**, 240–248.
- 894 Moore A, Russell IC, Potter ECE (1990) The effects of intraperitoneally implanted dummy acoustic
895 transmitters on the behaviour and physiology of juvenile Atlantic salmon, *Salmo salar* L. *Journal of*
896 *fish biology*, **37**, 713–721.
- 897 Morin PA, Luikart G, Wayne RK, the SNP workshop group (2004) SNPs in ecology, evolution and
898 conservation. *Trends in ecology & evolution*, **19**, 208–216.
- 899 Morin PA, Pease VL, Hancock BL *et al.* (2010) Characterization of 42 single nucleotide
900 polymorphism (SNP) markers for the bowhead whale (*Balaena mysticetus*) for use in discriminating
901 populations. *Marine Mammal Science*, **26**, 716–732.

- 902 Mrakovčić M, Buj I, Mustafić P, Čaleta M, Zanella D (2007) *Croatian Red List: Freshwater fish*.
903 Department of Zoology, Faculty of Science, Zagreb.
- 904 Navodaru I, Buijse AD, Staras M (2002) Effects of Hydrology and Water Quality on the Fish
905 Community in Danube Delta Lakes. *International review of hydrobiology*, **87**, 329–348.
- 906 Nei M (1987) *Molecular evolutionary genetics*. Columbia University Press, New York.
- 907 Nesbø CL, Fossheim T, Vøllestad LA, Jakobsen KS (1999) Genetic divergence and
908 phylogeographic relationships among European perch (*Perca fluviatilis*) populations reflect glacial
909 refugia and postglacial colonization. *Molecular ecology*, **8**, 1387–1404.
- 910 Van Oosterhout C, Hutchinson WF, Wills DPM, Shipley P (2004) micro-checker: software for
911 identifying and correcting genotyping errors in microsatellite data. *Molecular ecology notes*, **4**,
912 535–538.
- 913 Peery MZ, Kirby R, Reid BN *et al.* (2012) Reliability of genetic bottleneck tests for detecting recent
914 population declines. *Molecular ecology*, **21**, 3403–3418.
- 915 Petit RJ, El Mousadik A, Pons O (1998) Identifying Populations for Conservation on the Basis of
916 Genetic Markers. *Conservation biology: the journal of the Society for Conservation Biology*, **12**,
917 844–855.
- 918 Pritchard JK, Stephens M, Donnelly P (2000) Inference of population structure using multilocus
919 genotype data. *Genetics*, **155**, 945–959.
- 920 R Core Team (2013) *R: a language and environment for statistical computing*, Vienna, Austria.
- 921 Ramachandran S, Deshpande O, Roseman CC *et al.* (2005) Support from the relationship of genetic
922 and geographic distance in human populations for a serial founder effect originating in Africa.
923 *Proceedings of the National Academy of Sciences of the United States of America*, **102**, 15942–
924 15947.

- 925 Rasmussen H (1959) Fish ponds and fish rearing. In: *Kulturhistoriskt lexikon för nordisk medeltid*
926 (eds: Andersson I, Granlund J), pp. 307–309, Malmö, Allhem.
- 927 Reyjol Y, Hugueny B, Pont D *et al.* (2006) Patterns in species richness and endemism of European
928 freshwater fish. *Global ecology and biogeography*, **16**, 65–75.
- 929 Rylková K, Kalous L, Bohlen J, Lamatsch DK, Petrtýl M (2013) Phylogeny and biogeographic
930 history of the cyprinid fish genus *Carassius* (Teleostei: Cyprinidae) with focus on natural and
931 anthropogenic arrivals in Europe. *Aquaculture*, **380**, 13–20.
- 932 Salzburger W, Brandstätter A, Gilles A *et al.* (2003) Phylogeography of the vairone (*Leuciscus*
933 *souffia*, Risso 1826) in Central Europe. *Molecular ecology*, **12**, 2371–2386.
- 934 Savini D, Occhipinti-Ambrogi A, Marchini A *et al.* (2010) The top 27 animal alien species
935 introduced into Europe for aquaculture and related activities. *Journal of applied ichthyology*, **26**, 1–
936 7.
- 937 Sayer CD, Copp GH, Emson D *et al.* (2011) Towards the conservation of crucian carp *Carassius*
938 *carassius*: understanding the extent and causes of decline within part of its native English range.
939 *Journal of fish biology*, **79**, 1608–1624.
- 940 Schwartz MK, McKelvey KS (2009) Why sampling scheme matters: the effect of sampling scheme
941 on landscape genetic results. *Conservation genetics*, **10**, 441–452.
- 942 Simic, V, Simic S, Cirkovic M, Pantovic N (2009) *Preliminary red list of the fishes of Serbia*.
943 COMBAFF-First Conference on Conservation and Management of Balkan Freshwater Fishes.
- 944 Simon A, Gozlan RE, Robert Britton J, van Oosterhout C, Hänfling B (2014) Human induced
945 stepping-stone colonisation of an admixed founder population: the spread of topmouth gudgeon
946 (*Pseudorasbora parva*) in Europe. *Aquatic sciences*, **77**, 17–25.

- 947 Svanberg I, Bonow M, Olsén H (2013) Fish ponds in Scania, and Linnaeus's attempt promote
948 aquaculture in Sweden. In: *Svenska Linnésällskapets årskrift* (eds David B, Gunnar D), pp. 85–
949 100. Svenska Linnésällskapet, Uppsala.
- 950 Svårdson G (1998) Plostglacial dispersal and reticulate evolution of Nordic Coregonids. *Nordic*
951 *journal of freshwater research*, **74**, 3–32.
- 952 Takada M, Tachihara K, Kon T *et al.* (2010) Biogeography and evolution of the *Carassius auratus*-
953 complex in East Asia. *BMC evolutionary biology*, **10**, 7.
- 954 Tamura K, Stecher G, Peterson D, Filipiński A, Kumar S (2013) MEGA6: Molecular Evolutionary
955 Genetics Analysis version 6.0. *Molecular biology and evolution*, **30**, 2725–2729.
- 956 Tarkan AS, Cucherousset J, Zięba G, Godard MJ, Copp GH (2010) Growth and reproduction of
957 introduced goldfish *Carassius auratus* in small ponds of southeast England with and without native
958 crucian carp *Carassius carassius*. *Journal of applied ichthyology*, **26**, 102–108.
- 959 Tavaré S (1986) Some probabilistic and statistical problems in the analysis of DNA sequences. In:
960 *Lectures in mathematics in the life sciences* (ed Miura RM), pp. 57–86. American Mathematical
961 Society, Providence, RI.
- 962 Tsipias G, Tsiamis G, Vidalis K, Bourtzis K (2009) Genetic differentiation among Greek lake
963 populations of *Carassius gibelio* and *Cyprinus carpio carpio*. *Genetica* **136**, 491–500.
- 964 Urho L, Lehtonen H (2008) Fish species in Finland. Finnish Game and Fisheries Research Institute,
965 Helsinki.
- 966 Van Oppen MJH, Rico C, Turner GF, Hewitt GM (2000) Extensive Homoplasy, Nonstepwise
967 Mutations, and Shared Ancestral Polymorphism at a Complex Microsatellite Locus in Lake Malawi
968 Cichlids. *Molecular Biology and Evolution*, **17**, 489–498.

- 969 Weir B, Cockerham C (1984) Estimating F-statistics for the analysis of population structure.
970 *Evolution*, **38**, 1358-1370.
- 971 Wheeler A (2000) Status of the crucian carp, *Carassius carassius* (L.), in the UK. *Fisheries*
972 *management and ecology*, **7**, 315–322.
- 973 Wolfram G, Mikschi E (2007) Rote Liste der Fische (Pisces) Österreichs. In: *Rote Liste gefährdeter*
974 *Tiere Österreichs, Teil 2*. Grüne Reihe des Lebensministeriums Band 14/2. (ed Zulka K), pp. 61–
975 198. Böhlau-Verlag, Wien.
- 976 Wouters J, Janson S, Lusková V, Olsén KH (2012) Molecular identification of hybrids of the
977 invasive gibel carp *Carassius auratus gibelio* and crucian carp *Carassius carassius* in Swedish
978 waters. *Journal of fish biology*, **80**, 2595–2604.
- 979 Xu P, Zhang X, Wang X *et al.* (2014) Genome sequence and genetic diversity of the common carp,
980 *Cyprinus carpio*. *Nature genetics*, **46**, 1212-1219.

981

982 **Author contributions**

983 DLJ collected, samples, performed lab work, analysed data and wrote the manuscript. BH was
984 involved with conception of the project, advised on all steps of analyses and commented on the
985 manuscript. GHC was involved in the conception of the project, contributed samples and
986 commented on the manuscript. LJLH advised on the analysis and commented on the manuscript.
987 CDS and KHO provided samples and commented on manuscript.

988

989 **Data accessibility**

990 Genbank accession numbers for mtDNA sequences are provided in Table 1 of this manuscript. The
991 microsatellite data files for all DAPC analyses, mantel test matrices, mtDNA raw sequences,

992 sequence alignments, model testing outputs, tree files, RADseq loci catalog and VCF files used for
993 analyses and the DIYABC project files (containing all inputs, scenarios and parameter priors for
994 each analysis stage) have now been uploaded to Dryad (<http://dx.doi.org/10.5061/dryad.t2j45>). All
995 scripts used for DAPC, mantel tests and comparisons of RADseq and microsatellite datasets can be
996 found on GitHub (<https://github.com/DanJeffries/Jeffries-et-al-2016-crucian-phylogeography>). All
997 demultiplexed RADseq reads have been uploaded to the short read archive (Project accession:
998 SRP063043).

999

1000

1001 Figure 1. Population structure of *C. carassius* in Europe. a) Sampling locations (sites sampled with
1002 nuclear and mtDNA markers = red dots, mtDNA only = blue dots) and population cluster
1003 memberships from DAPC analysis. Pie chart size corresponds to microsatellite allelic richness. Pie
1004 chart colours for Danubian populations and RUS1 correspond to clusters in the broad scale DAPC
1005 analysis b) and for all northern European populations colours correspond to clusters in the northern
1006 European DAPC analysis (mtDNA lineage 1 only) c). The Danube river catchment is shaded dark
1007 grey.

1008

1009 Figure 2. Maximum credibility tree calculated in BEAST for 100 *C. carassius cytb* sequences. For
1010 the three maximally supported nodes, age is given above and the posterior probability distribution is
1011 given below, with 95% CI's represented by blue bars.

1012

1013 Figure 3. Comparison of DAPC results using a) RADseq dataset, b) M2 dataset and c) M3 dataset.
1014 Colours correspond between DAPC scatter plots and maps within but not between panels.

1015

1016 Figure 4. The postglacial recolonisation of *C. carassius* in Europe. Arrows represent the
1017 relationships between population pools used in DIYABC (grey circles) as inferred from Stage 1,
1018 scenario 9 (arrows outlined in black) and Stage 3, scenario 14d (arrows with no outline) analyses on
1019 RADseq data. Bottlenecks are represented by white-striped sections of arrows. Posterior time
1020 estimates in years for each demographic event are given in black, and estimates of N_e are given in
1021 blue. Blue diamonds represent ancestral populations inferred by DIYABC and the labels (a-f)
1022 correspond to their mention in the text. Hypothetical expansion fronts are represented by dashed
1023 contour lines and the Danube river catchment is shaded red. Hypothetical glacial refugia are
1024 represented by dashed blue circles (I - III). The blue dashed box (?) represents our inference that *C.*
1025 *carassius* expanded into central and perhaps northern Europe during the Riss-Würm interglacial,
1026 however we cannot estimate this range.

1027 SI Figure 1. DIYABC scenarios used in broad-scale analysis (Stage 1). See text for population
1028 poolings. See Table 3 for population poolings and prior parameter values.

1029

1030 SI Figure 2. All scenarios tested in stage 2 a) and stage 3 b) of DIYABC analysis. See Table 3 for
1031 population poolings and prior parameter values.

1032

1033 SI Figure 3. Filtering out merged ohnologs. a) Distribution of SNP locus coverage prior to
1034 removing loci that had observed heterozygosity higher than 0.5 in one or more population. b)
1035 Distribution of locus coverage after filtering, showing a loss of many high coverage loci and a
1036 reduction in mean SNP coverage. Note the loss of loci with high coverage.

1037

1038 SI Figure 4. Linear regressions for all samples a) *Ar* against latitude; b) *Ar* against longitude and for
1039 only samples in mtDNA lineage 1 c) *Ar* against latitude; d) *Ar* against longitude.

1040

1041 SI Figure 5. DAPC analysis of a) full microsatellite dataset (Excluding NOR2); for results used in
1042 Fig. 1) and b) Full RADseq dataset.

1043

1044 SI Figure 6. Isolation by distance a) in M1 dataset for mtDNA lineage 1 only (excluding NOR2), b)
1045 full RADseq dataset, c) M2 dataset and d) M3 dataset.

1046

1047 SI Figure 7. DAPC scatter plot for the 1000 SNP RADseq dataset used in the DIYABC analysis,
1048 showing the same population structure as inferred from the full RADseq dataset.

1049

1050 SI Figure 8. Broad scale DIYABC analysis (Stage 1) results. a) Direct approach (left) and Logistic
1051 regression (right) showing support for scenario 9. b) Model checking for scenario 9, showing that
1052 the observed data fall well within the cloud of datasets simulated from the posterior parameter
1053 distribution. c) Scenario 9 schematic.

1054

1055 SI Figure 9. Fine scale DIYABC analysis in northern Europe. a) Stage 2 - major topological
1056 variants of scenarios. Direct approach (top left) and Logistic regression (top right) showing support
1057 for scenario 14 and 13 respectively. Model checking (Middle) for scenario 14 (bottom), showing
1058 that the observed data fall well within the cloud of datasets simulated from the posterior parameter
1059 distribution. Note the model checking placed the observed data outside of the cloud of posterior
1060 datasets for scenario 13. b) Stage 3 - Minor scenario variants of scenario 14 from stage 2. Direct

1061 approach (top left), logistic regression (top right) and model checking (middle) all support scenario
1062 14d (bottom).

1063

1064 SI Figure 10. Comparison of spatial patterns of uniformity in geographic sampling regimes of the
1065 full M1 dataset locations (a, c) and the sampling location subset used in M2, M3, and RAD datasets
1066 (b,d). Estimates of G and L from true sampling locations are plotted using the black solid lines.
1067 Estimates of G and L from simulated locations based on random Poisson distribution is represented
1068 by the red dashed line. Grey shaded areas are the 95% confidence intervals around the random
1069 estimates. Both the G and L function estimates show that there is more clustering of sampling
1070 locations in the M1 dataset than in the M2, M3 and RAD subsets.

1071

1072 SI Figure 11. Change in a) number of RAD tags and b) average tag coverage for three individuals
1073 used in the preliminary Stacks tag mismatch parameter (M) tests.

1074

1075 SI Figure 12. Results of parameter tests for the Stacks module Populations. a) Number of SNP loci
1076 in final dataset for incrementing values of parameters $-p$, $-r$ and $-m$; b) average coverage per SNP
1077 and per sample for the same parameter values; c) the number of loci which drop out in each
1078 population for each test value of the $-p$ parameter

1079

1080

1081 Table 1. Location, number, genetic marker sampled, and accession numbers of samples and sequences used
 1082 in the present study for microsatellite and mitochondrial DNA analyses. mtDNA sequence accession
 1083 numbers can be found in SI table 2.

Code	Accession	Location	Country	Drainage	Coordinates		Microsatellites	mtDNA	RADseq
					lat	long			
GBR1		London	U.K.	U.K	51.5	0.13	9		
GBR2		Reading	U.K.	U.K	51.45	-0.97	4		
GBR3		Norfolk	U.K.	U.K	52.86	1.16	7		
GBR4		Norfolk	U.K.	U.K	52.77	0.75	27		9
GBR5		Norfolk	U.K.	U.K	52.77	0.76	14		
GBR6		Norfolk	U.K.	U.K	52.54	0.93	29	3	
GBR7		Norfolk	U.K.	U.K	52.9	1.15	24	1	10
GBR8		Hertfordshire	U.K.	U.K	52.89	1.1	37	3	9
GBR9		Norfolk	U.K.	U.K	52.8	1.1	27		
GBR10		Norfolk	U.K.	U.K	52.89	1.1	14		
GBR11		Norfolk	U.K.	U.K	52.92	1.16	20		
BEL1		Bokrijk	Belgium	Scheldt River	50.95	5.41	13	1	
BEL2		Meer van Weerde	Belgium	Scheldt River	50.97	4.48	12		
BEL3		Meer van Weerde	Belgium	Scheldt River	50.97	4.48	8		
GER1*		Kruegersee	Germany	Elbe River	52.03	11.97		3	
GER2		Münster	Germany	Rhine River	51.89	7.56	21	3	
GER3		Bergheim	Germany	Danube River	48.73	11.03	9	3	
GER4		Bergheim	Germany	Danube River	48.73	11.03	8	3	
CZE1		Lužnice	Czech Republic	Danube River	48.88	14.89	9	3	
POL1		Sarnowo	Poland	Vistula River	52.93	19.36	33		
POL2		Kikót-Wies	Poland	Vistula River	52.9	19.12	34		
POL3		Tupadly	Poland	Vistula River	52.74	19.3	17	3	10
POL4		Orzysz	Poland	Vistula River	53.83	22.02	13	3	10
EST1		Tartu	Estonia	Baltic Sea	58.39	26.72	5	3	
EST2		Vehendi	Estonia	Baltic Sea	58.39	26.72	5		
RUS4*		Small lake, Velikaya river	Russia	Baltic Sea	55.9	30.25	29	3	
FIN1		Joensuu	Finland	Baltic Sea	62.68	29.68	32	3	
FIN2		Helsinki	Finland	Baltic Sea	60.36	25.33	32		
FIN3		Jyväskylä	Finland	Baltic Sea	62.26	25.76	37	3	10
FIN4		Oulu	Finland	Baltic Sea	65.01	25.47	7	3	8
FIN5		Salo	Finland	Baltic Sea	60.37	23.1	10	3	
FIN6		Åland Island	Sweden	Baltic Sea	60.36	19.85	8	3	
SWE1		Gränbrydammen	Sweden	Baltic Sea	59.87	17.67	25		
SWE2		Stordammen	Sweden	Baltic Sea	59.8	17.71	21	3	10
SWE3		Östhammar	Sweden	Baltic Sea	60.26	18.38	27	3	
SWE4		Umeå	Sweden	Baltic Sea	63.71	20.41	9	3	
SWE5		Kvicksund	Sweden	Baltic Sea	59.45	16.32	9		
SWE7		Grillby	Sweden	Baltic Sea	59.64	17.37	10		
SWE8		Skabersjo	Sweden	Baltic Sea	55.55	13.15	19	3	10
SWE9		Märsta	Sweden	Baltic Sea	59.6	17.8	31	3	
SWE10		Norrköping	Sweden	Baltic Sea	58.56	16.27	29		9
SWE11		Gotland Island	Sweden	Baltic Sea	57.85	18.79	11	3	
NOR1		Oslo	Norway	North Sea	60.05	9.94	2		
NOR2		Lake Prestvattnet, Tromsø	Norway	North Sea	69.65	18.95	16		9
BLS			Belarus	Dnieper	52.47	30.52	7	1	
RUS1		Proran Lake	Russia	Don River	47.46	40.47	10	3	9
DEN1		Copenhagen	Denmark	Baltic Sea	60.21	17.79	12		10
DEN2		Pederstrup	Denmark	Baltic Sea	55.77	12.55	14		8
DEN3		Gammel Holte	Denmark	Baltic Sea	56	12.5	14		
DEN4		Bornholm Island	Denmark	Baltic Sea	55.17	14.86			5
SWE12		Osterbybruk Mansion	Sweden	Baltic Sea	55.73	12.34	14		9
SWE14		Wengnarn Castle	Sweden	Baltic Sea	59.66	18.95	16		9
RUS2*		Karma	Russia	Volga River	52.9	58.4		2	
RUS3*		Saygach'yedake	Russia	Volga River	47.5	48.5		4	
TNO			Netherlands	North Sea	-	-		1	
HUN1		Gödöllő	Hungary	Danube River	47.61	19.36		2	6
HUN2		Vörösmocsár	Hungary	Danube River	46.49	19.17			

848 83 160
 Total number of fish = 867

Genbank mtDNA Sequences

Code	Accession	Reference	Country	Drainage
GER6	DQ399917	Kalous et al. (2007)	Germany	Baltic sea
GER6	DQ399918	Kalous et al. (2007)	Germany	Baltic sea
GER6	DQ399919	Kalous et al. (2007)	Germany	Baltic sea
GER7	JN412540	Rylková et al. (2013)	Germany	Hunte River
GER7	JN412541	Rylková et al. (2013)	Germany	Hunte River
GER7	JN412542	Rylková et al. (2013)	Germany	Hunte River
GER7	JN412543	Rylková et al. (2013)	Germany	Hunte River
GER8*	JN412537	Rylková et al. (2013)	Germany	Lahn River
GER8*	JN412538	Rylková et al. (2013)	Germany	Lahn River
CZE2	GU991399	Rylková et al. (2013)	Czech Republic	Elbe drainage
Milevsko	DQ399938	Kalous et al. (2012)	Czech Republic	Elbe drainage
AUS1	JN412534	Rylková et al. (2013)	Austria	Danube river
AUS1	JN412533	Rylková et al. (2013)	Austria	Danube river
AUS2	JN412535	Rylková et al. (2013)	Austria	Danube river
AUS3	JN412536	Rylková et al. (2013)	Austria	Danube river
GBR12	JN412539	Rylková et al. (2013)	U.K.	U.K

GBR12	GU991400	Kalous et al. (2012)	U.K.	U.K
SWE15	JN412545	Rylková et al. (2013)	Sweden	Baltic sea
SWE16	JN412544	Rylková et al. (2013)	Sweden	Baltic sea
Ccarp1	AB158807	Mabuchi et al (2005)	Japan	-
Ccarp2	DQ868875	Tsipas et al. (2009)	Greece	-
Ccarp3	KF574490	Unpublished	India	-

1084 † Also present

1085 * Location on Map (Fig. 1.a) is approximate

1086

For Review Only

1087 Table 2. Population pools, parameter priors used and median posterior parameter values inferred in the three
1088 stages of DIYABC analysis.

Analysis stage	Population Pools	Scenarios tested	Parameter priors	Most likely Scenario	Median of posterior distributions of most likely scenario
1	Pool 1 – GBR4, GBR7, GBR8, DEN1, DEN2, DEN3, FIN3, FIN4, POL3, POL4, SWE2, SWE8, SWE9, SWE10, SWE12, SWE14, NOR2 Pool 2 – DEN1, DEN2, DEN3 Pool 3 – FIN3, FIN4	1 - 11	N1 = 10E+03 - 500E+03 Nb1 = 10 - 100E+03 N2 = 100 - 100E+03 N3 = 100 - 200E+03 t1 = 1E+03 - 1E+06 gens t2 = 1E+03 - 3E+06 gens ra = 0.001-0.999 rb = 0.001-0.999 rc = 0.001-0.999 db = 10- 10E+03 gens	9	N1 =34700 Nb1 =23700 N2 =74900 N3 =140000 t1 =135000 db =4460 t2 =1090000
			N1 = 10-4E+03 N2 = 10 - 10E+03 N3 = 10 - 20E+03 N4 = 10 - 50E+03 N5 = 10 - 20E+03 N6 =10 - 400 t1 = 100- 10E+03 gens t1a = 100- 10E+03 gens t2 =100- 10E+03 t2a =100- 5E+03 gens t2b = 500-20E+03 gens t2c = 100 - 10E+03 gens t2d = 100 - 10E+03 gens t3 = 500 - 20E+03 gens t3c =100 - 10E+03 gens t3d =100 - 10E+03 gens t4 =500 - 20E+03 gens ra = 0.001-0.999 rb = 0.001-0.999		14
2	Pool 1 – GBR4, GBR7, GBR8 Pool 2 – DEN1, DEN2, DEN3 Pool 3 – FIN3, FIN4	12 - 16	N1 = 10-4E+03 Nb1 = 10-10E+03 N2 = 10 - 10E+03 N3 = 10 - 20E+03 Nb3 = 10-10E+03 N4 = 10 - 50E+03 N5 = 10 - 20E+03 N6 =10 - 400 Nb6 =10-10E+03 t1 = 100- 10E+03 gens t1a = 100- 10E+03 gens t2d = 100 - 10E+03 gens t3d = 100 - 10E+03 gens t4 = 500 - 20E+03 gens rb = 0.001-0.999 da = 10 - 10E+03 gens db = 10 - 10E+03 gens dc = 10 - 10E+03 gens dd = 10 - 10E+03 gens de = 10 - 10E+03 gens	14d	
			Pool 4 – POL3, POL4 Pool 5 – SWE2, SWE8, SWE9, SWE10, SWE12, SWE14 Pool 6 – NOR2		14a - 14f

1089

1090

1091 Table 3. Summary statistics for M1, M2, M3 and RADseq datasets. RAD contains all RADseq data, M1
 1092 contains all microsatellite data, M2 contains only microsatellite for the individuals used in the RADseq, and
 1093 M3 contains all microsatellite data for all individuals that were available in populations that were used in
 1094 RADseq.

Dataset	Description	N samples	Mean N samples/pop	N. loci	Mean N.alleles/pop	Mean N.alleles/locus
RAD	RADseq data only	149	8.95 ± 1.4	13189	6723	2
M1	Full Microsatellite dataset	848	17.2 ± 9.5	13	27 ± 8.8	7.6
M2	Microsatellites for RADseq samples only	146	9.13 ± 0.8	13	24.4 ± 7.3	7.84 ± 5.1
M3	Microsatellites for all samples in populations used in RADseq	313	19.6 ± 9.0	13	27.4 ± 8.1	11.23 ± 7.6

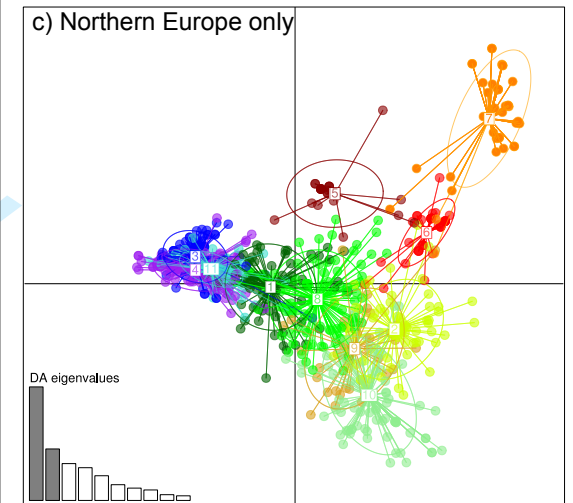
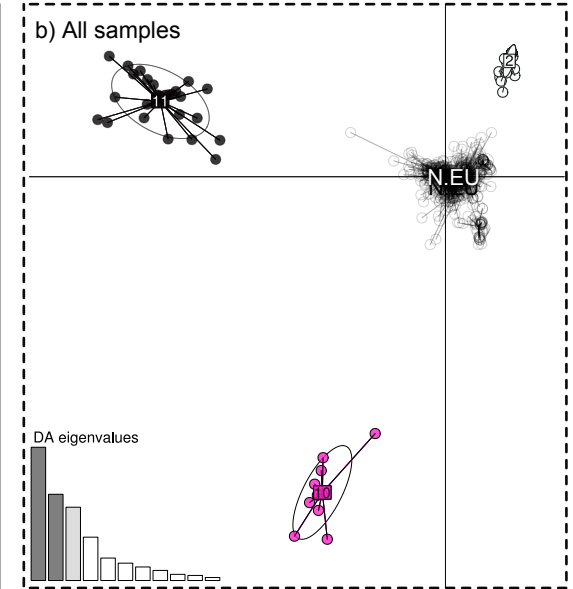
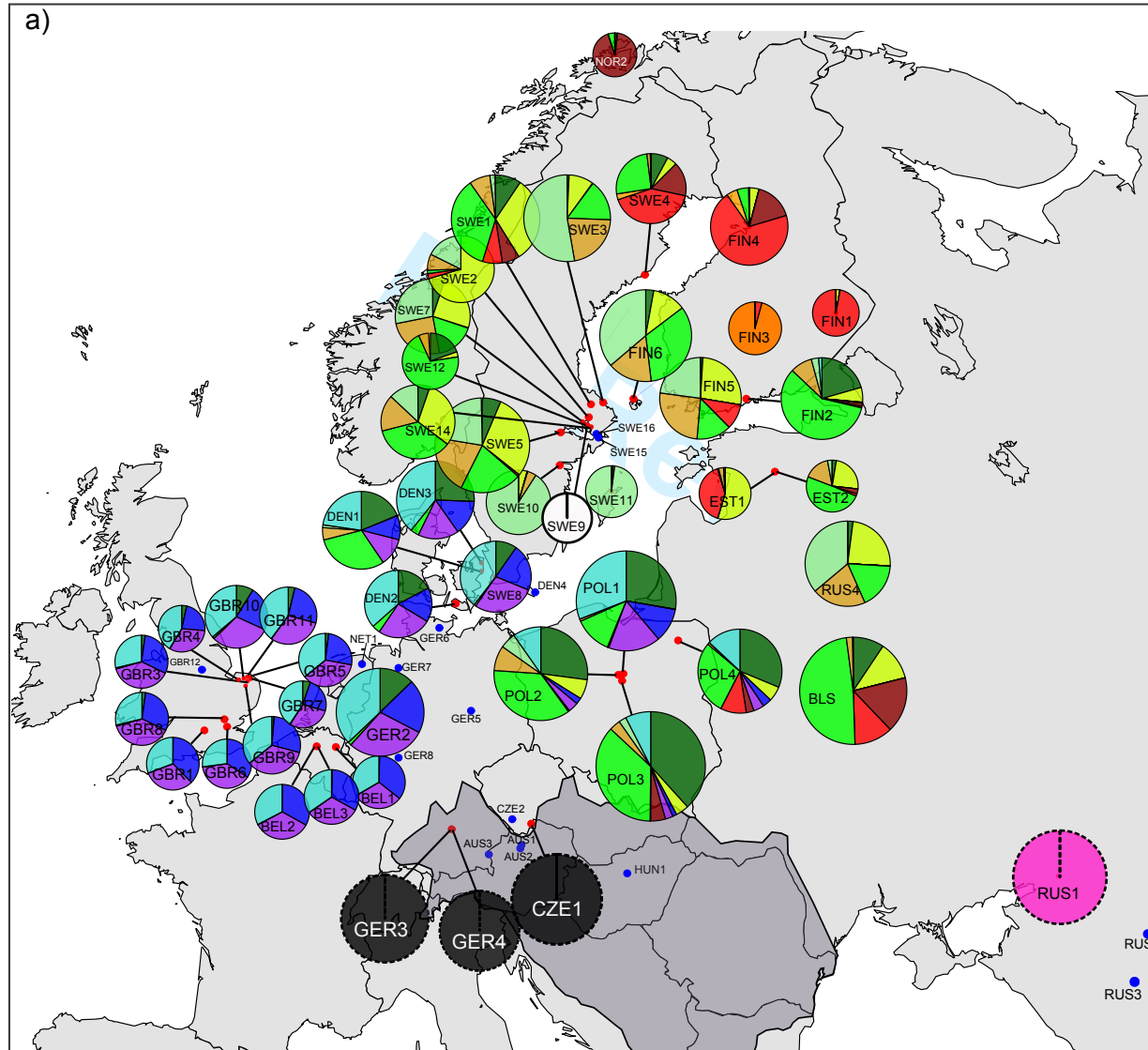
1095

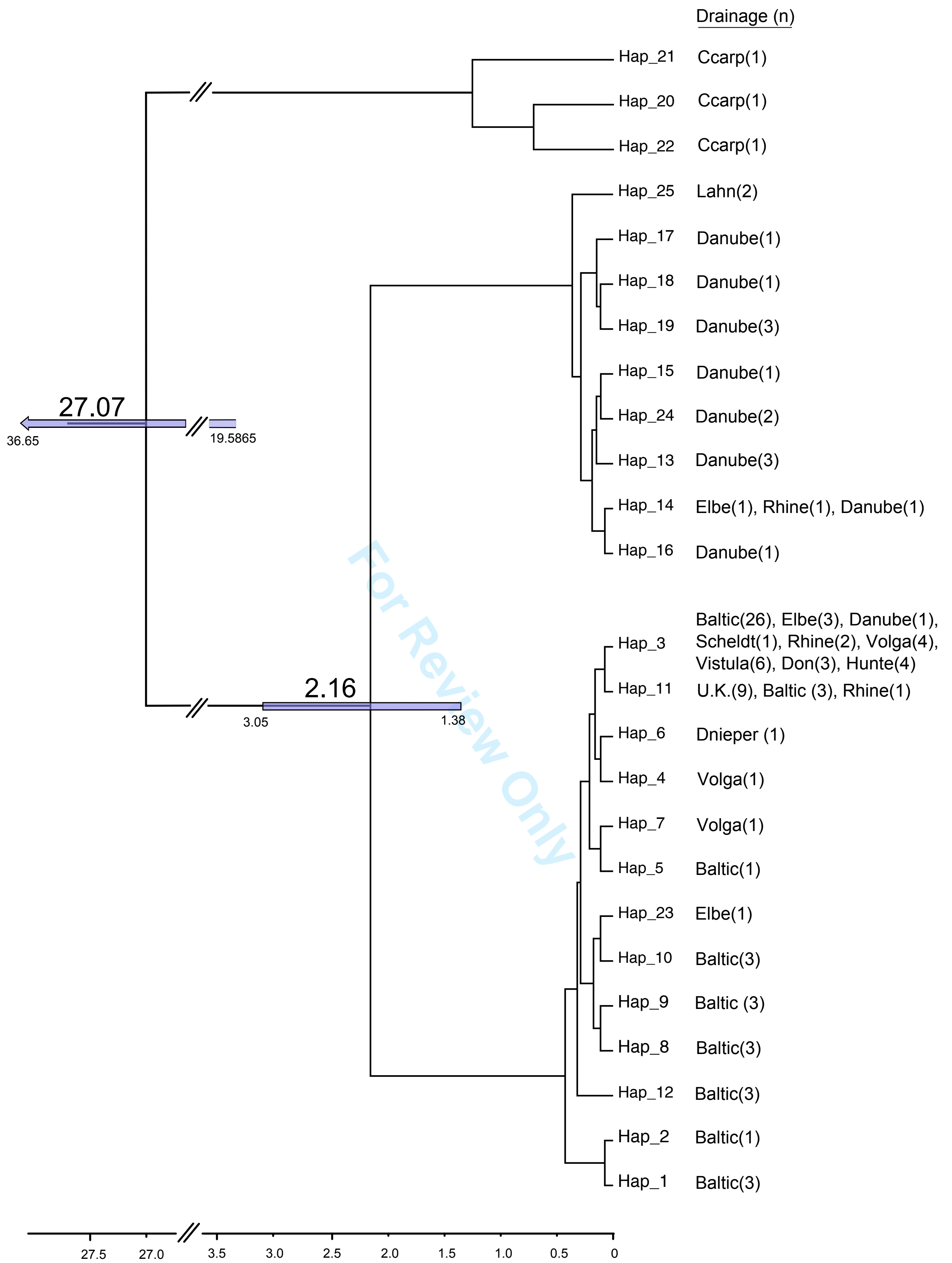
1096

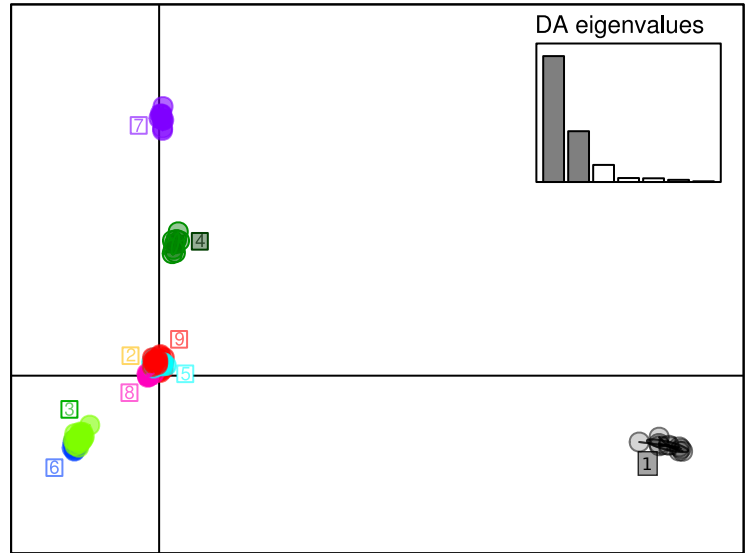
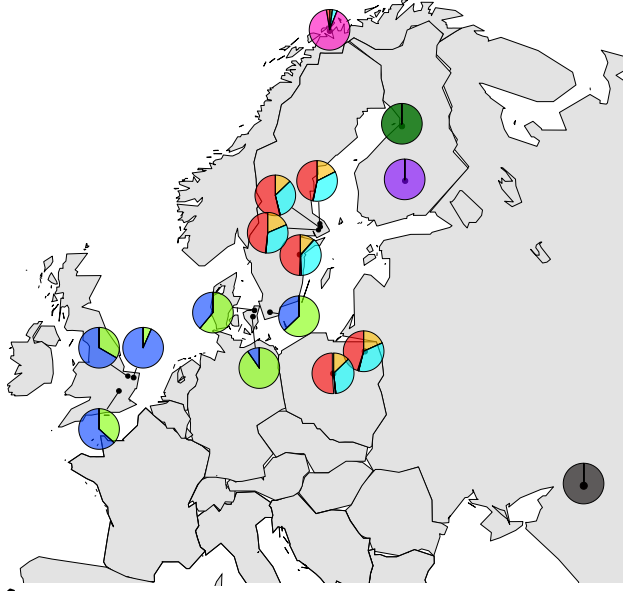
1097 Table 4. Pearson's product-moment correlation coefficients and paired t-tests comparing heterozygosities
 1098 and F_{ST} s between M2, M3 and RADseq datasets. *** $P = < 0.001$, ** $P = < 0.005$, * $P = < 0.05$.

Heterozygosities (df = 18)		Pearsons correlation coefficient (t)		
Paired T-tests		M2	11.13***	3.85**
		-2.4*	M3	3.86**
		-9.71***	-9.29***	RAD
F_{ST} (df = 105)		Pearsons correlation coefficient (t)		
Paired T-tests		M2	46.26***	10.09***
		-6.21***	M3	9.05***
		13.74***	15.12***	RAD

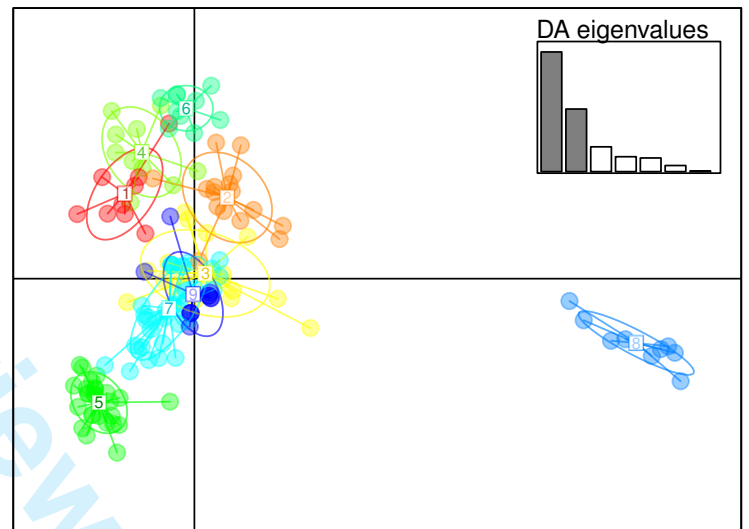
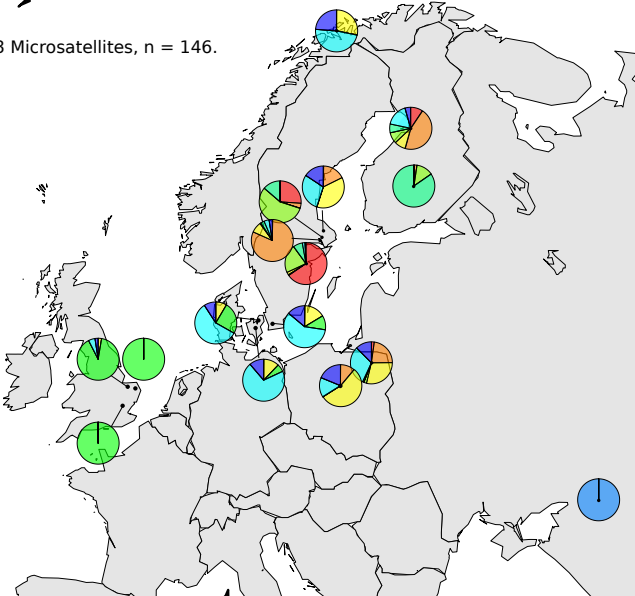
1099



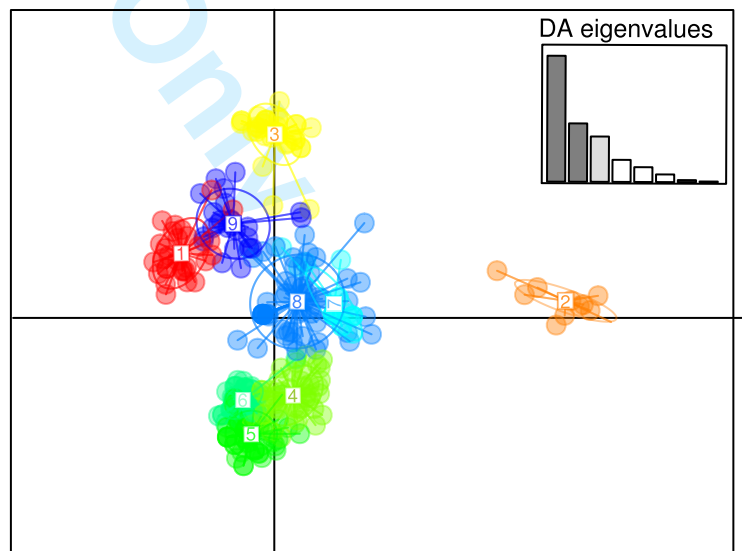
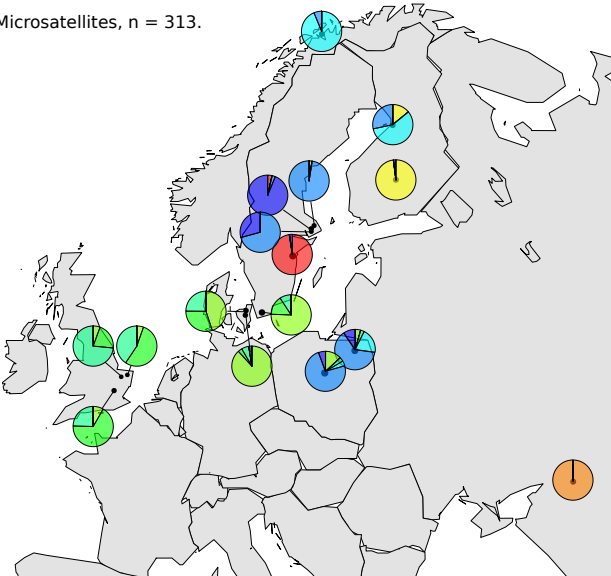


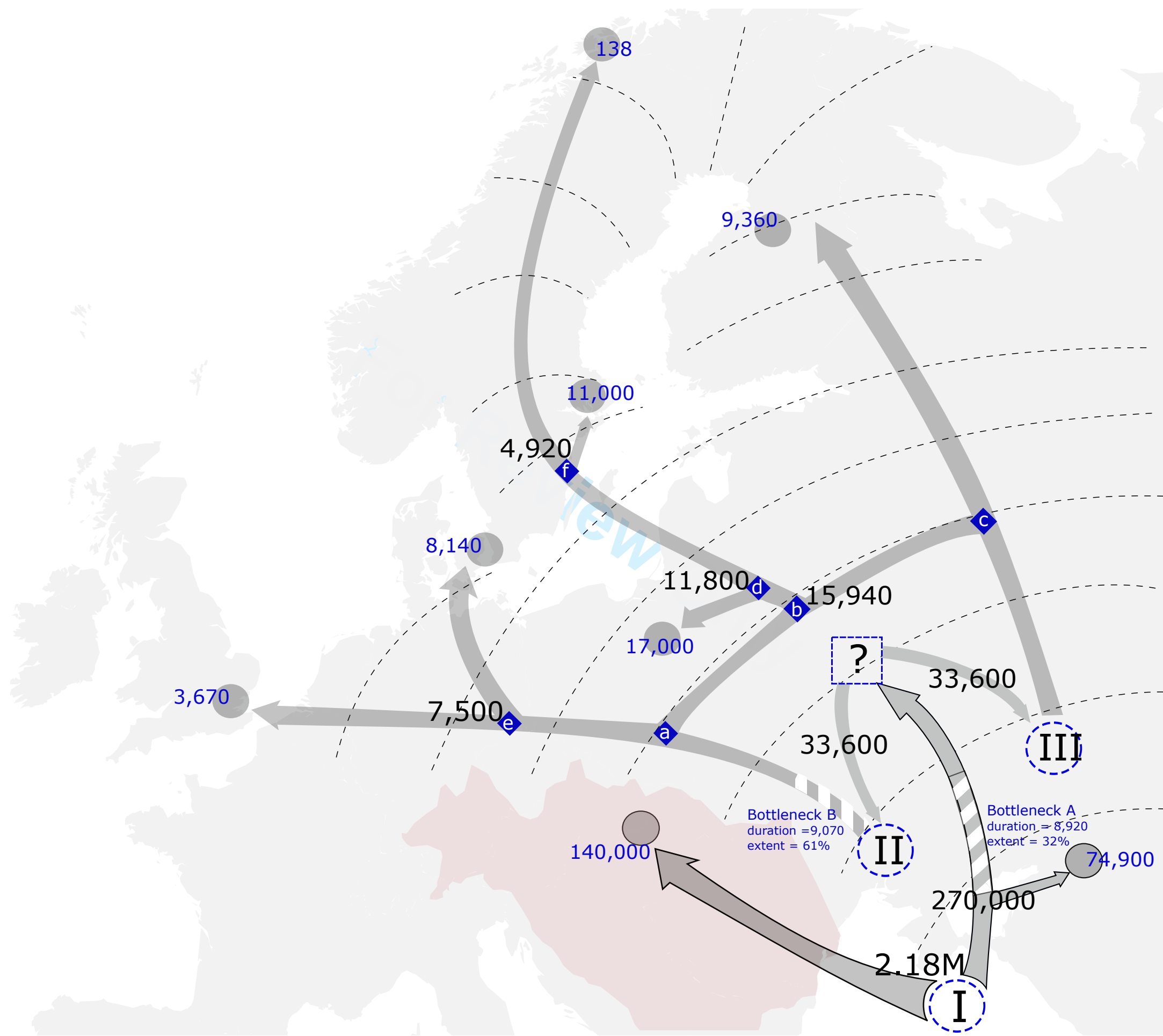


B) M2 - 13 Microsatellites, n = 146.



B) M3 - 13 Microsatellites, n = 313.





1 Comparing RADseq and microsatellites to infer
2 complex phylogeographic patterns, a real data
3 informed perspective in the Crucian carp, *Carassius*
4 *carassius*, L.

5
6 **Authors:** ¹Daniel L Jeffries, ²Gordon H Copp, ¹Lori Lawson Handley, ³K. Håkan Olsén, ⁴Carl D
7 Sayer, ¹Bernd Hänfling

8

9 Supporting Information

10 *Detecting hybrids*

11 *Methods*

12 In total we acquired tissue samples of 1354 fish from 72 populations. All samples were first
13 genotyped using multiplex 1 (SI table 1) which contained the 6 species diagnostic microsatellite
14 loci. These data were then analysed using the NewHybrids v. 1.1 (Anderson & Thompson 2002)
15 software package in order to determine whether each fish was *C. carassius*, *C. auratus*, *C. gibelio*
16 or a hybrid between any of these species.

17

18 NewHybrids uses allele frequencies to give a likelihood probability that an individual belongs to
19 one species or another, or if the individual belonged to one of several hybrid classes (F1, F2 or
20 backcross). Data from 20 *C. carassius* samples, which were confidently identified as pure from both
21 morphology and genotypes, and were not sympatric with non-native species, were included in each
22 analysis as baseline data. Priors were then added to the analyses specifying that these individuals
23 were indeed pure in order to give the software more power with which to assess allele frequencies
24 associated with *C. carassius*. To be sure to account for allele frequency differences between
25 different geographic regions, only pure individuals from regions neighbouring the hybrid population

26 were used. Individuals which had more than a 25% chance of being an F1 hybrid, F2 hybrid, or a
27 backcross were removed from population structure analyses and were not genotyped at the
28 additional 7 microsatellite loci (Multiplexes 2.1 and 2.2, SI table 1).

29

30 *Results*

31 Of the 1354 fish which were genotyped with microsatellites, 942 individuals across 55 populations
32 (86.7%) were identified as pure *C. carassius* using the first set of 6 species diagnostic loci in
33 NewHybrids analyses. 19 (1.8%) from 2 different populations were identified as *C. auratus*, 15 fish
34 (1.4%) from 4 populations were identified as *C. gibelio* and 10 fish (0.93%) from two populations
35 were identified as *C. carpio*. NewHybrids identified 60 (5.5%) *C. carassius* x *C. auratus* hybrids,
36 25 (2.2%) *C. carassius* x *C. gibelio* hybrids, and 16 (1.5%) *C. carassius* x *C. carpio* hybrids. Of the
37 942 fish identified as pure *C. carassius*, 867 existed in locations (49 populations) where hybrids
38 or non-native species were not detected by microsatellite genotyping. To safeguard against cryptic
39 introgression which may produce erroneous results only these 867 pure *C. carassius* were used for
40 the main phylogeographic analyses and tests using either microsatellites, mtDNA or RADseq.

41

42 *RADseq data filtering and Stacks analysis parameter testing*

43 RADseq analyses were performed using only the first-end reads from the paired-end sequencing, as
44 coverage across the length of the second-end contigs was not consistent enough to call SNPs in all
45 individuals. For these first-end reads, raw data was first quality checked using FastQC (Andrews
46 2010), which assesses the per-base sequence quality and content of reads, and provides
47 comprehensive graphical outputs with which to assess the overall quality of raw sequencing data.
48 These analyses did not identify any individuals that had low overall sequence quality, therefore all
49 samples were retained for further analyses.

50

51 Preliminary analyses were also carried out using PyRAD (Eaton 2014), which allows for the
52 incorporation of allelic variants resulting from insertions and deletions. However, no significant
53 difference in the number of usable loci was shown. As Stacks provides more downstream
54 populations genetics facilities, this program was used for the final analyses.

55

56 Raw RADseq reads were first, demultiplexed using the “process_radtags” module distributed with
57 Stacks and our inline barcodes. Second, reads were filtered for any sequences containing Illumina
58 adapters or primers and trimmed to a length of 92 bp. Third, PCR duplicates introduced during
59 library preparation were removed using the “clone_filter” program (also distributed with Stacks).
60 Finally, preliminary tests of parameter values for each module of the de novo stacks pipeline were
61 performed in order to identify “optimal” parameter values (i.e. where loci number and read depth
62 were stable) for use in the final Stacks analysis. These tests were carried out for 5 sets of 3
63 randomly chosen individuals from the RADseq dataset and, for each test, all non-test parameters
64 were kept as default. In the ustacks module, which groups identical reads into stacks and then
65 stacks into loci, Parameters M and m were tested (See Catchen et al. 2013 for detailed description
66 of parameters). M values were increased in increments of 2 from 0 to 10. The efficiency of ustacks
67 in finding real loci was then examined with simple counts of the number of constructed loci at each
68 M parameter value and the read coverage of these loci. The expectation was that, at low parameter
69 values, divergent alleles (percentage divergence > M) at a locus will not merge (under-merging),
70 thus increasing the number of loci overall and decreasing the average coverage. In contrast high
71 parameter values could cause over-merging of paralogous loci and have the opposite effects on the
72 number of loci and coverage (Catchen et al. 2013). SI Fig. 11 shows the outputs for a single subset
73 of *C. carassius* samples, which was typical of all 5 subsets tried. In ustacks, an ‘m’ parameter value
74 of zero (minimum of 0 reads required to form a stack) resulted in a very large number of tags
75 (49000-54000) as expected. Likely due to many single reads containing sequencing error being
76 called as loci. The number of loci decreased by approximately 3000 – 4000 tags in the samples

77 tested at a required read depth of 2 (approx. 50,000), after which further increases in ‘m’ resulted in
78 small decreases in the number of tags. This likely reflects merging of paralogous loci, or low
79 coverage loci. Mean coverage across all loci within an individual of course reflected the ‘m’
80 parameter increase, jumping initially from approx. 16 reads per locus with zero read depth required,
81 to 20-35 at a minimum required depth of two reads. On the basis of these results we chose an $m = 8$,
82 to ensure high power for SNP calling.

83

84 Incrementing over values of ‘M’ again met our expectations, with the number of loci dropping
85 significantly as the ‘M’ parameter was increased from zero to 2 mismatches allowed, and then
86 dropping more slowly with higher mismatch allowance. These further drops may again be allowing
87 for paralog merging between loci. The mean coverage of loci behaved as expected, with higher
88 mismatch allowance, more divergent reads can be added to existing stacks, inflating coverage for
89 those loci. On the basis of these results $M=2$ was chosen for final analyses.

90 Parameter tests were also performed for the cstacks parameter N, which is responsible for setting
91 the maximum mismatch threshold allowed between homologous loci among individuals in the locus
92 catalog. First, ustacks was run using chosen “optimal” parameters to obtain the inputs necessary for
93 cstacks. Cstacks was then run separately on each of the 5 sample subsets with values of N between
94 0 – 10, with increments of 2.

95

96 Finally, we tested three core parameters in the Populations module of Stacks, -m which is analogous
97 to the parameter of the same name in the ustacks module, -r, which specifies the number of
98 individuals within a give population that a locus must be present in, and -p which specifies the
99 number of populations that a locus must be present in (above the -r threshold) for it to be retained
100 in the final dataset (SI Fig. 12). -p was tested for values of between 13 – 19 populations, -r was
101 tested for values between 0.5 – 1.0 and -m was tested for values between 1-8 however, a the dataset
102 had previously been filtered at previous stages for loci present with a depth of 8 reads or higher, the

103 tests of $-m$ in the populations stage were redundant.

104

105 *Final running parameters used*

106 For all parameter tests, the optimal values were taken to be those where the rate of change in either
107 RAD tag number, or coverage began to decrease. In ustacks, a maximum of two mismatches were
108 allowed between alleles at a given locus ($M=2$) and at least eight identical reads per stack ($m=8$)
109 were required. Default values were used for all other parameters. ustacks also called SNPs within
110 individuals at each locus. The cstacks module was then used to merge loci across individuals into a
111 catalog, where $N=2$ mismatches were allowed between individuals at a given locus. Individuals
112 were then searched against this catalog using Sstacks to determine their genotype at each catalog
113 locus. For the Populations module, optimal values were chosen so that loci that were shared
114 between at least 70% of individuals in each population ($-r = 0.7$), allowing loci to drop out in one or
115 two individuals in a population for reasons of low DNA sample quality or low coverage. Loci must
116 have also been present in 17 of the 19 populations ($-p = 17$), and have read depth of at least 8 ($-m 8$)
117 in each individual.

118

119 *DAPC & Running parameters*

120 *Methods*

121 Population structure was examined using Discriminant Analyses of Principal Components (DAPC,
122 (Jombart *et al.* 2010)) in adegenet. Similar to the more commonly used program, STRUCTURE
123 (Pritchard *et al.* 2000), DAPC is an individual-based approach that uses Principal Components
124 Analysis (PCA) to transform population genetic data and Discriminant Analysis (DA) to identify
125 clusters. The number of clusters is assessed using the K-means method, which is also used in
126 STRUCTURE (Pritchard *et al.* 2000). Unlike STRUCTURE, DAPC does not assume underlying
127 population genetics models such as Hardy-Weinberg Equilibrium (Jombart *et al.* 2010) and is

128 therefore more suitable for analysing *C. carassius* since populations are often bottlenecked
129 (Hänfling *et al.* 2005). An additional benefit of DAPC is that it maximizes between-group variation,
130 while minimizing variation within groups, allowing for optimal discrimination of between-
131 population structure (Jombart *et al.* 2010).

132

133 *Results*

134 For the full microsatellite dataset (M1), BIC scores indicated that between 11 and 19 genetic
135 clusters (**Error! Reference source not found.**) would be an appropriate model of the variation in the
136 data. We therefore chose 11 clusters to use in the discriminant analysis, retaining 8 principal
137 components as recommended by the spline interpolation a-scores (**Error! Reference source not
138 found.c**) and we kept 2 linear discriminants for plotting (**Error! Reference source not found.b**).

139

140 Three major lineages were found, one located in the Danube, one in the Don, and one spread across
141 northern Europe. However the large amount of divergence between them masked the population
142 structure present in northern Europe. We therefore subsetted the data, separating NEU populations
143 from RUS1, GER3, GER4, CZE1 (and SWE9, which was an outlier within NEU, **Error! Reference
144 source not found.b**) and reanalysed them with DAPC in order to better infer fine population structure
145 between them.

146

147 For the RADseq dataset, BIC scores suggested between 9 and 14 genetic clusters, similar to the
148 range inferred in the microsatellite data, we therefore chose 9 clusters to take forward in the
149 analysis. As recommended by spline interpolation, we retained 7 principal components and we kept
150 2 of the linear discriminants from the subsequent discriminant analysis

151

152 *Assessment of spatial uniformity of sampling locations*

153 *Methods*

154 In order to assess the geographic uniformity of the sampling regimes in each data subset, we used
155 two measures of spatial patterns. The nearest neighbour distance distribution function (G), measures
156 the distance of each sampling location to its nearest neighbour (Ripley 1991). The L-function is a
157 transformation (for ease of interpretation) of Ripley's K-function (Ripley 1991), which measures
158 the number of sampling locations within a given radius from each point. K has the advantage of
159 assessing the uniformity of the sampling regime over multiple scales, as opposed to only measuring
160 distances between closest neighbours as with G. In both cases, the estimates of G or K from our
161 sampling locations were compared against random Poisson distributions, which would represent
162 uniformly spaced sampling locations. 5% and 95% confidence thresholds for these Poisson
163 distributions were also calculated to allow us to determine whether our sampling regimes
164 significantly deviated from random ($p < 0.05$). These calculations were performed using the Gest
165 and Lest functions (for G and L respectively) in the package "spatstats" in R (Baddeley & Turner
166 2005).

167

168 *Results*

169 Both methods used for the assessment of geographic uniformity of sampling locations shows that
170 the M1 dataset locations are more patchily distributed than those of the M2, M3 and RAD datasets
171 (**Error! Reference source not found.**).

172

173 *Additional discussion*174 *Population structure in northwest Europe*

175 An intriguing result lies in the genetic similarity between populations in England with those in
 176 Belgium and Germany. *C. carassius* has been designated as native to England, however this status
 177 has been contentious in the past (Maitland 1972). Under the assumption that it is native, and
 178 considering the observed diversity and divergence times between populations across mainland
 179 Europe, we would expect to see stronger population structure between English and continental
 180 Europe, which have been separated for approximately 7800 years (Coles 2000). Given the observed
 181 diversity between populations across mainland Europe, which, according to DIYABC analysis, has
 182 arisen relatively recently. Clearly further examination of this issue is warranted and molecular data
 183 would be a value addition to the current evidence, which is predominantly anecdotal.

184

185 SI table 1. Microsatellite loci used, grouped by their combinations in multiplex reactions. Multiplex primer
 186 mix ratios for PCR were chosen so as to give even peak strengths when analysing PCR products. Allele size
 187 ranges are those present in *C. carassius* for all 43 putatively pure crucian populations.

Locus	Multiplex #	Primer mix Ratios*	# Alleles	Allele size range	Ho	GenBank Accession no.	Reference
GF1	1	0.1	1	299	0	U35614	Zheng et al. 1995
GF17	1	0.1	2	182-186	0.024	U35616	Zheng et al. 1995
GF29	1	0.2	8	191-226	0.348	U35618	Zheng et al. 1995
J7	1	0.07	10	202-228	0.109	AY115095	Yue & Orban 2002
MFW2	1	0.1	1	161	0	-	Croojmans et al. 1997
Ca07	1	0.2	9	122-140	0.286	D85428	Yue & Orban 2004
TE Buffer	1	0.23					
J69	2.1	0.4	14	213-241	0.404	AY115106	Yue & Orban 2002
HJLY17	2.1	0.1	9	152-168	0.223	DQ378986	Zhi-Ying et al. 2006
HJLY35	2.1	0.1	18	261-307	0.377	DQ403242	Zhi-Ying et al. 2006
TE Buffer	2.1	0.4					
J20	2.2	0.2	9	171-218	0.149	AY115099	Yue & Orban 2002
J58	2.2	0.1	14	119-147	0.398	-	Yue & Orban 2002
MFW7	2.2	0.35	25	160-206	0.464	-	Croojmans et al. 1997
MFW17	2.2	0.35	26	185-262	0.41	-	Croojmans et al. 1997

188 * All primers used at 10mM per ul concentration, diluted in ddH2O from 100mM per ul stock

189 SI table 2. Genbank accession numbers for the mtDNA sequences used in this study.

Sample code	Accession number
FIN5_01	KT630314
FIN5_02	KT630315
FIN5_03	KT630316
EST1_02	KT630317
GER1_01	KT630318
EST1_01	KT630319
GER1_03	KT630320
FIN6_01	KT630321
FIN6_02	KT630322
FIN6_03	KT630323
BEL1_03	KT630324
EST1_03	KT630325
GER2_02	KT630326
GER2_03	KT630327
GER4_02	KT630328
NOR1_01	KT630329
NOR1_02	KT630330
SWE11_01	KT630331
SWE11_02	KT630332
SWE11_03	KT630333
RUS2_02	KT630334
RUS4_01	KT630335
RUS4_03	KT630336
FIN1_01	KT630337
FIN1_02	KT630338
FIN1_03	KT630339
FIN4_01	KT630340
FIN4_02	KT630341
FIN4_03	KT630342
POL4_01	KT630343
POL4_02	KT630344
POL4_03	KT630345
RUS1_01	KT630346
RUS1_02	KT630347
RUS1_03	KT630348
SWE8_01	KT630349
SWE8_02	KT630350
SWE8_03	KT630351
POL3_01	KT630352
POL3_02	KT630353
POL3_03	KT630354
SWE4_01	KT630355
SWE4_02	KT630356
SWE4_03	KT630357
RUS3_01	KT630358
RUS3_03	KT630359
RUS3_04	KT630360
RUS2_01	KT630361
RUS4_02	KT630362
BLS_03	KT630363
RUS3_02	KT630364
SWE3_01	KT630365
SWE3_02	KT630366
SWE3_03	KT630367
SWE2_01	KT630368
SWE2_02	KT630369
SWE2_03	KT630370
SWE9_01	KT630371
SWE9_02	KT630372
SWE9_03	KT630373
GBR7_01	KT630374
GBR6_01	KT630375
GBR8_01	KT630376
GBR8_02	KT630377
GBR8_03	KT630378
GBR6_02	KT630379
GBR6_03	KT630380
CZE1_01	KT630381
CZE1_02	KT630382
CZE1_03	KT630383
GER4_01	KT630384
GER4_03	KT630385
GER1_02	KT630386
GER2_01	KT630387
FIN3_01	KT630388
FIN3_02	KT630389
FIN3_03	KT630390
HUN1_02	KT630391
GER3_01	KT630392
GER3_02	KT630393
GER3_03	KT630394

191 SI table 3. Haplotype memberships for 101 Cytochrome B sequences used in Fig. 2.

Lineage	Haplotype	N	Drainage (n populations)	Sample code	
1	1	3	Baltic	FIN5 1-3	
	2	1	Baltic	EST1 2	
	3	49	Elbe(2), Baltic(9), Scheldt(1), Rhine(2), North sea(2), Vistula(6), Volga(4), Don(3), Danube(1), Hunte(4)	GER1 1,3, EST1 1, 3, SWE6 1 -3, BEL1 3 , GER2 2, 3, GER4 2, NOR 1, 2, SWE11 1-3, RUS2 2, RUS4 1, 3, FIN1 1-3, FIN4 1-3, POL4 1-3, RUS1 1-3, SWE8 1-3, POL5 1-3, SWE4 1-3, RUS3 1, 3, 4, CZE2 1, GER6 1 – 4, SWE14 1, SWE15 1	
	4	1	Volga	RUS2 1	
	5	1	Baltic	RUS4 2	
	6	1	Dnieper	BLS 3	
	7	1	Volga	RUS3 2	
	8	3	Baltic	SWE3 1-3	
	9	2	Baltic	SWE2 1 - 3	
	10	3	Baltic	SWE9 1-3	
2	11	13	UK(4), Rhine(1), Baltic (2)	GBR7 1, GBR6 1-3, GBR8 1-3, NET 1, GER5 1-3, GBR12 1, 2	
	12	3	Baltic	FIN3 1-3	
	13	3	Danube	GER4 1, 2, AUS3 1	
	14	3	Elbe(1), Rhine(1), Danube(1)	GER1 2, GER2 1, AUS2 1	
	15	1	Danube	CZE1 1	
	16	1	Danube	CZE1 2	
	17	1	Danube	CZE1 3	
	18	2	Danube	HUN 1, 2	
	19	3	Danube	GER3 1-3	
	23	1	Elbe	CZE2 2	
	24	2	Danube	AUS1 1, 2	
	25	2	Lahn	GER7 1, 2	
	Outgroup	20	1		Ccarp 1
		21	1		Ccarp 2
		22	1		Ccarp 3

192

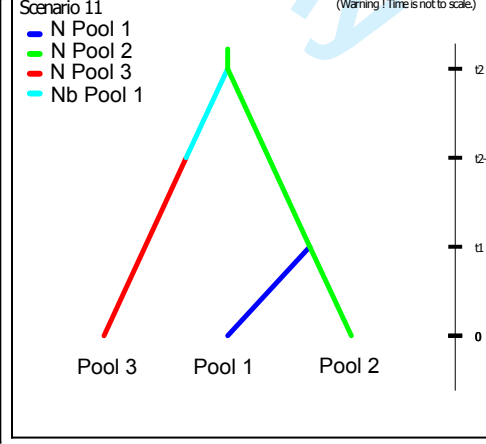
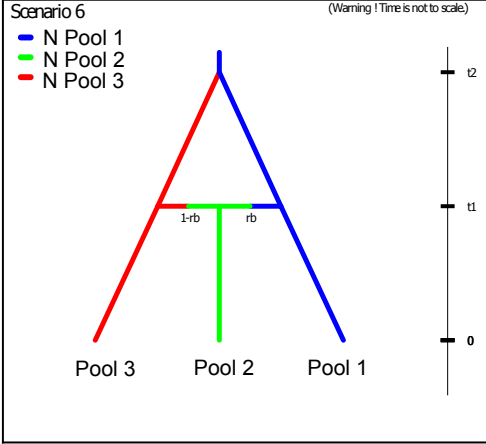
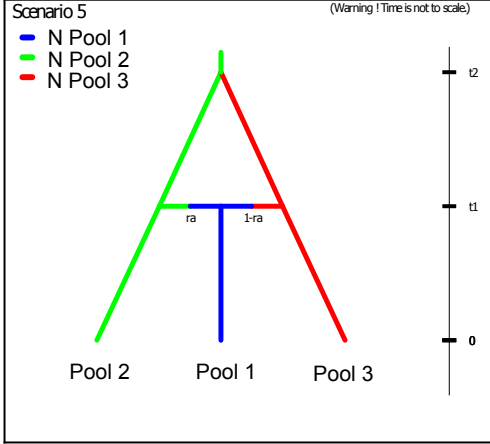
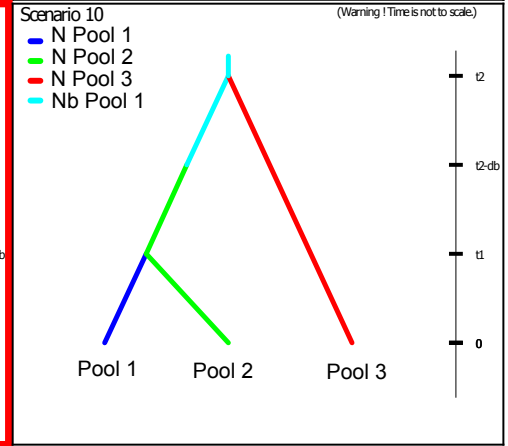
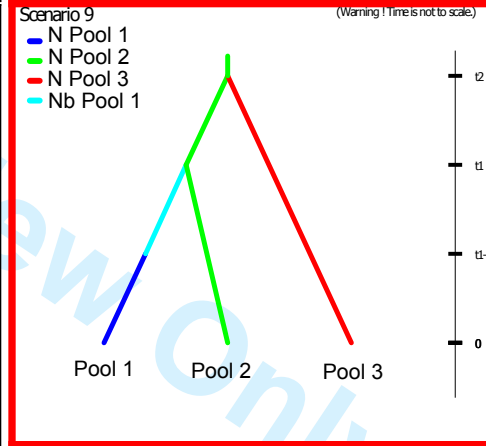
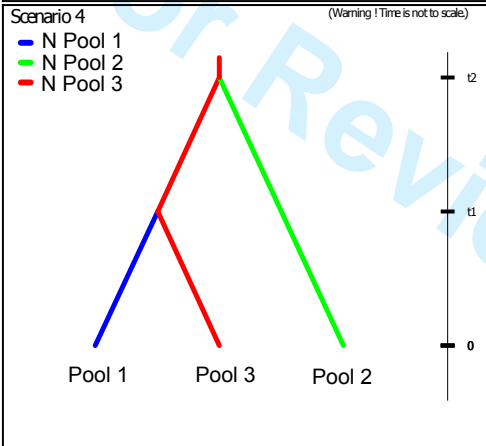
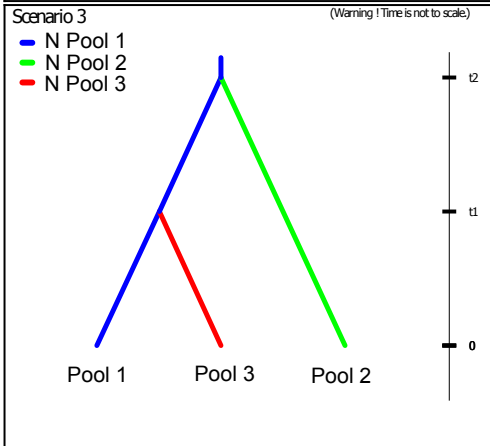
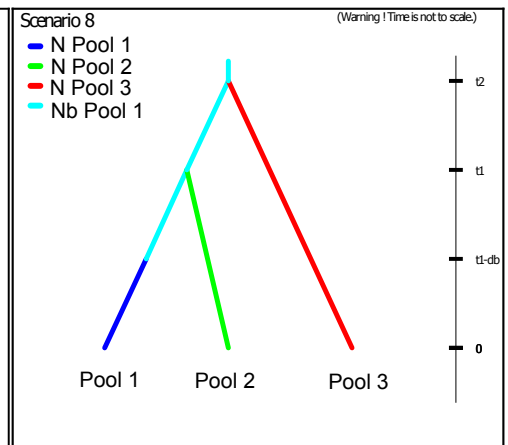
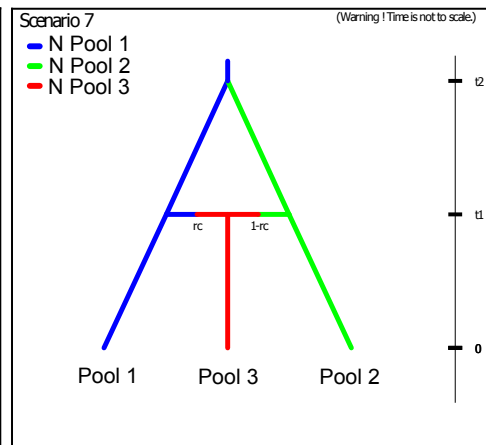
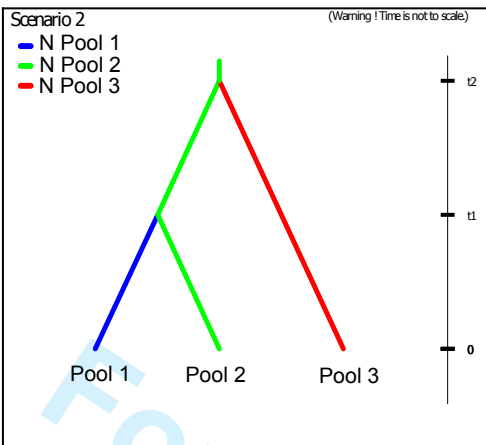
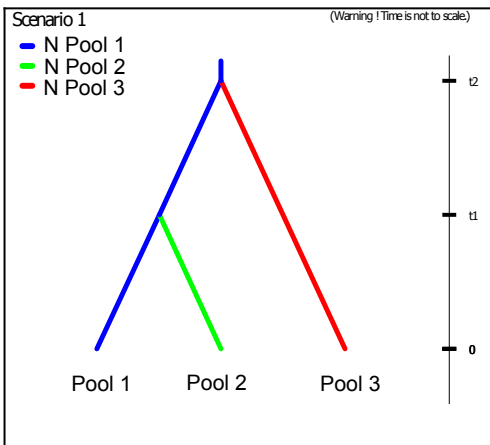
193

194

195 SI table 4. Pairwise FST values calculated using the M1 dataset.

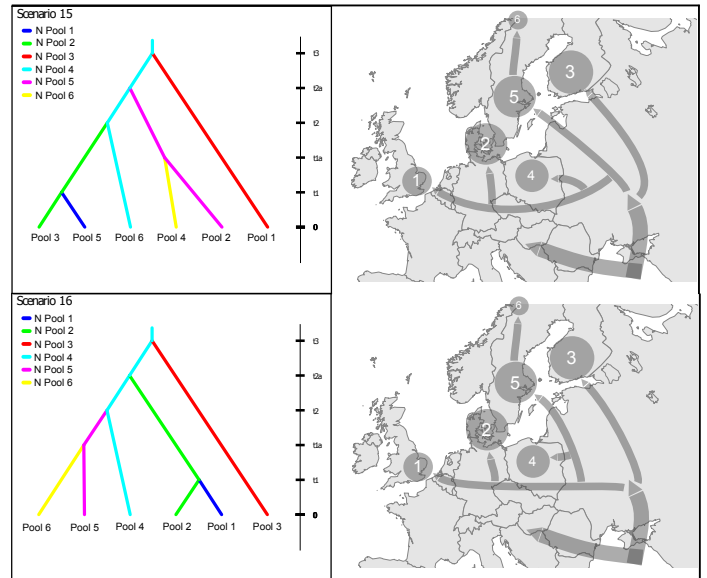
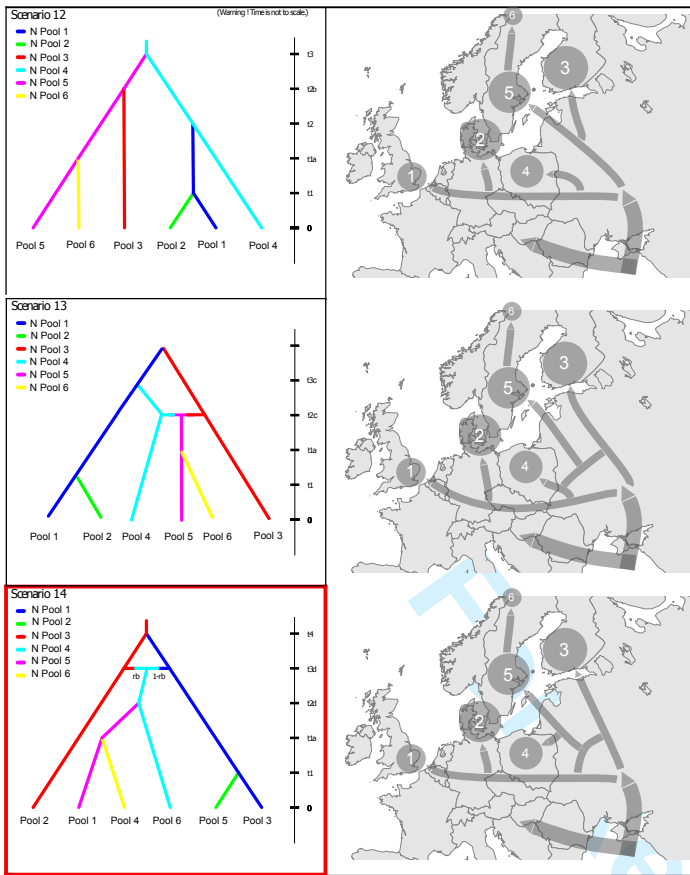
	GBR1	GBR2	GBR4	BEL1	BEL2	BEL3	FIN1	RUS4*	FIN2	CZE1	GER2	GER3	GER4	POL1	POL2	POL3	POL4	GBR7	GBR3	GBR8	GBR9	GBR11	GBR5	GBR6	GBR10	SWE4	SWE3	SWE5	FIN6	SWE7	SWE2	SWE1	SWE9	SWE10	SWE11	SWE8	FIN5	FIN3	FIN4	EST1	EST2	BLS	RUS1	DEN1	SWE12	DEN2	NOR2	SWE14	DEN3
GBR1		0.307	0.531	0.312	0.198	0.346	0.785	0.472	0.407	0.604	0.256	0.613	0.628	0.226	0.291	0.342	0.368	0.436	0.364	0.378	0.518	0.317	0.517	0.302	0.376	0.479	0.444	0.419	0.458	0.542	0.591	0.404	0.839	0.548	0.793	0.39	0.428	0.72	0.596	0.628	0.526	0.491	0.623	0.319	0.626	0.261	0.768	0.457	0.233
GBR2	NS		0.67	0.316	0.247	0.366	0.783	0.482	0.446	0.588	0.332	0.6	0.618	0.266	0.309	0.357	0.378	0.611	0.535	0.562	0.716	0.381	0.651	0.451	0.501	0.476	0.478	0.443	0.518	0.566	0.594	0.396	0.853	0.616	0.826	0.454	0.444	0.725	0.572	0.645	0.522	0.459	0.59	0.346	0.664	0.357	0.864	0.454	0.268
GBR4	*	NS		0.588	0.445	0.532	0.774	0.498	0.327	0.69	0.267	0.708	0.716	0.19	0.325	0.315	0.484	0.15	0.401	0.288	0.223	0.248	0.185	0.432	0.145	0.508	0.41	0.433	0.422	0.543	0.57	0.402	0.817	0.506	0.774	0.501	0.439	0.717	0.601	0.663	0.497	0.488	0.683	0.472	0.648	0.362	0.627	0.525	0.312
BEL1	*	NS	*		0.065	0.023	0.732	0.479	0.427	0.601	0.253	0.609	0.617	0.284	0.293	0.359	0.347	0.512	0.36	0.442	0.523	0.295	0.502	0.291	0.436	0.449	0.447	0.446	0.483	0.524	0.586	0.412	0.8	0.583	0.75	0.47	0.436	0.696	0.569	0.614	0.481	0.467	0.608	0.363	0.569	0.362	0.73	0.462	0.283
BEL2	*	NS	*	NS		0	0.711	0.438	0.363	0.571	0.195	0.582	0.588	0.193	0.24	0.288	0.296	0.396	0.24	0.361	0.38	0.156	0.356	0.249	0.278	0.39	0.395	0.374	0.393	0.465	0.525	0.359	0.779	0.536	0.705	0.425	0.359	0.673	0.508	0.558	0.394	0.398	0.57	0.327	0.523	0.287	0.683	0.422	0.198
BEL3	NS	NS	*	NS	NS		0.724	0.447	0.382	0.563	0.204	0.573	0.581	0.232	0.249	0.303	0.296	0.472	0.306	0.423	0.482	0.215	0.439	0.279	0.353	0.407	0.412	0.381	0.418	0.474	0.54	0.368	0.807	0.561	0.731	0.462	0.369	0.686	0.521	0.577	0.41	0.39	0.559	0.352	0.534	0.34	0.738	0.428	0.233
FIN1	*	NS	*	*	*	*		0.498	0.537	0.742	0.586	0.746	0.745	0.513	0.475	0.508	0.532	0.745	0.761	0.738	0.797	0.695	0.763	0.718	0.737	0.419	0.515	0.532	0.587	0.627	0.55	0.437	0.75	0.642	0.796	0.685	0.56	0.569	0.43	0.521	0.456	0.487	0.717	0.632	0.697	0.666	0.676	0.485	0.591
RUS4*	*	*	*	*	*	*		0.309	0.484	0.33	0.506	0.51	0.311	0.3	0.286	0.334	0.462	0.416	0.482	0.5	0.41	0.434	0.442	0.437	0.291	0.301	0.215	0.191	0.354	0.367	0.262	0.555	0.38	0.462	0.433	0.286	0.494	0.304	0.28	0.113	0.231	0.495	0.367	0.455	0.371	0.522	0.27	0.317	
FIN2	*	NS	*	*	*	*	*		0.488	0.225	0.526	0.521	0.191	0.142	0.125	0.235	0.286	0.302	0.325	0.395	0.286	0.314	0.312	0.302	0.284	0.142	0.166	0.161	0.212	0.295	0.172	0.649	0.271	0.482	0.271	0.182	0.442	0.289	0.28	0.137	0.168	0.484	0.265	0.264	0.206	0.448	0.193	0.159	
CZE1	NS	NS	*	*	*	*	*	*		0.38	0.342	0.364	0.43	0.421	0.364	0.462	0.573	0.546	0.572	0.672	0.596	0.637	0.555	0.571	0.471	0.444	0.347	0.408	0.445	0.587	0.456	0.791	0.555	0.615	0.448	0.395	0.69	0.535	0.479	0.402	0.388	0.477	0.384	0.484	0.44	0.677	0.418	0.408	
GER2	*	NS	*	*	*	*	*	*	*		0.379	0.381	0.146	0.189	0.181	0.232	0.142	0.111	0.113	0.269	0.177	0.226	0.139	0.168	0.263	0.256	0.2	0.186	0.275	0.39	0.226	0.654	0.355	0.507	0.207	0.22	0.552	0.351	0.358	0.228	0.237	0.458	0.168	0.337	0.146	0.453	0.299	0.128	
GER3	NS	NS	*	*	*	NS	*	*	*	NS	*		0.113	0.445	0.445	0.397	0.48	0.579	0.543	0.567	0.673	0.61	0.649	0.542	0.57	0.502	0.492	0.402	0.454	0.492	0.609	0.489	0.805	0.589	0.642	0.438	0.441	0.708	0.532	0.499	0.435	0.412	0.472	0.411	0.54	0.467	0.691	0.47	0.435
GER4	NS	NS	*	*	*	NS	*	*	*	NS	*	NS		0.442	0.443	0.399	0.465	0.584	0.553	0.569	0.687	0.612	0.661	0.546	0.575	0.488	0.487	0.387	0.45	0.494	0.61	0.486	0.812	0.593	0.657	0.439	0.435	0.697	0.54	0.501	0.435	0.405	0.492	0.415	0.542	0.481	0.703	0.463	0.431
POL1	*	*	*	*	*	*	*	*	*	*	*	*	*		0.105	0.074	0.191	0.182	0.202	0.242	0.21	0.153	0.175	0.237	0.105	0.218	0.195	0.194	0.183	0.246	0.3	0.187	0.587	0.317	0.477	0.235	0.186	0.487	0.259	0.298	0.156	0.161	0.426	0.194	0.314	0.138	0.356	0.246	0.111
POL2	*	*	*	*	*	*	*	*	*	*	*	*	*	*		0.061	0.113	0.292	0.253	0.317	0.358	0.237	0.298	0.243	0.242	0.241	0.148	0.149	0.169	0.111	0.219	0.146	0.598	0.266	0.417	0.244	0.112	0.438	0.228	0.239	0.125	0.114	0.427	0.203	0.184	0.157	0.422	0.17	0.124
POL3	*	NS	*	*	*	NS	*	*	*	*	*	*	*	*	*		0.142	0.31	0.271	0.368	0.392	0.234	0.274	0.294	0.227	0.246	0.16	0.16	0.185	0.214	0.283	0.154	0.642	0.253	0.448	0.26	0.154	0.456	0.197	0.261	0.086	0.057	0.355	0.203	0.268	0.155	0.427	0.194	0.117
POL4	*	NS	*	*	*	*	*	*	*	*	*	NS	*	*	*	*		0.416	0.301	0.418	0.491	0.323	0.413	0.281	0.358	0.263	0.285	0.184	0.246	0.24	0.34	0.22	0.69	0.391	0.547	0.344	0.211	0.446	0.269	0.269	0.204	0.177	0.464	0.266	0.286	0.261	0.53	0.257	0.202
GBR7	*	NS	*	*	*	*	*	*	*	*	*	*	*	*	*	*		0.153	0.072	0.364	0.164	0.244	0.286	0.134	0.497	0.405	0.388	0.391	0.514	0.529	0.321	0.8	0.452	0.74	0.355	0.426	0.685	0.542	0.63	0.424	0.406	0.608	0.37	0.606	0.277	0.637	0.499	0.279	
GBR3	NS	NS	*	NS	NS	NS	*	*	NS	NS	NS	NS	NS	*	*	*	NS		0.021	0.422	0.09	0.336	0.097	0.22	0.435	0.387	0.322	0.343	0.479	0.525	0.297	0.827	0.516	0.751	0.284	0.364	0.673	0.509	0.573	0.396	0.394	0.592	0.232	0.591	0.182	0.752	0.442	0.175	
GBR8	*	*	*	*	*	*	*	*	*	*	*	*	*	*	*	*	*	NS		0.42	0.184	0.31	0.181	0.22	0.518	0.444	0.426	0.424	0.534	0.561	0.356	0.784	0.479	0.734	0.301	0.464	0.686	0.564	0.636	0.453	0.447	0.631	0.332	0.605	0.254	0.641	0.524	0.287	
GBR9	*	NS	*	*	*	*	*	*	*	*	*	NS	*	*	*	*	*	NS	*		0.205	0.021	0.38	0.159	0.577	0.483	0.528	0.517	0.661	0.621	0.458	0.841	0.528	0.814	0.61	0.529	0.728	0.651	0.723	0.519	0.495	0.652	0.553	0.751	0.504	0.757	0.608	0.395	
GBR11	*	NS	*	*	*	*	*	*	*	*	*	*	*	*	*	*	*	NS	*		0.178	0.235	0.138	0.369	0.346	0.342	0.336	0.438	0.475	0.285	0.746	0.509	0.689	0.368	0.344	0.641	0.46	0.542	0.342	0.384	0.603	0.287	0.52	0.211	0.584	0.418	0.161		
GBR5	NS	NS	*	*	*	*	*	*	*	*	*	*	*	*	*	*	*	NS	*	NS		0.339	0.161	0.452	0.367	0.387	0.365	0.538	0.555	0.375	0.819	0.489	0.759	0.489	0.398	0.681	0.561	0.604	0.401	0.415	0.619	0.422	0.645	0.366	0.655	0.483	0.27		
GBR6	*	NS	*	*	*	*	*	*	*	*	*	*	*	*	*	*	*	NS	*	*		0.278	0.452	0.39	0.358	0.36	0.463	0.533	0.366	0.773	0.474	0.686	0.293	0.387	0.634	0.513	0.519	0.398	0.413	0.599	0.272	0.511	0.235	0.666	0.429	0.228			
GBR10	NS	NS	*	*	*	*	*	*	*	*	*	NS	NS	*	*	*	*	NS	*	*		0.403	0.352	0.332	0.346	0.447	0.478	0.325	0.787	0.469	0.703	0.376	0.335	0.662	0.481	0.537	0.378	0.365	0.571										

For Review Only



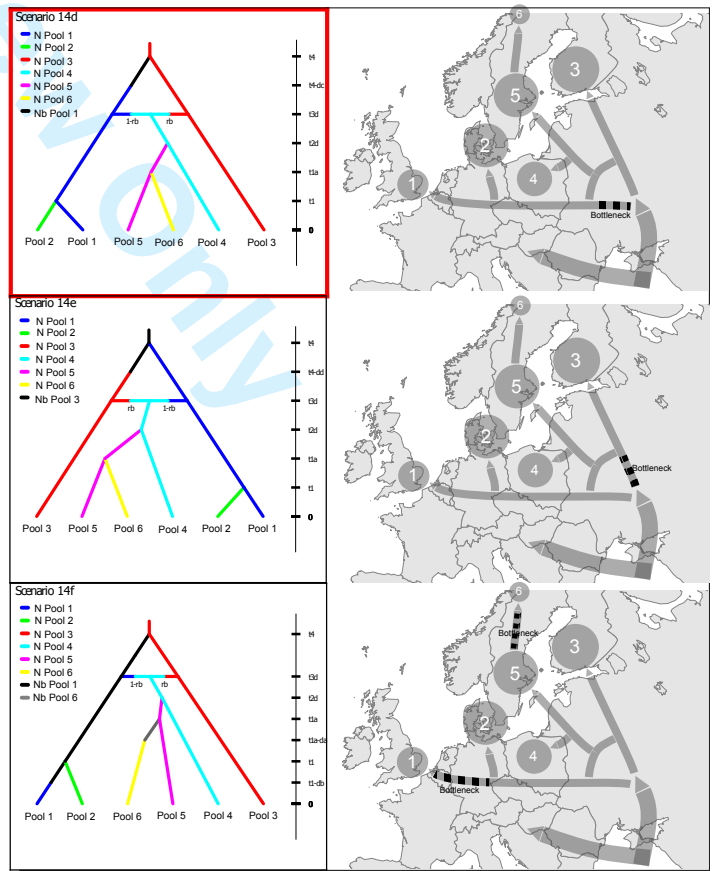
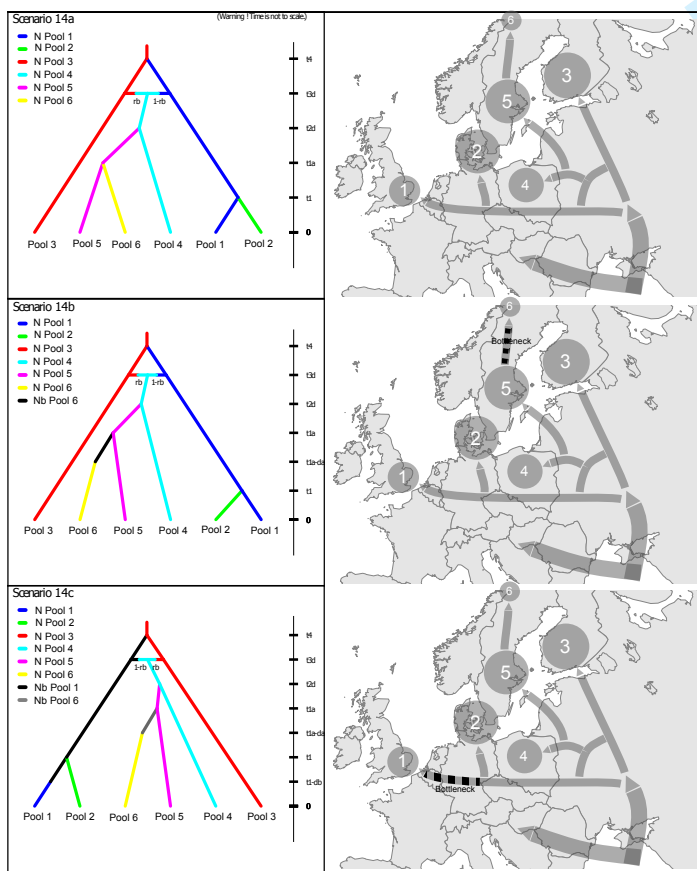
Pool 1 - Northern Europe
 Pool 2 - Don river
 Pool 3 - Danube River

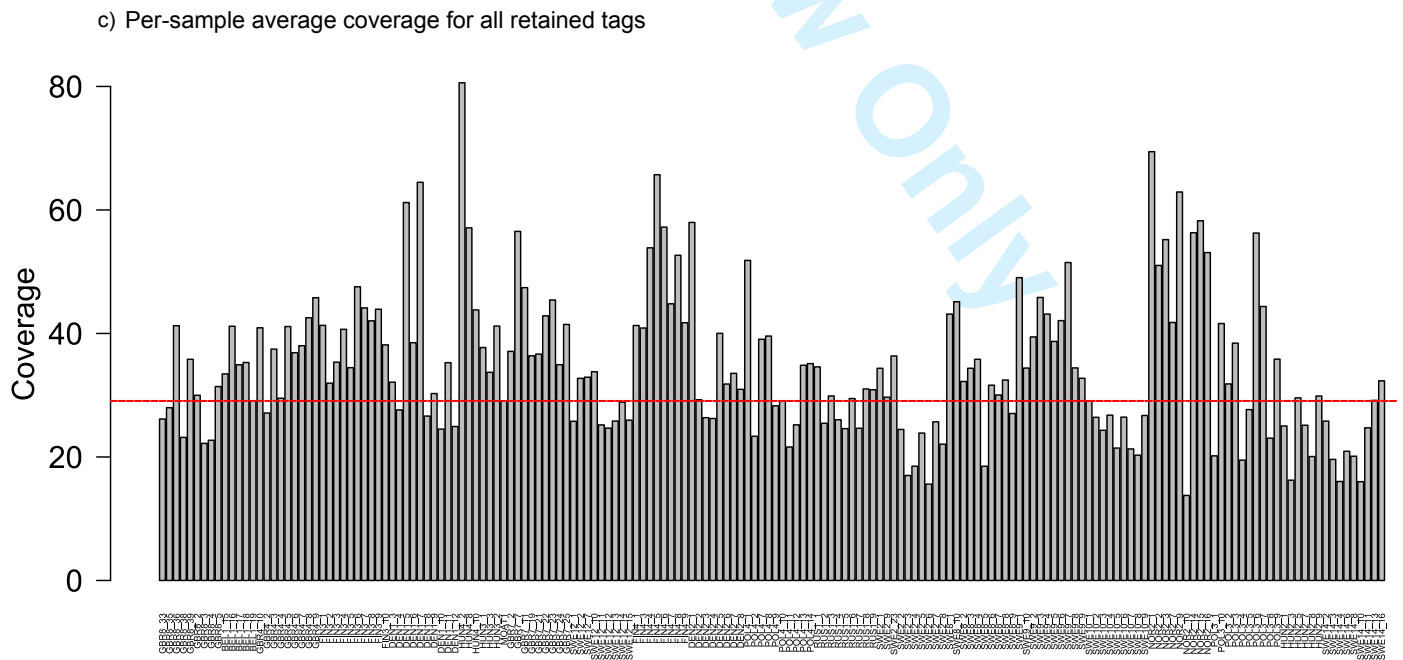
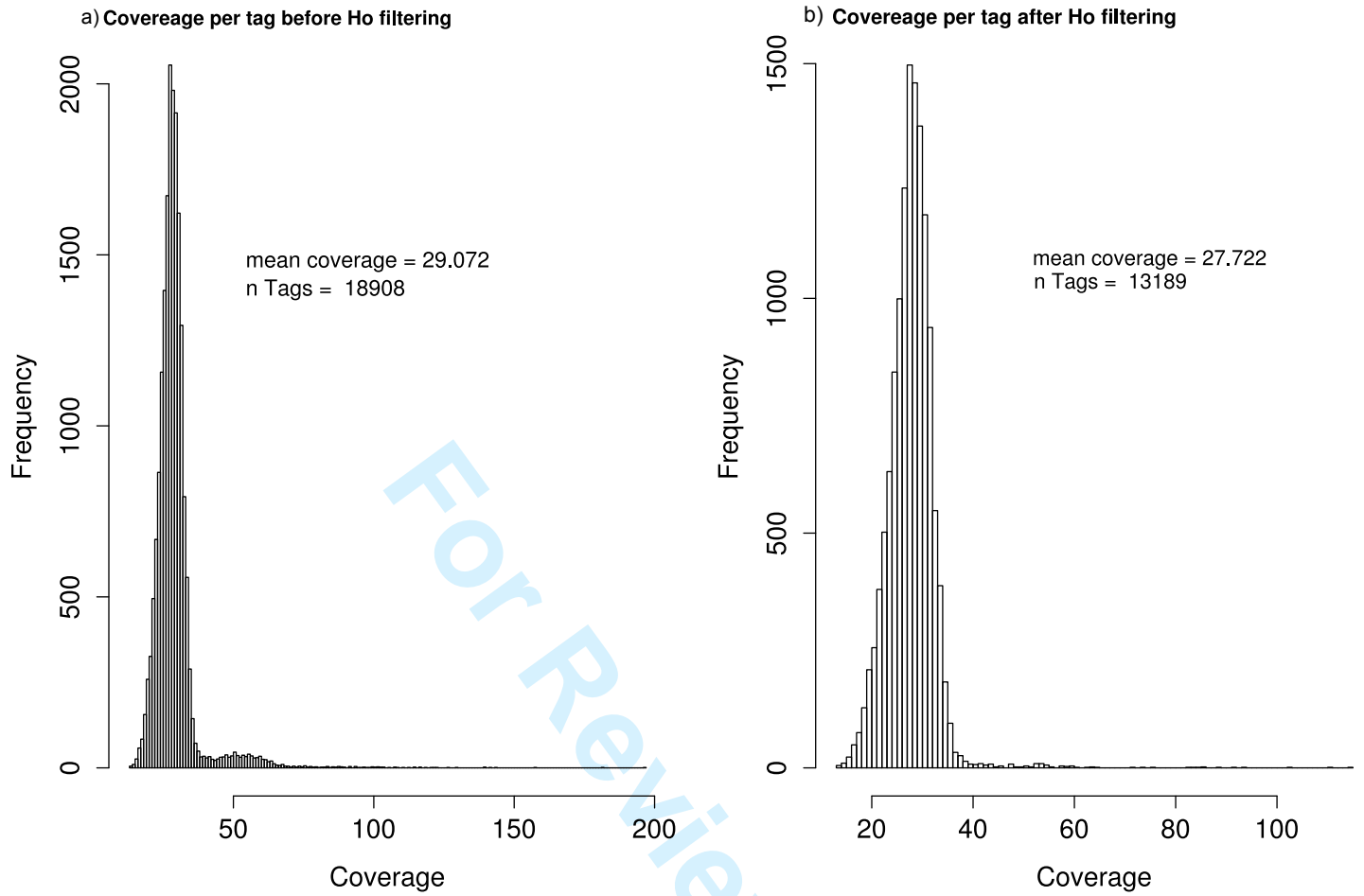
a) Stage 2. NEU Major variants



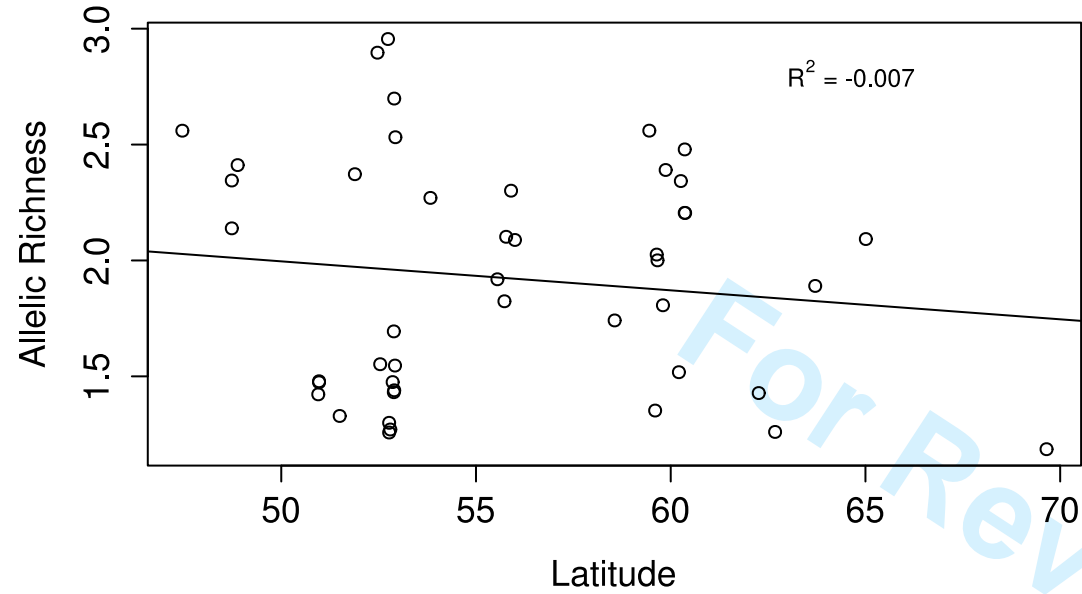
Pool 1 - UK
 Pool 2 - Denmark / S.Sweden
 Pool 3 - Finland
 Pool 4 - Poland
 Pool 5 - Sweden
 Pool 6 - Tromsø

b) Stage 3. Scenario 14 Minor variants

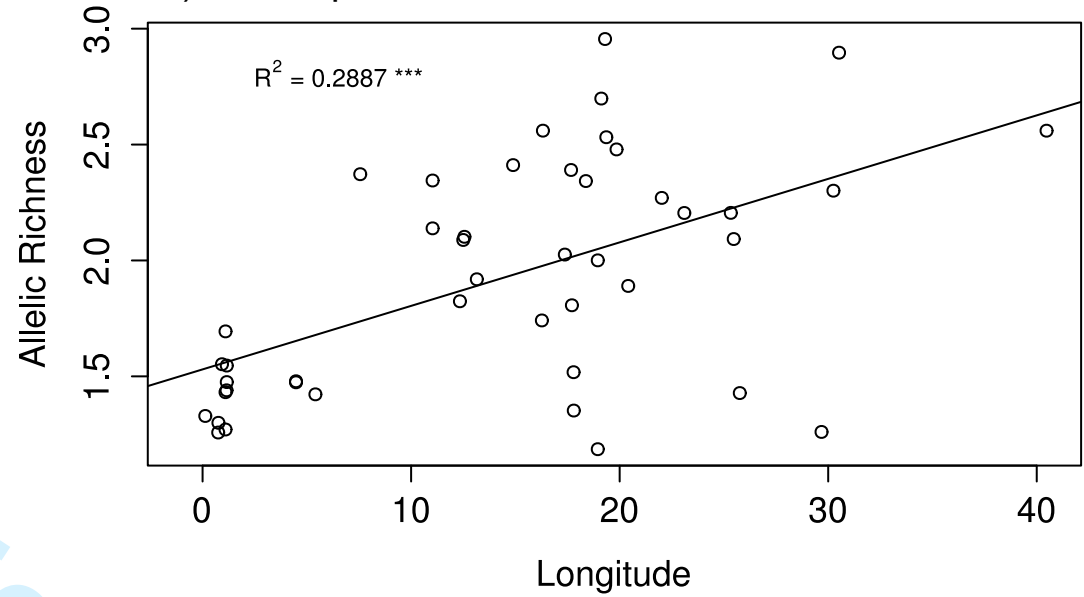




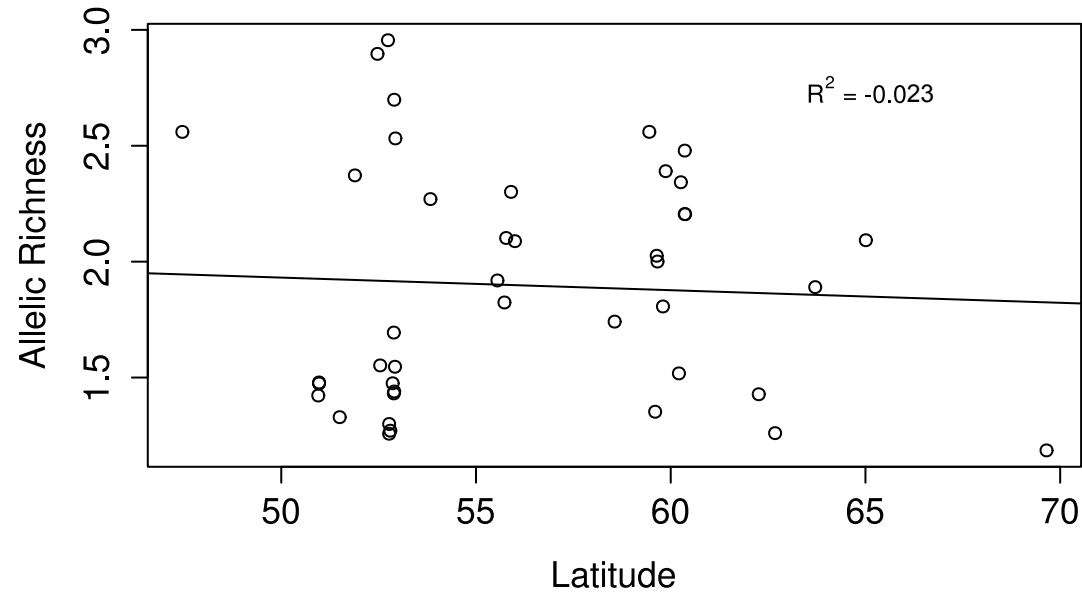
a) All samples



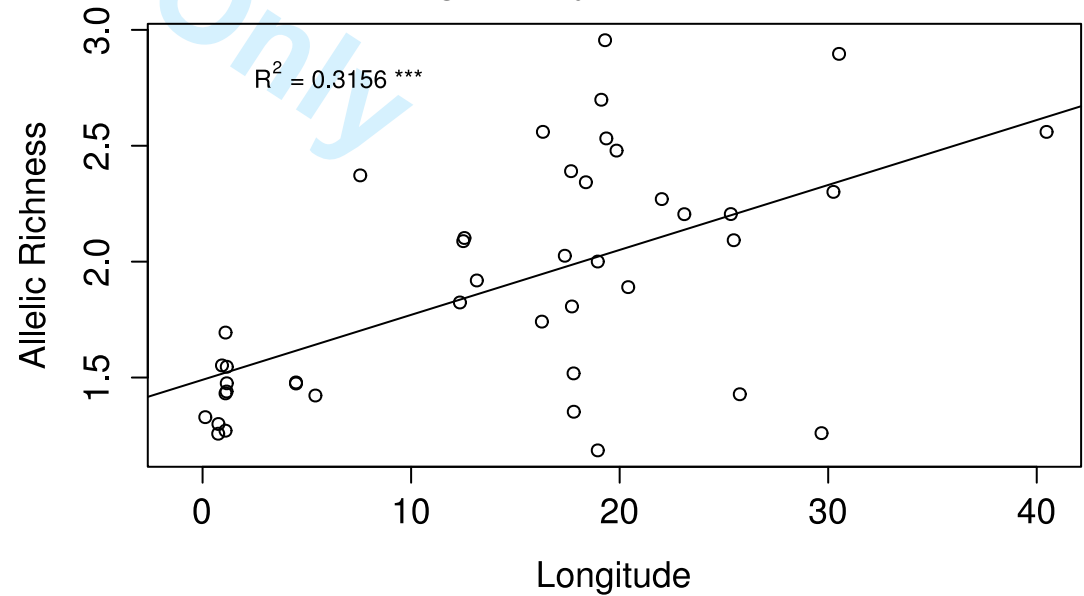
b) All samples

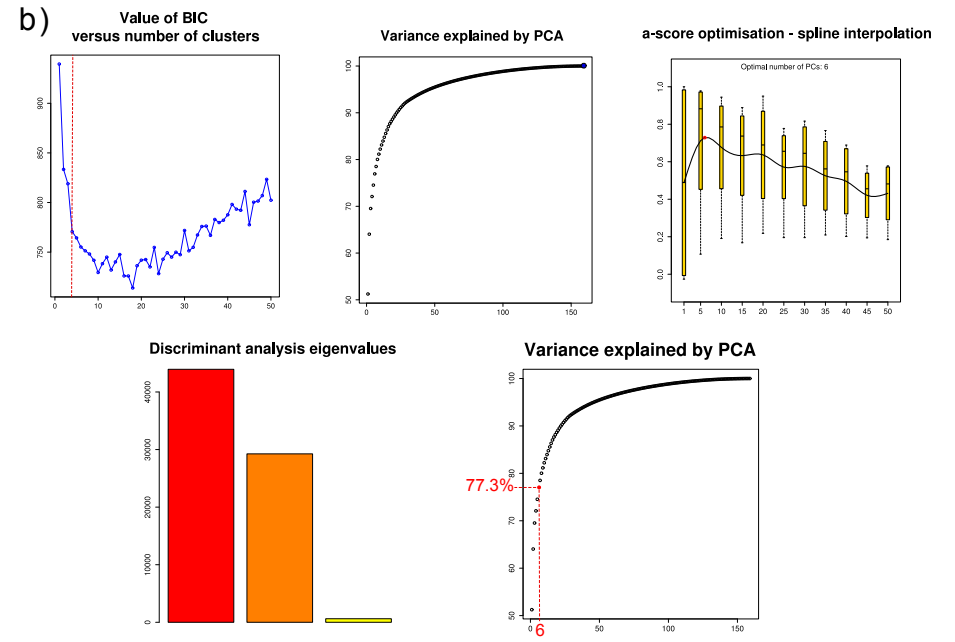
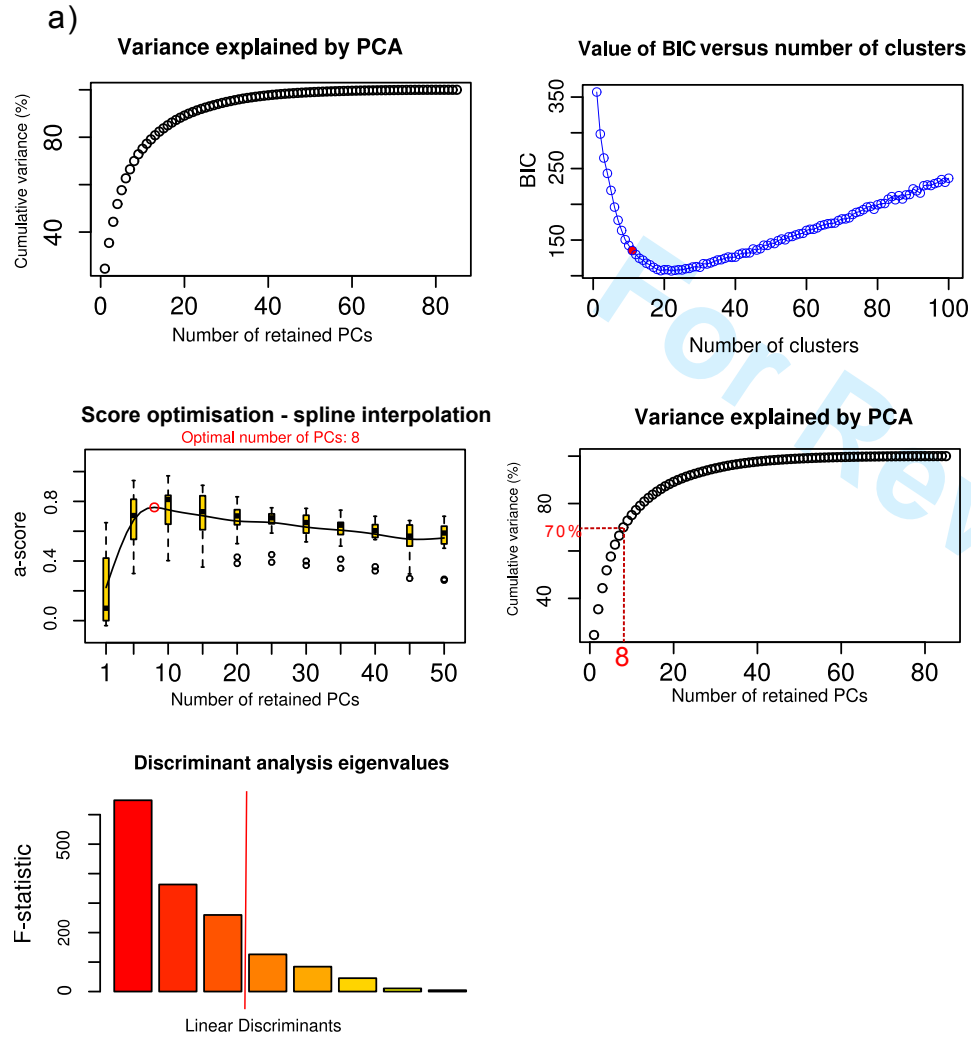


c) mtDNA Lineage 1 only

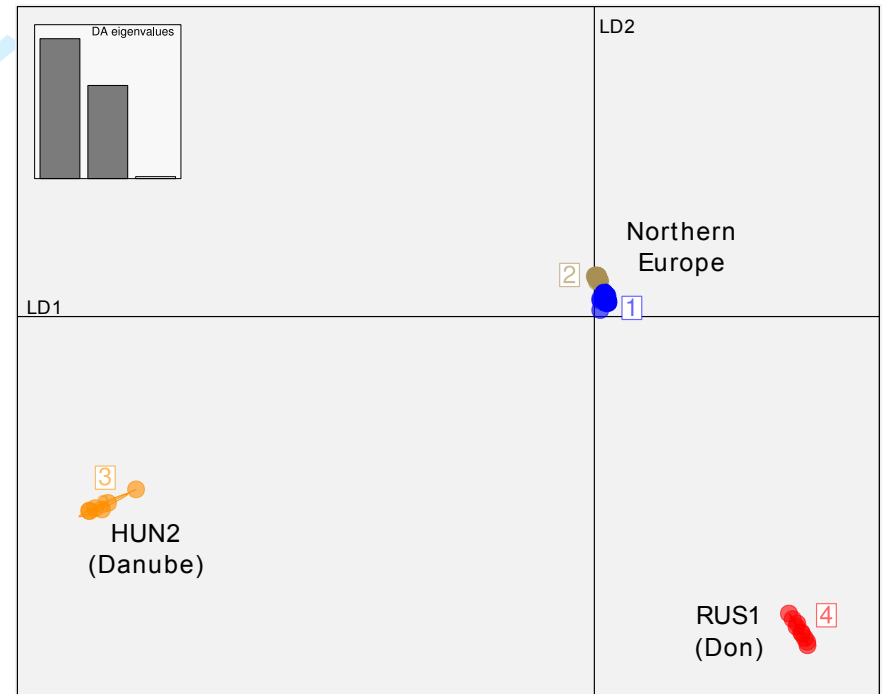


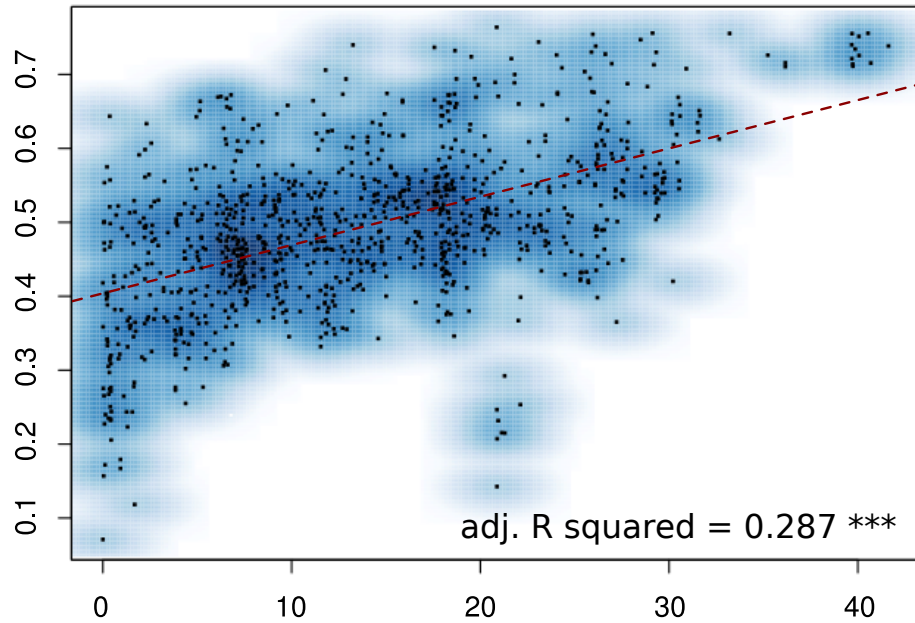
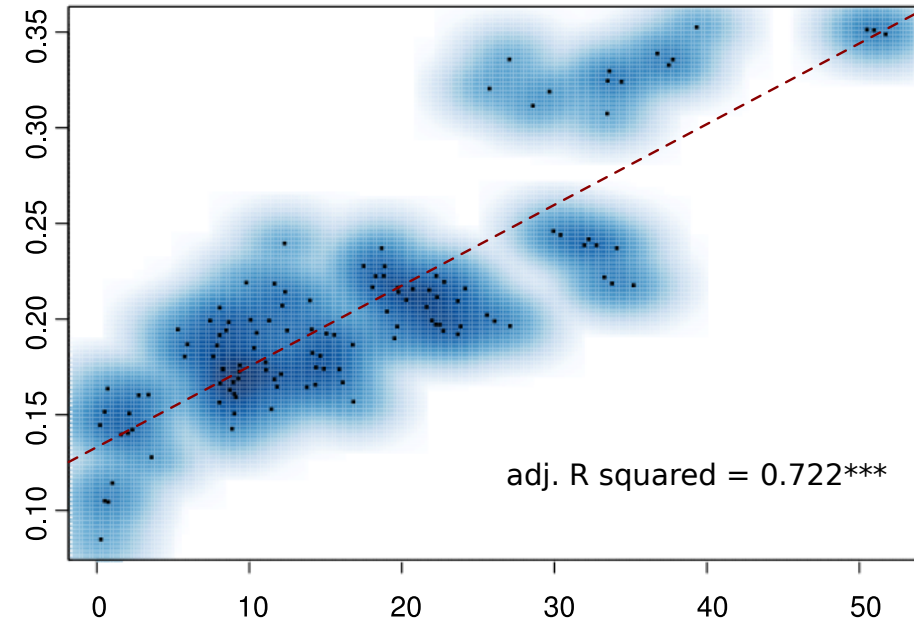
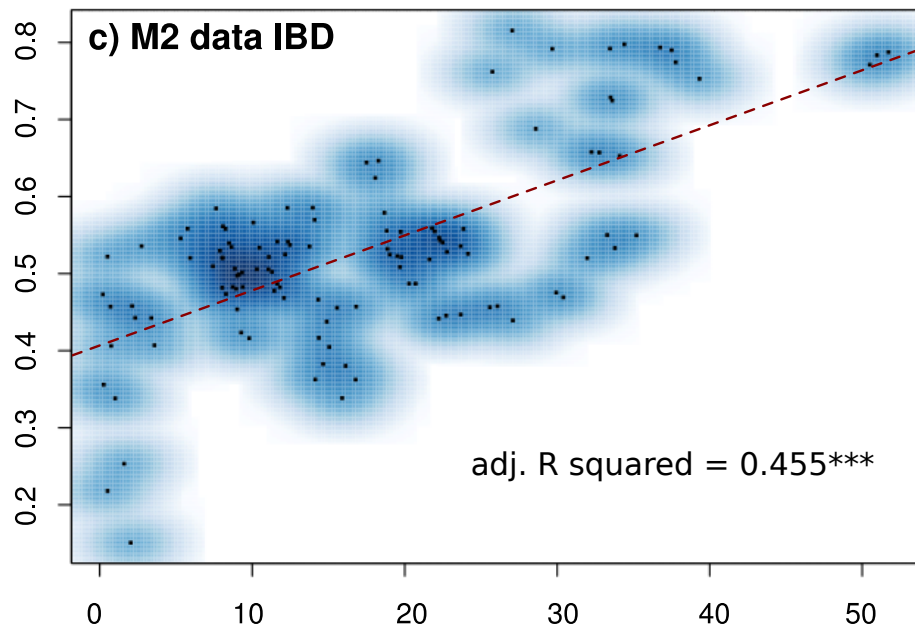
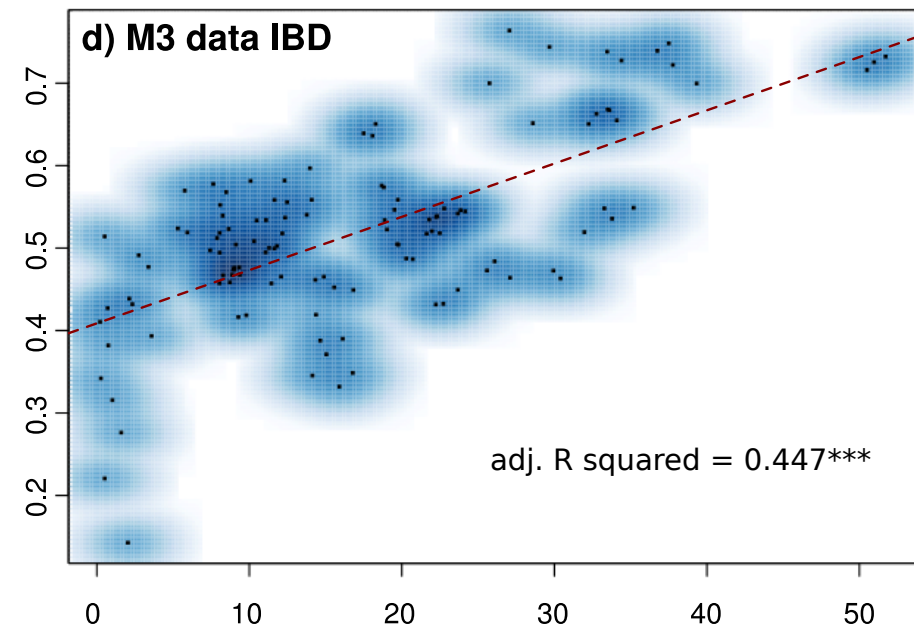
d) mtDNA Lineage 1 only

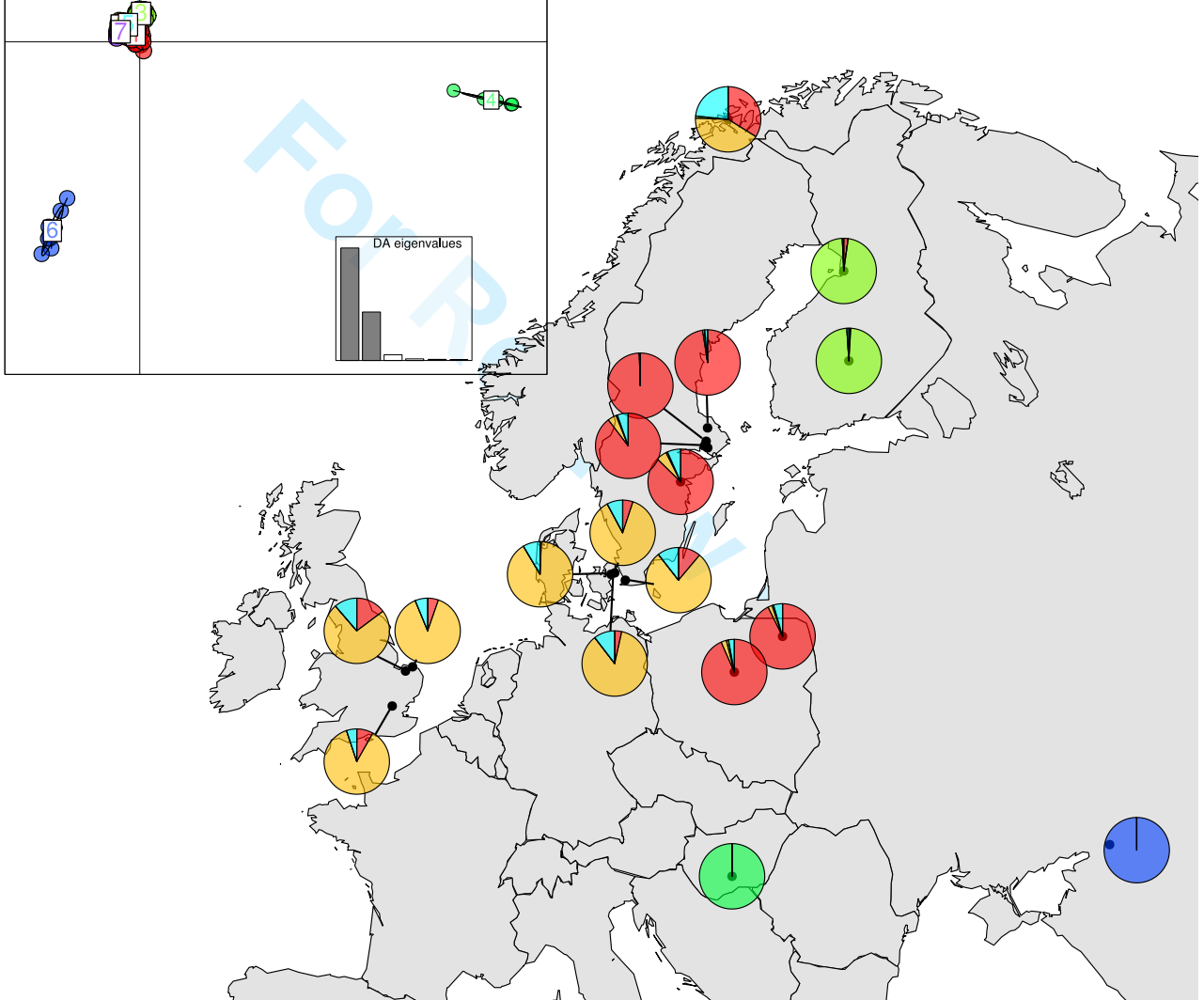


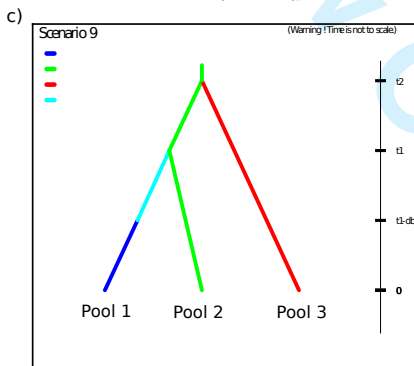
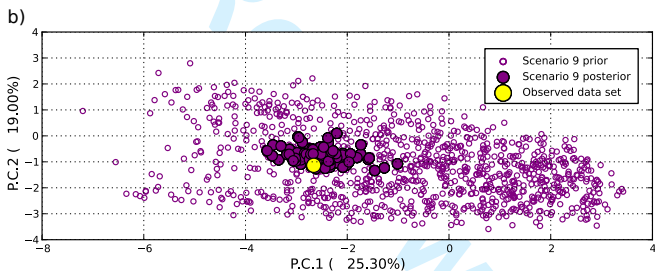
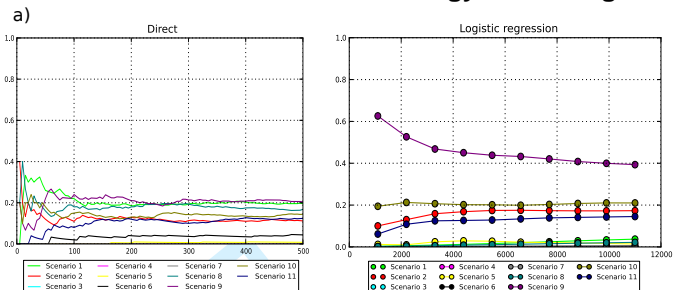


DAPC Scatter plot - Full RADseq dataset



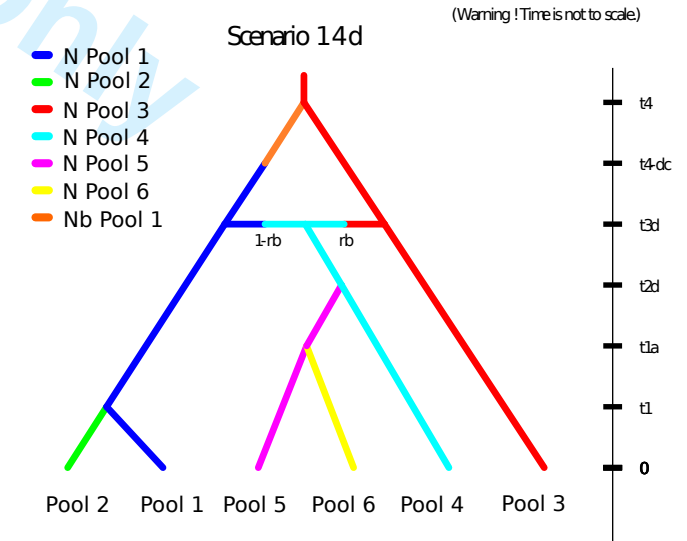
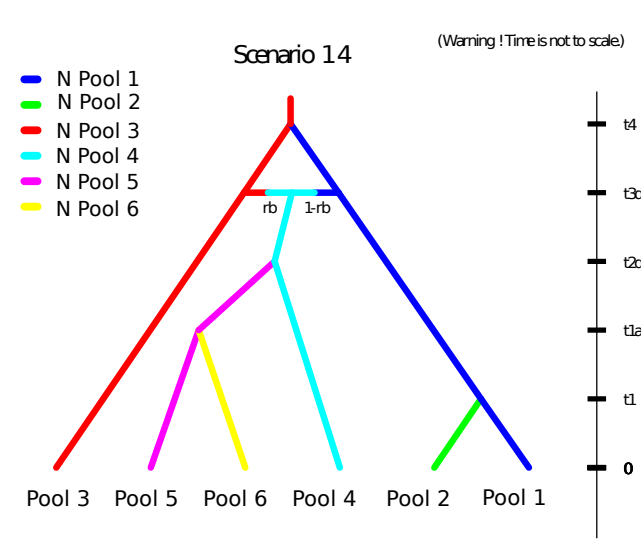
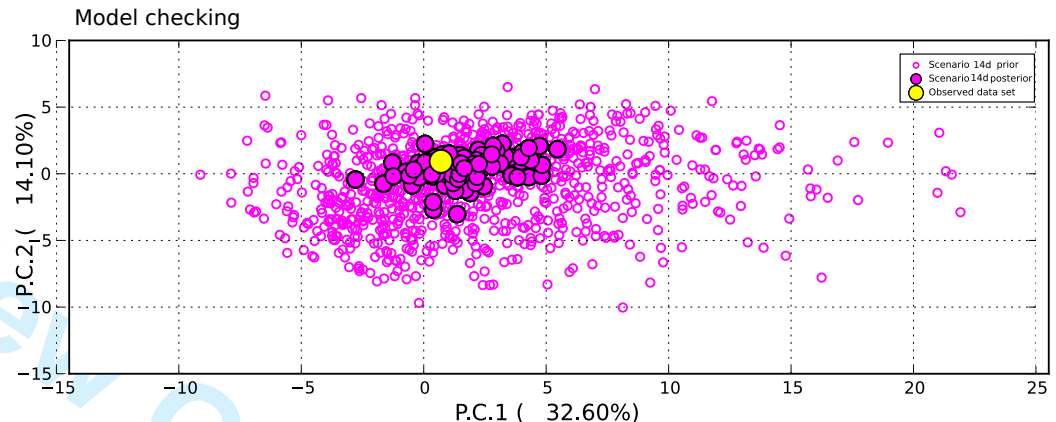
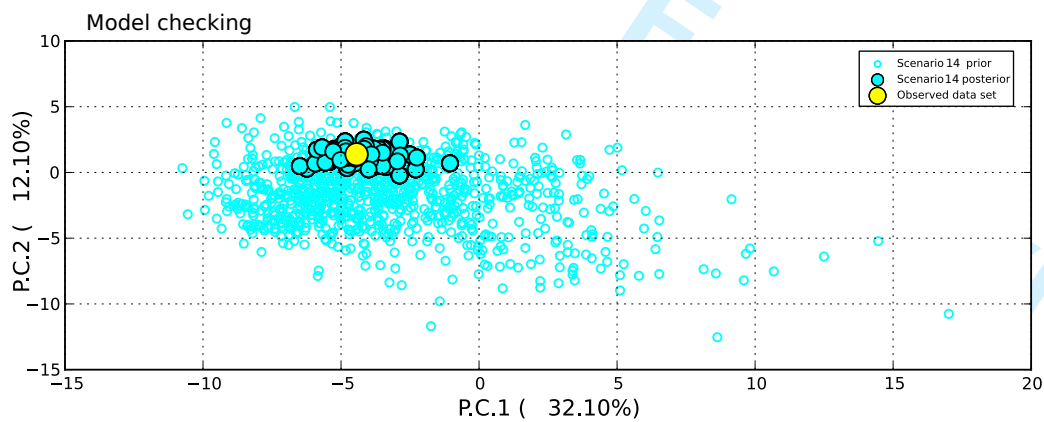
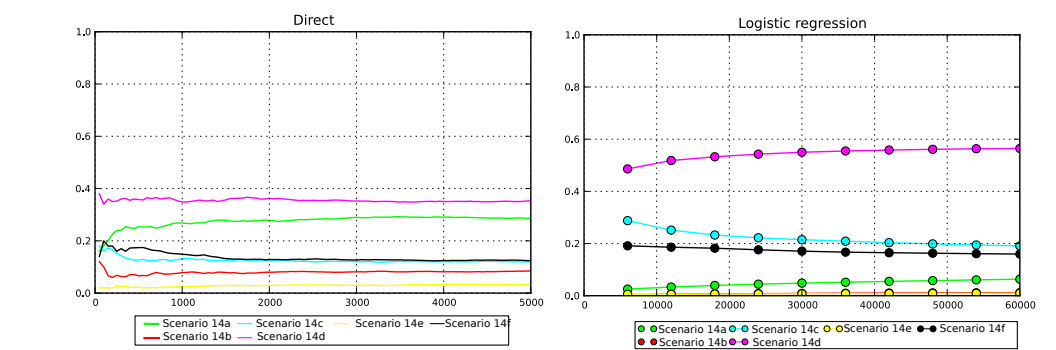
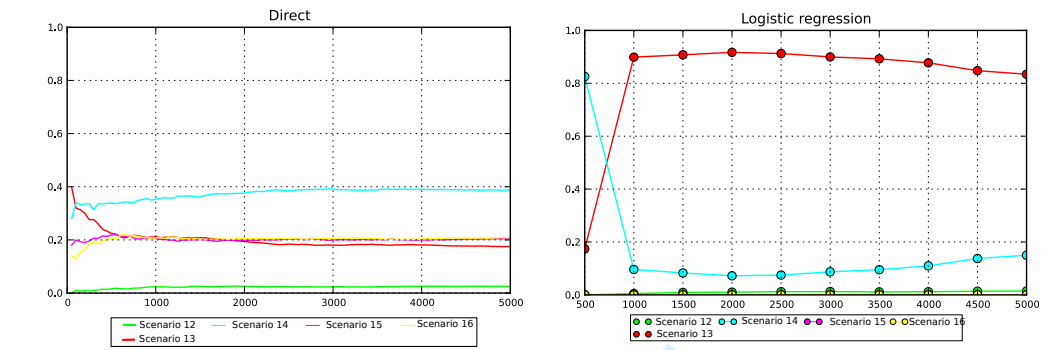
a) M1, Lineage 1 only (excluding NOR2)**b) RADseq data IBD****c) M2 data IBD****d) M3 data IBD**





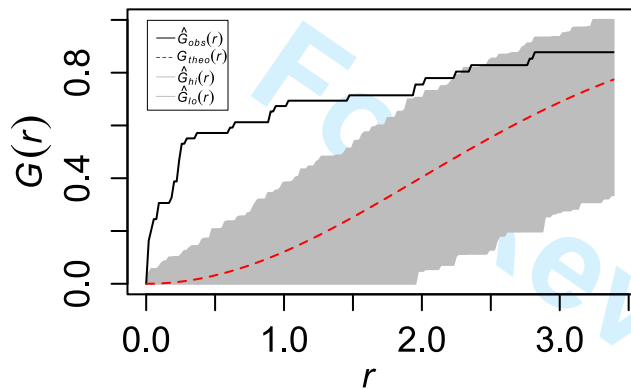
a) Stage 2. NEU major variants

b) Stage 3. NEU minor variants

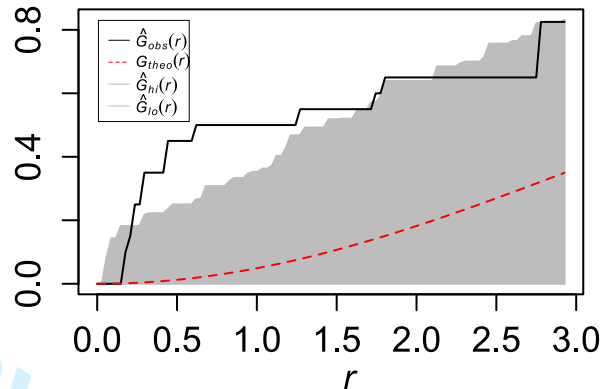


(Warning ! Time is not to scale)

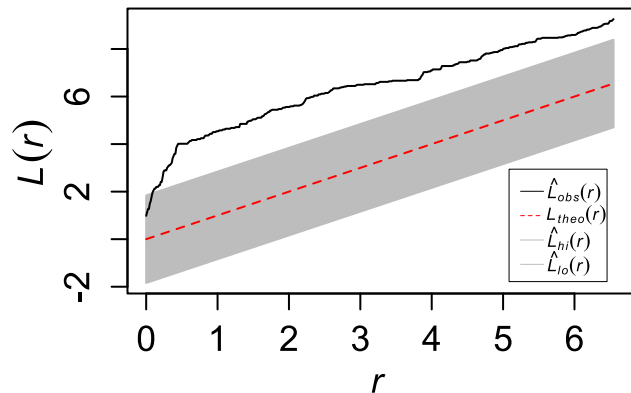
M1 Gest



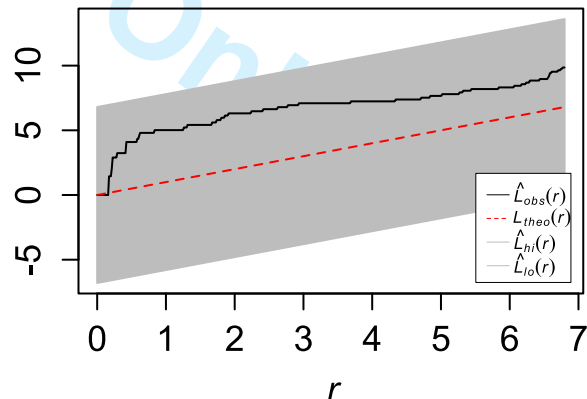
M2 Gest



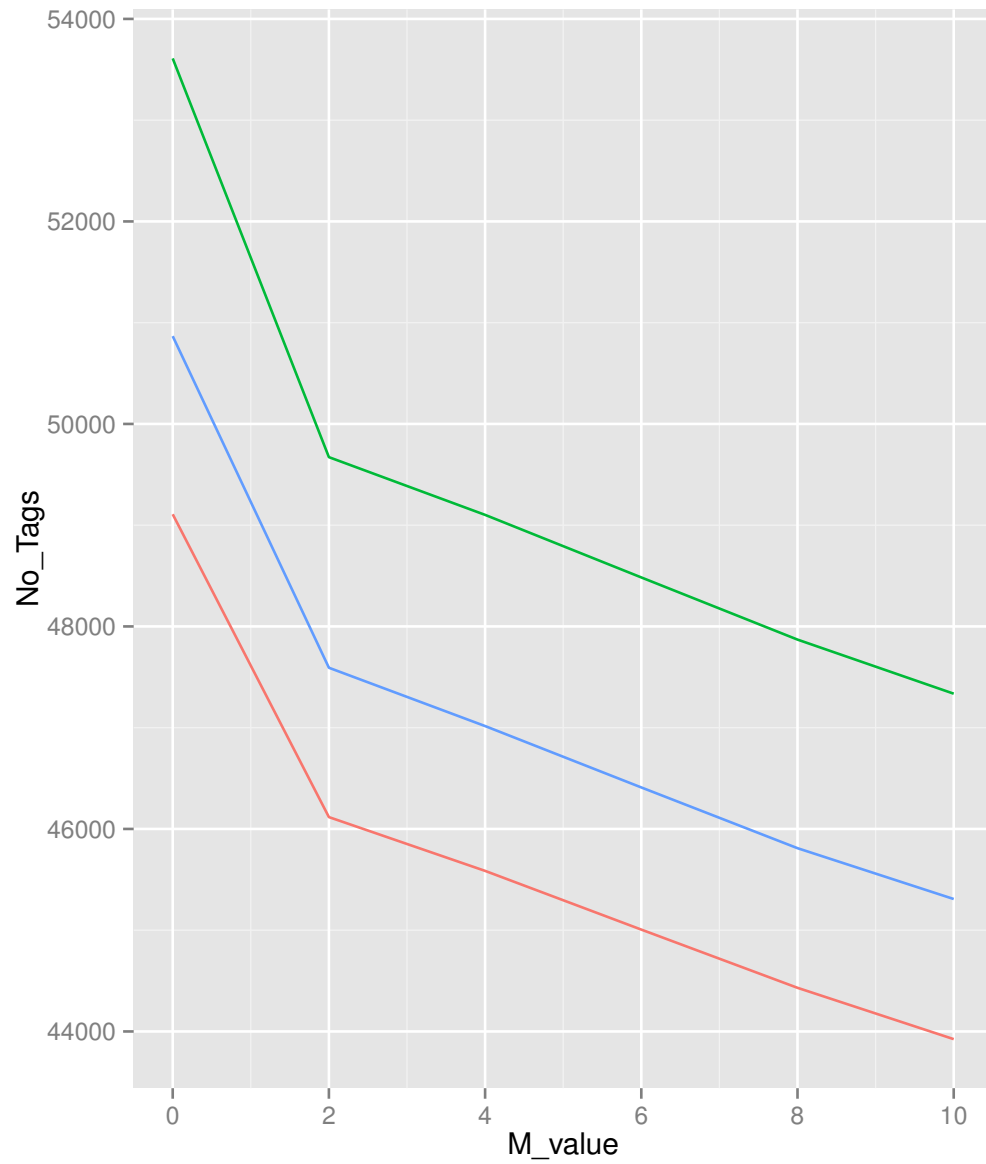
M1 Lest



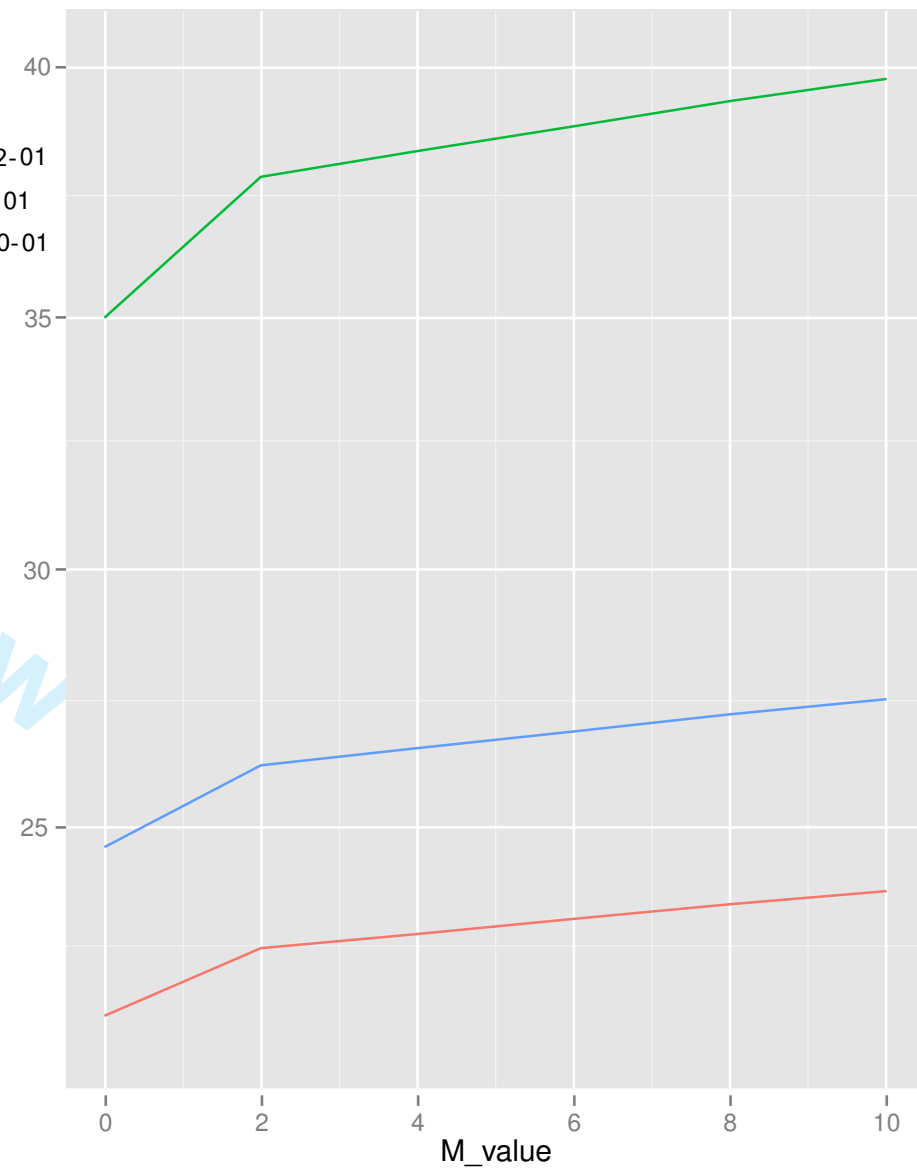
M2 Lest

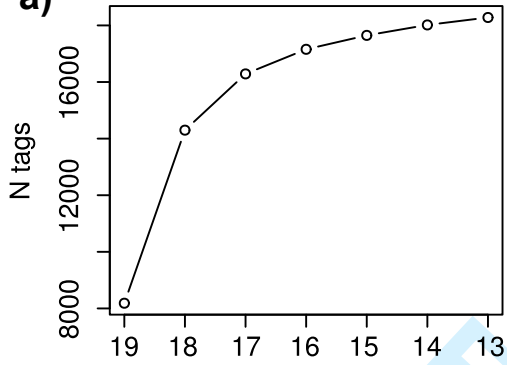
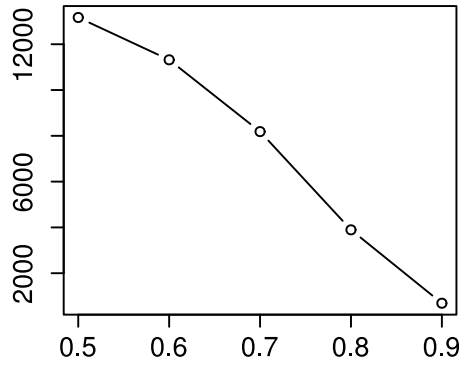
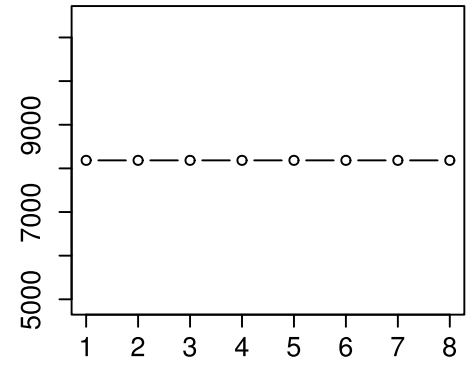
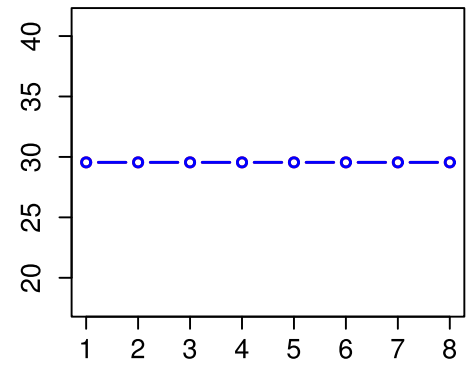
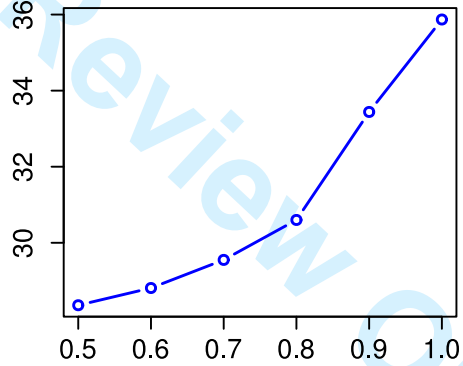
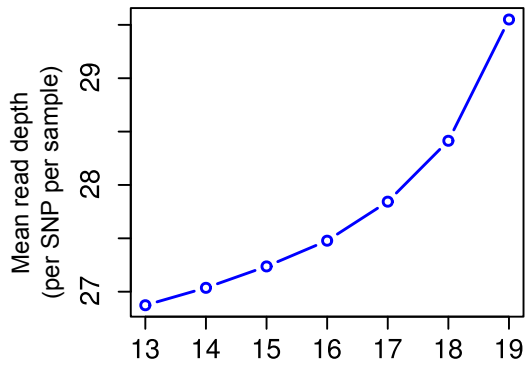
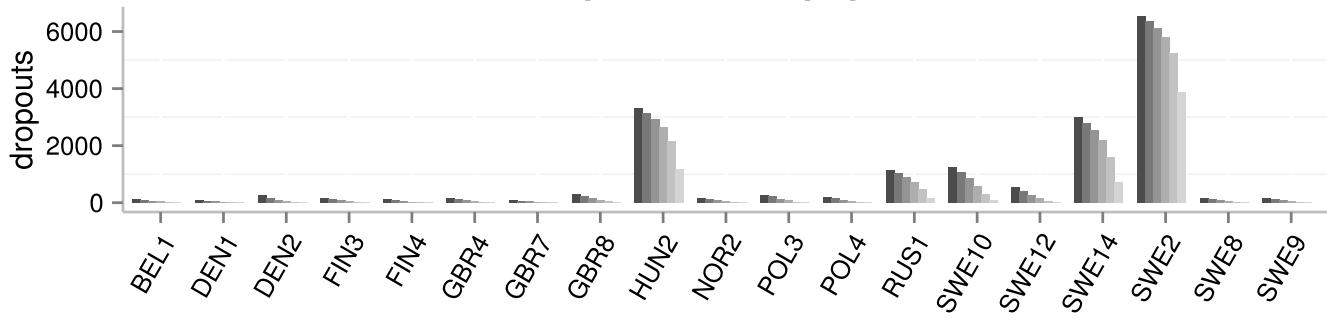


a) Change in number of tags with incrementing M value



b) change in average tag coverage with incrementing M value



-p**a)****Molecular Ecology****-r****-m****b)****c)****SNP dropout across populations****p**

13

14

15

16

17

18

19